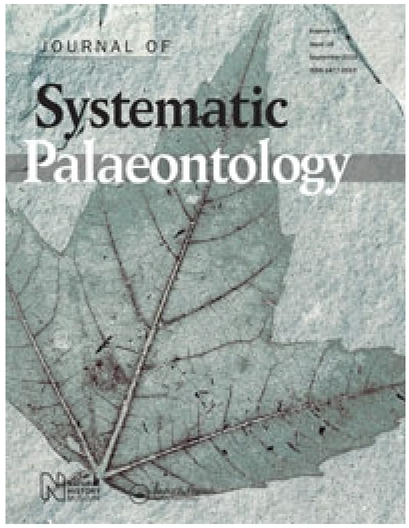


# The evolution of Eocene planktonic foraminifera *Dentoglobigerina*


| | |
|---|---|
| Journal: | *Journal of Systematic Palaeontology* |
| Manuscript ID | TJSP-2020-0041.R1 |
| Manuscript Type: | Original Article |
| Keywords: | Eocene, Planktonic foraminifera, <i>Dentoglobigerina</i>, <i>Subbotina</i>, <i>Acarinina</i>, Phylogeny |
| | |

# The evolution of Eocene planktonic foraminifera *Dentoglobigerina*

Florent Fayolle[a]* and Bridget S. Wade[a]

[a]*Department of Earth Sciences, University College London, Gower Street, London, United Kingdom. WC1E 6BT.*

*Corresponding author: Tel: +44 (0)20 3108 6359; Email: florent.fayolle.18@alumni.ucl.ac.uk

# The evolution of Eocene planktonic foraminifera *Dentoglobigerina*

*Dentoglobigerina* is a diverse genus of planktonic foraminifera ranging from the Eocene to Recent. However, the ancestry of *Dentoglobigerina* has been controversial. A growing body of evidence indicates the genus *Dentoglobigerina* to have been spinose in life and evolved from Eocene *Subbotina,* whilst others have suggested its origins to stem from *Acarinina*. Here we explore whether *Subbotina* or *Acarinina* is the ancestor of *Dentoglobigerina* by examining 35 specimens, evaluating their morphology and their occurrences through the middle to late Eocene, from worldwide localities. We find that *Dentoglobigerina* evolved ~4 million years earlier than previously documented, with the species *Dentoglobigerina pseudovenezuelana* and '*Dentoglobigerina*' *eotripartita* recorded in middle Eocene Zone E9. Morphological convergences between *Dentoglobigerina* and *Subbotina* were found with *D. galavisi* and *D. pseudovenezuelana*, and between *Dentoglobigerina* and *Acarinina* with '*D.*' *eotripartita*. Spine holes were observed in *D. galavisi* and *D. pseudovenezuelana*, though not uniformly found in all forms. Our findings suggests that there are two distinct lineages, (1) *Dentoglobigerina* encompassing the species *D. pseudovenezuelana* and *D. galavisi* as a descendant of *Subbotina*, and (2) '*Dentoglobigerina*' (including '*D.*' *eotripartita*) as descendant of *Acarinina*. Our results contribute to a better understanding of *Dentoglobigerina* biostratigraphy, phylogeny and evolution, and have implications for the taxonomy.

**Keywords:** *Dentoglobigerina*, *Subbotina*, *Acarinina*, phylogeny, planktonic foraminifera, Eocene, International Ocean Discovery Program

# Introduction

*Dentoglobigerina* is a genus of planktonic foraminifera that ranges from the middle Eocene to Recent, reaching its highest diversity during the Oligocene and lower Miocene (Wade *et al*. 2018a). However, this genus has a complex taxonomic and phylogenetic history due to its resemblance and evolutionary convergence with species of other genera. There are two opposing theories on the origins of *Dentoglobigerina*; (1) the *Acarinina* ancestor theory by Olsson *et al.* (2006a) and (2) the *Subbotina* ancestor theory implied by Pearson & Wade (2015) and Wade *et al.* (2018a). Questions regarding its first occurrence, potential ancestor, wall texture type and conservation of spine holes through evolution remain unresolved. Here we examine specimens of *Dentoglobigerina*, *Acarinina* and *Subbotina* in samples from worldwide localities and dated from the middle to late Eocene. We also analyse spine hole data from Miocene *Dentoglobigerina* forms, whose images are available in our IODP data report Fayolle & Wade (2020).



## Historical context of *Dentoglobigerina* taxonomy

The genus *Dentoglobigerina* was erected by Blow (1979) and has recently been reviewed by Olsson *et al.* (2006a) and Wade *et al.* (2018a). Blow's genus concept was based on the presence of an umbilical tooth and the requirement of a globogeriniform morphology, hence including forms now recognized as *Subbotina* by Wade *et al.* (2018b) (which also can show tooth in their aperture area) and excluding forms where the tooth is not prominent (e.g., *Dentoglobigerina tapuriensis*). Blow's concept was followed by Spezzaferri & Premoli Silva (1991) by recognising Oligocene forms such as *D. globularis* and *D. larmeui*. In the Atlas of Eocene planktonic foraminifera, Olsson *et al.* (2006a) recognised three species of *Dentoglobigerina* in the Eocene; *galavisi, pseudovenezuelana* and *tripartita*, with the ancestor *D. galavisi* ranging from middle Eocene Zone E13. Wade *et al.* (2018) acquired scanning electron micrographs (SEMs) of the holotype of *Globigerina tripartita* Koch (1926), which indicated a large, subspherical test, more typical of specimens encountered in the Oligocene. *Dentoglobigerina eotripartita* Pearson, Wade and Olsson, was named for the smaller, more compact morphotypes commonly found in the Eocene. Wade *et al.* (2018a) proposed *D. eotripartita* evolved in upper Eocene Zone E14, and was the ancestor of *D. tripartita*, which evolved in the lower Oligocene Zone O2.

[Insert Fig. 1 here]

**Controversy around *Dentoglobigerina* phylogeny**

Two main theories on the evolution of Eocene *Dentoglobigerina* have been proposed and are synthetized in Fig. 2. It was initially implied by Blow (1979) that *Dentoglobigerina* likely evolved from *Subbotina*, as strong morphological resemblances were observed and two specimens showing transitional features between *Dentoglobigerina* and *Subbotina* were illustrated (Blow 1979, pl.191, figs 8-9). However, *Subbotina* possesses spinose wall texture, and as there was no evidence for a spinose wall texture in *Dentoglobigerina* (Hemleben & Olsson 2006), Olsson *et al.* (2006a) placed the genus within the non-spinose Family Globoquadrinidae. They pointed to the *Globoquadrina*-type wall texture, believed by Hemleben & Olsson (2006) to have evolved from the *muricate*-type, and suggested the dentoglobigerinids evolved from muricate *Acarinina*.

Geochemical analysis reveals *Acarinina* had a mixed-layer habitat (Pearson *et al.* 2001; Wade 2004) while *Dentoglobigerina* calcified in a deeper water thermocline habitat (Pearson & Palmer 1999; Pearson *et al.* 2001), similar to *Subbotina yeguaensis* (Olsson et al. 2006b). Therefore, Hemleben & Olsson (2006) hypothesized that the *Globoquadrina*-type wall texture would have developed in response to the occupation of a deeper water habitat by *Dentoglobigerina*, resulting in the loss of pustules and an increase in porosity. According to Berggren *et al.* (2006), the omnipresence of pustules in *Acarinina* wall texture would be the result of a high symbiont activity. As a consequence, Hemleben & Olsson (2006) related the less pustulose *Globoquadrina*-type wall texture with the loss of symbiont activity with *Dentoglobigerina* in deeper water habitats.

In contrast, more recent studies have reported spine holes in several forms of *Dentoglobigerina* from the late middle Eocene Zone E13 (Sexton *et al.* 2006), late Eocene (Pearson & Wade 2015), Oligocene (Wade *et al.* 2018a) and Miocene (Fox & Wade 2013), strongly supporting the *Subbotina* ancestor theory. Due to the evidence of spine holes on various species, Wade *et al.* (2018a), in the Atlas of Oligocene planktonic foraminifera, placed the genus within the Family Globigerinidae, and proposed the dentoglobigerinids evolved from a subbotinid ancestor. However, none of these studies investigated the evolution of *Dentoglobigerina*, or provided evidence of transitional forms.

So far, however, there is relative paucity of studies describing potential morphological intermediates that could show evolutionary transitions between *Dentoglobigerina* and either *Acarinina* or *Subbotina*. Although Olsson *et al.* (2006a) suggested an acarininid ancestor, there was no evidence for specimens showing transitional morphological traits between the two genera, and nothing similar to the two unusual specimens illustrated by Blow (1979) were found.

Research thus far has not been able to determine whether or not spines are a conservative trait in *Dentoglobigerina* forms. Only one study has assessed the occurrence of spine holes in *Dentoglobigerina* specimens from the middle Eocene, Zone E13 (Sexton *et al.* 2006). Pearson & Wade (2015) recorded the presence of spine holes in *Dentoglobigerina galavisi*, *Dentoglobigerina pseudovenezuelana* and *Dentoglobigerina eotripartita* in the late Eocene and early Oligocene of Tanzania at Zones E15/E16 and O1. Fox & Wade (2013) and Wade *et al.* (2018a) recorded spine holes in several Miocene forms, however, there has been no accumulated evidence of spine holes in specimens older than Zone E13. As yet, spine holes have not been observed in all species of *Dentoglobigerina*, suggesting there could be two clades with similar morphologies, one spinose and one non-spinose, or that spines could have been lost through evolution.

Much uncertainty still exists about the first occurrence of *Dentoglobigerina* during the middle Eocene. The oldest documented occurrence of *Dentoglobigerina* is from middle Eocene Zone E12 with ancestral species *D. galavisi* (Krasheninnikov & Hoskins 1973), however it is proposed by Wade *et al.* (2018a) that the genus could have evolved earlier than thought (Fig. 2).

Our objective was to obtain data to resolve the biostratigraphic gaps of the middle Eocene by updating the stratigraphic range of Eocene *Dentoglobigerina* and by establishing phylogenetic relationships with other Eocene taxa. For that, this project addresses the following objectives: (1) Establish the ancestor of *Dentoglobigerina* by selecting specimens of Eocene *Dentoglobigerina* and potential morphological intermediates with *Subbotina* and *Acarinina* from multiple sites across the world with a stratigraphic coverage from the middle Eocene, Zone E9 to late Eocene, Zone E16; (2) Document when the genus evolved by determining the lowermost occurrences and updating the stratigraphic range of Eocene *Dentoglobigerina* species; (3) Examine test morphology, chamber shape and arrangement to determine evolutionary intermediates and ancestor-descendent relationships; (4) Record the presence of spine holes in the wall texture of Eocene and Miocene *Dentoglobigerina* forms in order to assess the conservation of spines through evolution or the potential existence of two lineages (one spinose and one non-spinose).

[Insert Fig. 2 here]

# Materials and methods

## Site locations

*Dentoglobigerina* specimens were explored from multiple ocean basins with samples ranging from middle Eocene (Zone E9) to late Eocene (Zone E16), and early Miocene (Subzone M1b) to middle Miocene (Subzone M9a). The middle Eocene to late Eocene samples are from core sediments recovered from five expeditions as part of Ocean Drilling Program (ODP) and field samples from Mississippi (Fig. 3). The early to late Miocene samples have been recovered from core sediments as part of Integrated Ocean Drilling Program and International Ocean Discovery Program (IODP). The sites were chosen based on the availability of samples covering those intervals, previous biostratigraphic works and preservation state (our preservation approach is addressed in detail in a subsequent section). Table 1 provides further details in the number of samples analysed, the core sections, depth intervals, coordinates, biostratigraphic ages and preservation quality for the Eocene interval. Details concerning Miocene samples can be found in the IODP data report Fayolle & Wade (2020).

The biostratigraphy of each site was calibrated to the Planktonic Foraminiferal Zonation of Wade *et al.* (2011). Ages were established based on previous initial and scientific reports referenced under Table 1 for Eocene samples and were calibrated to Cande & Kent (1995) for consistency with the Atlas of Eocene Planktonic Foraminifera (Pearson *et al.* 2006). We also have updated the sample ages to the Geologic Timescale of 2020 (GTS2020) following Speijer *et al.* 2020.

[Insert Fig. 3 and Table 1 here]

**Scanning Electron Microscope and z-stacking imaging**

An Olympus z-stacking light microscope from the Micropalaeontology laboratory of UCL was used to take images in three views (umbilical, edge and spiral view) of the selected specimens. This experiment aimed to show the overall preservation of the test and detailed morphological traits such as the wall texture, orientation of the tooth and the arrangement of chambers. Three to four specimens were selected across 21 samples based on their preservation potential and size (preferentially above 355 µm for better resolution). These were placed at the centre of a rectangular subdivision in a brass picking tray, then images were taken upon automatic calibration of the microscope and processed using the sharpen filters for clarity.

A Jeol JSM-6480LV high-performance scanning electron microscope from the UCL Earth Sciences laboratory was used on the selected specimens to get a higher resolution of their wall texture and investigate the presence of morphological features (spine holes and pustules) which could help in their taxonomic identification. Following Z-stacking microscopy the specimens were placed on stubs using double-sided tape. Each stub was sputter-coated in an argon and gold atmosphere using a sputter-coater machine to avoid charging. These steps were repeated for the selected specimens, in each of the three views. Spine holes were investigated across the three views of each specimens' test, and particularly on areas where pores were sufficiently preserved, pore ridges smooth and not affected by diagenetic processes.

**Wall texture, preservation and spine hole identification**

The identification of phylogenetic relationships between ancestor-descendant relies on overall test morphological features, including aperture position, chamber shape and arrangement. Being able to identify the original wall texture of selected specimens and the presence of spine holes is critical, hence the need to assess the preservation potential of their wall texture. In addition, we note the presence of pustules, which have been reported in both the *Globoquadrina*-type and *Dentoglobigerina*-type wall textures (Hemleben *et al.* 2018).

The quality of each sample (Table 1) was inferred from the number of its specimens showing a similar state of preservation. We observed that the preservation varies between specimens of the same sample, and even within areas of the wall texture. Therefore, the preservation of specimens may not always reflect this of the sample (two poorly preserved specimens in Fig. 9 in fairly preserved ODP Samples 1263B-7H-5W and 763B-6X-5W) and we infer the importance of looking at the state of preservation at the specimen and wall texture levels to help in identifying morphological features. We classified the states of preservation under three categories (Fig. 4):

- *Good*: (1) under light microscope: glassy, translucent reflective surface test, pore channels clearly visible through the chamber wall; (2) under SEM: the pores and pore ridges are visible and clear of micro-organism remains (e.g., frustules, coccoliths), the test surface is relatively smooth, spine holes may be identified.
- *Fair*: (1) under light microscope: pore channels usually discernible; (2) under SEM: the pore and pore ridges are visible in some parts and poorly preserved in others; (2) under SEM: some areas of the wall texture are smooth whereas others are affected by dissolution and/or recrystallization, spine holes may be identified in some parts of the test where the wall texture is relatively well preserved.
- *Poor*: (1) under light microscope: chalky, white, opaque, and hard to discern internal features; (2) under SEM: very high carbonate content (e.g., coccoliths fragments) that obscures the pores and pore intersections, spine holes may, most of the time, not be recognizable and be confused with coccolith fragments and the shape given by calcite crystals.

[Insert Fig. 4 here]

We identify spine holes as features found at the intersection of pores often up on small topographic highs and smaller than pores (Poole & Wade 2019). In this study, we observed spine holes, varying between 0.2 and 2.1 µm in diameter, that are circular to slightly triangular in shape, characteristic of the *Globigerina*-type (Hemleben *et al.* 1991). We infer that the identification of more convincing spine holes is preservation dependent. However, we do not consider that the total number of spine holes is completely preservation dependant. One may think that we may see more of them in better preserved specimens. However, sometimes, we were able to see more of them in specimens with 'fair' (a total of 11 spine holes in the specimen from Figure 15O-R) than with 'good' preservation (a total of 8 spine holes in the specimen from Figure 13G-K). More interesting, we pointed out that spine holes may not always be recognised in specimens with 'good' preservation (Figure 8Q-T). Poole & Wade (2019) suggested that abundant and systematically distributed spine holes are good evidence of spinosity. However, it should be noted, that even in species known to be spinose (e.g., *Trilobatus trilobus*), spine holes are not always evident due to gametogenic calcite (see Poole & Wade, fig. 6). The presence of morphological features analogous to spine holes has been assessed and split into two categories based on a similar approach:

- The term 'Evidence of spine holes' is used where (1) at least two spines holes per specimens could be observed, (2) spine holes are systematically distributed across the different views of the same specimen and/or across the same view, and where (3) the wall texture was not too affected by diagenetic processes. We placed an exception on the spine hole from Fig. 5A. This is because the hole is perfectly rounded and located at the pore intersection. Specimens with 'fair' or 'good' preservation sometimes result in cleaner and rounder holes (Fig. 5A-B). Fairly preserved specimens can sometimes show slit-like and/or elongated holes (Fig. 5C-D). With few exceptions only, poorly preserved specimens might show slit-like and elongated holes (Fig. 5E).

- The terms 'No evidence of spine holes' is used for specimens where their interpretation may be falsified by the presence of gaps between recrystallized crystals of calcite, especially in poorly preserved specimens (Fig. 14G-H). The presence of spine holes in the wall texture of '*D.' eotripartita* is uncertain because we were only able to observe one potential hole per specimen, hence not qualifying them for 'evidence of spine holes'. Consequently, we have circled them with white dashed lines in Fig. 5E-G.

[Insert Fig. 5 here]



**Open nomenclature and synonymy lists**

An open nomenclature is used in this study in order to express remarks on selected specimens where the genus and/or species assignment remain difficult. Shorthands used for the identification of this study specimens follows the model discussed by Bengtson (1988) and are as followed:

- 'sp.' indicates that the specimen cannot be associated to any identified species or that the identification of its species has not been attempted.
- 'cf.' is placed between a genus and species name to express a lesser degree of uncertainty compared with '?' when the genus can be confidently assigned but the species level suggested remains as an assumption.
- '?' to express great degree of uncertainty regarding the assignment of a specimen to a taxon.

**Systematic palaeontology overview**

In order to assess both ancestor theories (*Subbotina* vs *Acarinina*), images of Eocene *Dentoglobigerina*, *Subbotina*, *Acarinina* and morphological intermediates have been put into twenty-four plates (including supplementary materials). Each plate contains SEM images of the three views (umbilical, edge and spiral view), and wall texture together with z-stacker images. Interpretations in the morphological features (pustules; spine holes) and preservation character of the wall texture of each Eocene specimen have been recorded within Table 4 in supplementary materials and follow the methods used for assessing the preservation potential of the wall texture and the presence of spine holes.

Each specimen has been named based on morphological similarities with its respective holotype and has been recorded within Table 4 along with sample details. Nine specimens were difficult to assign to a species and/or a genus, hence the use of the open nomenclature to make comments and recognize similarities with taxa. We discuss the Miocene *Dentoglobigerina* forms in the 'Discussion' section as they allow us to trace the conservation of the spine character in *Dentoglobigerina*. However, we did not include their plates in this article as they do not relate directly to the origins of *Dentolgobigerina*. Therefore, their plates as well as their details can be found in the IODP data report Fayolle & Wade (2020). Recognized *Subbotina* specimens have been placed in the supplementary materials, except for *S. yeguaensis* which is of a great interest for this study, due to its possible relationship with *Dentoglobigerina*. The morphological intermediates between *Dentoglobigerina* and *Subbotina* or *Dentoglobigerina* and *Acarinina* have been described separately in the systematic palaeontology as those cannot be assuredly assigned to a particular species and/or genus.

## Systematic palaeontology

Order **Foraminiferida** d'Orbigny, 1826

Superfamily **Globigerinoidea** Carpenter, Parker & Jones, 1862

Family **Globigerinidae** Carpenter, Parker & Jones, 1862

Genus ***Dentoglobigerina*** Blow, 1979

**Type Species.** *Dentoglobigerina galavisi* (Bermúdez, 1961)

**Diagnosis.** Type of wall: Normal perforate, sparsely spinose in life, cancellate, pustulose on the umbilical area.

Test morphology: Trochospiral, globular, rounded to lobulate in outline with the final chamber leaning towards the umbilicus, weak to heavy concentration of pustules mostly around the umbilicus. Aperture commonly centered over the umbilicus and bordered with pustulose apertural lip or an asymmetrical triangular tooth. In some species the tooth is absent. A bulla can be common in late Oligocene and early Miocene forms.

**Remarks.** Wade *et al.* (2018a) differentiated the genus *Dentoglobigerina* from *Subbotina* by its (1) less globular central outline, (2) more appressed chambers leaning towards the aperture in edge view, (3) a greater concentration of pustules in the aperture area, (4) a more asymmetrical tooth than in *Subbotina* forms. Similarly, Pearson and Wade (2015) outlined the more compressed and appressed characters of the chambers of *Dentoglobigerina* as the preeminent difference with *Subbotina*. Olsson *et al.* (2006a) discerned *Dentoglobigerina* from *Subbotina* by its asymmetric extra-umbilical aperture, in contrast with the intra-extra umbilical aperture of subbotinid forms.

**Range.** Middle Eocene to recent

***Dentoglobigerina galavisi*** (Bermúdez, 1961)

(Figs 6, 7, 8, 9)

1961 *Globigerina galavisi*; Bermúdez: 1183, pl. 4, fig. 3.

1979 *Dentoglobigerina galavisi* (Bermúdez); Blow: 1301-1305, pl. 5 figs 1-3, pl. 6 fig. 5, pl. 16 fig. 4.

2006 *Dentoglobigerina galavisi* (Bermúdez); Olsson, Hemleben & Pearson: 403-404, pl. 13.1, figs 1-16.

2015 *Dentoglobigerina galavisi* (Bermúdez); Pearson & Wade: 54-55, pl. 15, figs 1-8.

2018 *Dentoglobigerina galavisi* (Bermúdez); Wade, Pearson, Olsson, Fraass, Leckie & Hemleben: 346-347, pl. 11.5, figs 1-16.



**Diagnosis.** Type of Wall: Cancellate, normal perforate, honeycomb, non-pustulose, and spinose in life (evidence for spine holes in Fig. 6G-H, 6O; Fig. 7G-H, O-P; Fig. 8G-J).

Test Morphology: Overall, the test is trochospiral, globular, oval to quadrate in equatorial outline and the chambers are globular. In spiral view 3½ ovoid chambers in ultimate whorl increasing rapidly in size can be observed. The sutures are moderately depressed, and straight to slightly curved. In umbilical view, 3½ ovoid chambers are increasing rapidly in size, the sutures are deeply incised and straight. The umbilicus is small, enclosed by surrounding chambers, the aperture centered over the umbilicus and is bordered by a thin irregular, triangular shaped lip that is centered below a well-defined apertural face. In edge view, the chambers are ovoid in shape and projecting over the umbilicus. The ultimate chamber shows a distinct bending and flattening into the umbilicus forming an indistinct umbilical face.

Size: 346-427 µm in width; 433-527 µm in length.

**Remarks.** Attributed as the type-species by Blow (1979), *D. galavisi* has a strong resemblance with *Subbotina*, and especially with *Subbotina yeguaensis* as seen in Fig. 13 (Stainforth 1974;

Bolli & Saunders 1985). Nevertheless, Wade *et al.* (2018a) distinguished it from most of *Subbotina* forms by its more (1) flattened spiral side, (2) radially compressed chambers in the umbilical side, (3) thin lip (also seen in *S. yeguaensis*) and (4) triangular umbilical shape (Pearson & Wade 2015).

Even though the lower occurrence of this species has been recorded in Zone E12, further research on older Eocene samples (Zone E10-E11) has been indicated in order to constrain its evolutionary first appearance (Wade *et al.* 2018a). Here we present *D. galavisi* specimens dated from Zone E11 (at around 42.3 Ma) on ODP Sample 763B-6X-5W at Exmouth Plateau, Indian Ocean.

**Taxonomic history.** *Globigerina galavisi* was described by Bermúdez (1961) from the upper Eocene of Mississippi. Bronnimann & Resig (1971) and Krasheninnikov & Hoskins (1973) followed by observing *Globigerina galavisi* (currently *Dentoglobigerina galavisi*) and pointing morphological features including a thin and plate-like lip and radially compressed chambers. Other studies such as Stainforth (1974) and Bolli & Saunders (1985) viewed it as a synonym of *Globigerina yeguaensis* (Weinzierl & Applin 1929). A separate study by Blow (1979) first recognized *D. galavisi* as a distinct and important morphotype of the genus *Dentoglobigerina* but his taxonomic concept was very broad, hence including in it very globular specimens that are now assigned to *Subbotina*. Olsson *et al.* (2006a) and Pearson & Wade (2015) applied a more restricted morphological concept which implied *D. galavisi* was the first species of the genus to evolve in the middle Eocene.

[Insert Figs 6, 7, 8, 9 here]

***Dentoglobigerina pseudovenezuelana*** (Blow & Banner, 1962)

(Figs 10, 11, 12, 13)

1962 *Globigerina yeguaensis pseudovenezuelana*; Blow & Banner: 100, pl. XI figs J-L, N-O.

1979 *Dentoglobigerina pseudovenezuelana* (Blow & Banner); Blow: 1307-1310, pl. 19 figs 1-2, pl. 244 figs 5-6.

2006 *Dentoglobigerina pseudovenezuelana* (Blow & Banner); Olsson, Hemleben & Pearson: 404-408, pl. 13.2 figs 1-16.

2015 *Dentoglobigerina pseudovenezuelana* (Blow & Banner); Pearson & Wade: 58-59, pl. 17 figs 1-6.

2018 *Dentoglobigerina pseudovenezuelana* (Blow & Banner); Wade, Pearson, Olsson, Fraass, Leckie & Hemleben: 356, pl. 11.9 figs 9-16.



**Diagnosis.** Type of Wall: Cancellate, normal perforate, pustulose on the umbilical area, spinose in life (evidence for spine holes in Fig. 10G-H; Fig. 11H, R-S; Fig. 12H-J; Fig.13G-J, Q-R).

Test Morphology: Overall, the test is large, trochospiral, compact, globular, subcircular in outline and the chambers are ovoid. In spiral view, 3½ ovoid chambers in ultimate whorl, increasing moderately in size can be observed. The sutures are moderately depressed and straight. In umbilical view, the 3½ ovoid chambers are increasing moderately in size, sutures are deeply depressed and straight, the umbilicus is moderate in size, the aperture is centered over the umbilicus and bordered by an irregular pustulose lip or tooth. In edge view, the chambers are ovoid in shape and are embracing. The ultimate chamber extends over the umbilicus and is oval to subcircular in outline.

Size: 375-500 µm in width; 425-566 µm in length.

**Remarks.** Olsson *et al.* (2006a) established the evolutionary transition of *D. pseudovenezuelana* in Zone E14 (at about 36.6 Ma). In contrast, Wade *et al.* (2018a) confirmed its lowest occurrence at Zone E12 based on Blow (1979). Here we find its lower datum at Zone E9 (at about 44.1 Ma) on ODP Sample 865C-7H-3 at Allison Guyot, western Pacific Ocean.

Wade *et al.* (2018a) distinguished *D. pseudovenezuelana* from *D. galavisi* by its (1) 3½ rather than 3 chambers as seen for *D. galavisi*, (2) more flattened and compact test and chambers, (3) highly pustulose around the lip and tooth, (4) and raggedy lip.

**Taxonomic history.** The species *pseudovenezuelana* was erected by Blow & Banner (1962) to accommodate one of the two species initially described by Bolli (1957) as *venezuelana*. Blow (1979) included *pseudovenezuelana* in his new genus *Dentoglobigerina* and thought that *S. yeguaensis* was its ancestor. This was rectified by Olsson *et al.* (2006a) to *D. galavisi* based on the belief that both of these species were non-spinose and placing them within the Globoquadrinidae Family. Although Wade *et al.* (2018a) agreed on its ancestor, *D. pseudovenezuelana* is constrained to the Globigerinidae Family as spine holes were observed in several specimens by Sexton *et al.* (2006) and Pearson & Wade (2015).

[Insert Figs 10, 11, 12, 13 here]

## Genus ***Subbotina*** Brotzen & Pozaryska, 1961

**Type species.** *Globigerina triloculinoides* (Plummer 1926)

**Diagnosis.** Type of wall: Normal perforate, spinose in life, wall cancellate, pustulose on the umbilical area.

Test morphology: According to Wade *et al.* (2018b) and Olsson *et al.* (2006b): low trochospiral, test rounded in outline consisting of 10 to 12 globular chambers with 3 to 4 rapidly increasing.

Aperture is umbilical to slightly extra-umbilical, narrow to broad lip with a symmetrical tooth in some species.

**Remarks.** The recent taxonomic work of Olsson *et al.* (2006b) and Wade *et al.* (2018b) now distinguish *Subbotina* by its (1) more rounded and globular chambers (especially seen in spiral view), (2) lobate periphery, (3) final whorl chamber leaning towards the aperture which is more globular in edge view than for dentoglobigerinoids forms, (4) an aperture which is more opened and intra umbilical (centered in umbilical view), (5) a symmetrical tooth, (6) and a more spinose and cancellate wall texture.

**Range.** Early Paleocene to late Oligocene

***Subbotina yeguaensis*** (Weinzierl and Applin, 1929)

(Fig. 14)

1929 *Globigerina yeguaensis;* Weinzierl & Applin: 409, pl. 43: fig. 1a-b.

1991 *Subbotina yeguaensis* (Weinzierl & Applin); Huber: 441, pl.5, fig. 2.

2006 *Subbotina yeguaensis* (Weinzierl & Applin); Olsson, Hemleben, Huber & Berggren: 162-163, pl. 6.18, figs 1-16.

**Diagnosis.** Type of wall: *ruber/sacculifer*-type wall texture, normal perforate, potentially spinose in life (evidence for spine holes in Fig. 14H, P, Q).

Test morphology: Overall, the test of specimens in Fig. 14 is rather elevated, trochospiral, globular and lobulated in outline. In umbilical view, 3½ chambers increase moderately in size, slightly embracing. The sutures are slightly depressed and curved. The aperture is umbilical and bordered by an irregular and broad lip that tapers both anteriorly and posteriorly. The ultimate chamber is equal to the penultimate chamber and is rather globular. In edge view, the chambers are globular in shape but are slightly embracing. The aperture is visible and bordered by a thin lip. In spiral view, globular chambers are more or less equal in size. The sutures are curved and not depressed.

Size: 350-466 μm in width; 450-600 μm in length.

[Insert Fig. 14 here]

## ***Subbotina* cf. *S. yeguaensis* (Weinzierl and Applin, 1929)**

(Figs 15, 16A-F)

1929 *Globigerina yeguaensis* Weinzierl & Applin:409, pl. 43: fig. 1a-b.

2006 *Subbotina yeguaensis* (Weinzierl & Applin); Olsson, Hemleben, Huber & Berggren: 162-163, pl. 6.18, figs 1-16.

**Diagnosis.** Type of wall: Cancellate, normal perforate, pustulose on the umbilical area (specimen in Fig. 15A-H) to non-pustulose (specimens in Figs 15I-R and 16A-F), probably spinose in life (evidence for spine holes in Fig. 15O-R; Fig. 16F).

Test morphology: Overall, the test is trochospiral, globular and moderately elevated, oval in equatorial outline and the chambers are ovoid (specimens from Figs 15I-R & 16A-F) to globular (specimen from Fig. 15A-H). The penultimate chamber equals the ultimate chamber. In umbilical view, the 3½ ovoid chambers are increasing moderately in size, sutures are deeply depressed and curved, the umbilicus is opened and large in size, the aperture is centered over the umbilicus and bordered by a well-defined lip (specimen from Figs 15I-R) or triangular and extra-umbilical tooth (specimen from Fig. 16A-F). The specimen of Fig. 15A-H does not show such features although the pustules are abundant in the apertural region. The last three chambers form about two-third of the entire test. In edge view, the chambers are ovoid in shape and are moderately embracing. The ultimate chamber is disposed straight over the umbilicus (specimen of Fig. 15A-H), bends lightly over the umbilicus for specimens of Figs 15I-R & 16A-F, and is oval to subcircular in outline. In spiral view, 3½ ovoid to globular chambers in ultimate whorl, increasing moderately in size can be observed. The sutures are moderately depressed and straight.

Size: 400-533 μm in width; 500-600 μm in length.

**Remarks.** Specimens in Figs 15 and 16A-F share strong affinity with the genus *Subbotina* by their more globular and elevated test compared to dentoglobigerinoids. At the species level, we made the assumption that they show their closest resemblance with *S. yeguaensis* but also at a lesser extent with the genus *Dentoglobigerina*, and in particular with *D. pseudovenezuelana*. Based upon the observations described in the 'Discussion' section under '*Subbotina – D. pseudovenezuelana* relationship', we recognise them as potential morphological intermediates between *Subbotina* and *D. pseudovenezuelana*.

[Insert Fig. 15 here]

***Subbotina* cf. *S. eocaena*** (Gümbel, 1868)

(Fig. 16G-P)

1868 *Globigerina eocaena* Gümbel:662, pl. 2, fig. 109a.b.

2006 *Subbotina eocaena* (Gümbel); Olsson and others:134-138, pl. 6.9, figs. 1, 2, 4-6, 9, 10.

**Diagnosis.** Type of wall: Cancellate and normal perforate, probably spinose in life (spine holes in Fig. 16P).

Test morphology: Overall, globular chambers and sub-triangular outline in spiral view, chambers increasing moderately in size. In umbilical view, thin and irregular lip in a low arched aperture, globular chambers and curved sutures. The ultimate chamber is large. In edge view, the ultimate chamber is appressed and bends slightly over the umbilicus such as for most of *Dentoglobigerina*. Chambers are ovoid in shape and embrace. In spiral view, globular chambers increase moderately in size, slightly curved sutures.

Size: 430 µm in width and 500 µm in length.

**Remarks.** The specimen in Fig. 16G-P shares morphological traits with the genus *Subbotina*. At the species level, we made the assumption that this specimen shows its closest resemblance to *S. eocaena* and at a lesser extent with *D. pseudovenezuelana*. We named specimen 22 as *S.* cf. *S. eocaena* and described it as a potential morphological intermediate between *Subbotina eocaena* and *Dentoglobigerina* in the 'Discussion' section under '*Subbotina* – *D. pseudovenezuelana* – *D. galavisi* relation'.

[Insert Fig. 16 here]

### *Subbotina* sp. 1

(Fig. 17)

**Diagnosis.** Type of wall: Cancellate, normal perforate, globular, non-pustulose, and spinose in life (spine holes in Fig. 17H-I, T).

Test morphology: Overall, the test is large, trochospiral, compact, globular, subcircular in outline and the chambers are ovoid. In umbilical view, the 3½ ovoid chambers are increasing rapidly in size, sutures are moderately depressed and curved. The umbilicus is large, the aperture is open, centered over the umbilicus and bordered by well-defined, irregular, triangular and extra-umbilical teeth. In edge view, the chambers are ovoid in shape and are embracing. The ultimate chamber extends over the umbilicus and is subcircular (specimen in Fig. 17A-J) to appressed (specimen in Fig. 17K-T) in outline. In spiral view, 3½ ovoid chambers in ultimate whorl, increasing moderately in size are observed. The sutures are moderately depressed and straight.

Size: 420-430 µm in width; 480-510 µm in length.

**Remarks.** The two specimens of Fig. 17 could not be associated with any identified species of *Subbotina*. Also, no other similar specimens were observed in the ODP Sample 865C-7H-3. Consequently, we defined these specimens as unusual and named them accordingly as *Subbotina* sp.1 to highlight their affinity to *Subbotina*. Both specimens potentially show a transition between *S. yeguaensis* and *D. pseudovenezuelana* and are addressed in the 'Discussion' section under '*Subbotina – D. pseudovenezuelana* relationship'.

[Insert Fig. 17 here]

**?*Subbotina*** or **?*Dentoglobigerina***

(Fig. 18)

**Diagnosis.** Type of wall: Cancellate, normal perforate, non pustulose, and spinose in life (spine holes in Fig. 18H).

Test morphology: Overall, the test is large and elevated, trochospiral, globular, oval in outline and the chambers are ovoid and globular. In umbilical view, the 3½ ovoid chambers are increasing moderately in size, sutures are moderately depressed and curved and the umbilicus is large in size. The aperture is open, centered over the umbilicus and bordered by a well-defined triangular and centered tooth. The last three chambers form about two-third of the entire test. The ultimate chamber is slightly detached from the rest of the test and seems appressed. In edge view, the chambers are ovoid in shape and are embracing. The ultimate chamber bends over the umbilicus and is appressed in outline. In spiral view, 3½ ovoid chambers in ultimate whorl, increasing rapidly in size can be observed. The sutures are moderately depressed and straight. Chambers are sub-circular in outline.

Size: 500 µm in width; 580 µm in length.

**Remarks.** The attribution of the specimen in Fig. 18 to the genus *Subbotina* or *Dentoglobigerina* is unclear as it shares morphological traits with both genera. We treat this specimen as a potential morphological intermediate between *Subbotina* and *Dentoglobigerina* and address its significance in the 'Discussion' section under '*Subbotina* – *D. pseudovenezuelana* – *D. galavisi* relation'.

[Insert Fig. 18 here]

Order **Foraminiferida** d'Orbigny, 1826

Superfamily **Globigerinoidea** Carpenter, Parker & Jones, 1862

Family **Globoquadrinidae** Blow, 1979

**Genus '*Dentoglobigerina*'**

Our study suggests that there are two lineages of *Dentoglobigerina*. One that evolved from *Subbotina*, including *D. galavisi and D. pseudovenezuelana*, and a second lineage that evolved from *Acarinina*, which we refer to here as '*Dentoglobigerina'*. However, the naming of a new genus has large implications for the phylogeny, beyond the Eocene, and future work is required to determine which species of the Oligocene and younger stratigraphic intervals belong in '*Dentoglobigerina*' lineage. Furthermore, new investigations are required into the genus *Globoquadrina*, to determine if the non-spinose 'dentoglobigerinids' that evolved from an acarininids ancestor, could be encompassed into the *Globoquadrina* lineage. We have examined Miocene forms as part of this study, and specimens from sites U1489 and U1490 are illustrated in Fayolle & Wade (2020). New analysis of Miocene *Dentoglobigerina* and their wall textures will be conducted by the Neogene planktonic foraminifera working group. In the meantime, we refer to specimens with an acarininid ancestor as '*Dentoglobigerina*' pending further investigations.



**'*Dentoglobigerina*' *eotripartita* Pearson, Wade and Olsson, 2018**

(Figs 19, 20, 21, 22A-H)

2018 *Dentoglobigerina eotripartita* (Koch); Wade, Pearson, Olsson, Fraass, Leckie & Hemleben: 343, pl. 11.4, figs 1-15.

**Diagnosis.** Type of wall: Normal perforate, cancellate, sometimes heavy pustulose in the umbilical and edge views (pustules on Figs 19I-P, 20A-F and 22A-F), and probably non-spinose in life.

Test morphology: Overall, the test is compact, globular and the chambers are arranged in a tight, low trochospiral, subcircular to subquadrate in equatorial outline, and are moderately lobate. In umbilical view, 3½ ovoid chambers in ultimate whorl, increasing rapidly in size are identified. Sutures are straight and incised, the umbilicus is moderate in size, the aperture is centered deep in the umbilicus and bordered by a thin, irregular, subtriangular-shaped lip or tooth which tends to point down the opposing suture. In edge view, the test is oval in outline, the chambers are ovoid in shape and the ultimate chamber projects above and bends over the umbilicus. In spiral view, 3½ ovoid compressed chambers in ultimate whorl, increasing rapidly in size can be observed. The chambers are accompanied by depressed and straight sutures (slightly curved in some cases).

Size: 275-414 μm in width; 305-498 μm in length.

**Remarks.** Wade *et al.* (2018a) distinguished *D. eotripartita* from *D. galavisi* by (1) an overall more compact structure, (2) three tightly coiled chambers increasing more rapidly in size and (3) a more compressed final whorl chamber. Wade *et al*. (2018a) proposed that *D. eotripartita* emerged from *D. galavisi* at Zone E13 (at around 38.6 Ma). Here we find its lowest occurrence at Zone E9 (at around 44.1 Ma) on ODP Sample 865C-7H-3 at Allison Guyot, western Pacific Ocean. Our results imply that *D. eotripartita* would not be a descendant of *D. galavisi* and would have in fact evolved from an acarininid ancestor, as supported by the evidence of morphological intermediates and similarities found between *Acarinina* and '*D.' eotripartita*. We refer to this separate lineage as '*Dentoglobigerina*'. The likely absence of spines holes in both '*D.*' *eotripartita* (one potential spine hole was found per specimen; Fig. 20H, Q; Fig. 22H) and '*D.*' *tripartita* maintain the hypothesis that the ancestral *D. eotripartita* would have given rise to the bigger and more globular '*D.*' *tripartita* somewhere in the early Oligocene (Wade *et al.* 2018a).

**Taxonomic history.** *Dentoglobigerina eotripartita* was erected by Pearson, Wade and Olsson in Wade *et al.* (2018a) to accommodate small and compact ancestral forms of *Dentoglobigerina tripartita* (plate 11.4, Wade *et al.* 2018a) and differentiate them from the larger and more globular specimens (plates 11.14 and 11.15, Wade *et al.* 2018a) that make the true *Dentoglobigerina tripartita*. As evidence for spines holes were found in *D. galavisi*, *D. pseudovenezuelana* and potentially in *D. eotripartita* by Pearson & Wade (2015), *D. eotripartita* was placed within the Family Globigerinidae by Wade *et al.* (2018a). In this study, we find that the morphological similarities with *Acarinina* suggests this species belongs within the Family Globoquadrinidae.

**Range.** Middle Eocene to early Oligocene

[Insert Figs 19, 20, 21 here]

Family **Truncorotaloididae** Loeblich and Tappan, 1961

Genus ***Acarinina*** Subbotina, 1953

**Type species.** *Acarinina acarinata* (Subbotina, 1953)

**Diagnosis.** Type of wall: Non spinose in life, muricate and pustules surrounding aperture. Test morphology according to Olsson et al. (1999): low to moderate trochospiral, ovoid shaped chambers, 4 to 7 chambers in final whorl, moderately to strongly muricate wall, umbilical or extra-umbilical aperture with occasionally a thin lip.

**Remarks.** *Acarinina* is primarily differentiated from *Dentoglobigerina* by its rather muricate and non-spinose wall texture. The test of *Acarinina* generally shows a more ovoid shape compared to the more lobulate form of *Dentoglobigerina*. Pustules are often more abundant and well distributed across the test in *Acarinina* than in *Dentoglobigerina* where pustules tend to be restricted to the apertural area.

**Range.** Middle Paleocene to late Oligocene

### *Acarinina mcgowrani* Wade & Pearson

(Fig. 22I-R)

2006 *Acarinina mcgowrani* (Wade & Pearson); Berggren, Pearson, Huber & Wade: 291-292, pl. 9.13, figs 1-16.

**Diagnosis.** Type of wall: Moderately muricate, non-spinose in life, normal perforate.

Test morphology: Overall, subquadrate outline, 4 inflated chambers in last whorl. In the umbilical view, 4 chambers gradually increase in size and weakly lobate outline, whereas the umbilicus is well defined, deep and lies under an oval ultimate chamber. In edge view, the chambers are sub-rounded and slightly compressed. In spiral view, the chambers are sub-rectangular in outline and potentially show a secondary aperture. The spiral sutures are deeply incised and radial to slightly curved .

Size: 390 μm in width, 470 μm in length.

[Insert Fig. 22 here]

### *Acarinina* cf. *A. triplex*

(Fig. 23A-J)

1953 *Acarinina triplex*; Subbotina: pl. 23, figs 1a-c

1993 *Acarinina triplex* (Subbotina); Pearson, Shackleton & Hall: 125, pl. 1, figs 11-12

2006 *Acarinina triplex* (Subbotina); Berggren, Pearson, Huber & Wade: 277, pl. 9.7, figs 5-7

**Diagnosis.** Type of wall: Moderately muricate, non-spinose in life, normal perforate.

Test morphology: Overall, subquadrate to weakly lobulate outline, 3 chambers in a last whorl. In umbilical view, the peripheral outline is broadly rounded, and the chambers are delimited by deep incised sutures. In edge view, the chambers are slightly rounded but delimited by deeply incised sutures in the specimen of Fig. 23A-J. In spiral view, the chambers are sub-rectangular in outline and potentially show a secondary aperture. The spiral sutures are deeply incised and radial to slightly curved.

Size: 390 μm in width; 465 μm in length.

**Remarks.** *Acarinina triplex* (Subbotina) was designated as a junior synonym of *Acarinina coalingensis* (Olsson *et al.* 1999; Berggren *et al.* 2006). *A. coalingensis* is thought to have gone extinct somewhere at the beginning of Zone E7, however, our results reveal a specimen consistent with *A. triplex* in Zone E9 approximatively 6 million years later than the latest occurrence of *A. coalingensis* (and its junior synonym *A. triplex*). This would suggest either that (1) *A. coalingensis* would have disappeared later than thought or that (2) *A. triplex* could no longer be synonymised in *A. coalingensis*.

On the question of the taxonomic attribution for the specimen on Fig. 23A-J, this study found that it shares morphological traits with both *Acarinina triplex* and '*D.*' *eotripartita*. It's rather sub-quadrate outline with broadly globular chambers arranged at distinct right angles and separated by deep incised sutures conform to the taxonomic description of *A. triplex* (Olsson *et al.* 1999; Berggren *et al.* 2006). *A. triplex* is also characterized by the rapidly increasing size of its chambers, which has not been noticed in this specimen, where those increase moderately in size instead such as for '*D.*' *eotripartita*. In addition, this study attributes to '*D.*' *eotripartita* the more enclosed aperture found in the elongation of umbilical depressed sutures of this specimen. We attribute this specimen as a potential transition between *A. triplex* and *'D.' eotripartita*.

### ***Acarinina* cf. *A. primitiva***

(Fig. 23K-S)

1947 *Globoquadrina primitiva*; Finlay: 291, pl. 8, figs 129-134

1993 *Acarinina primitiva* (Finlay); Pearson, Shackleton & Hall: 125, pl. 1, fig. 19

2006 *Acarinina primitiva* (Finlay); Berggren, Pearson, Huber & Wade: 304, pl. 9.17, figs 1-16

**Diagnosis.** Type of wall: Wall texture uncertain.

Test morphology: Overall, subquadrate to weakly lobulate outline, 3 chambers in a last whorl. In umbilical view, the chambers are sub-triangular to sub-circular and wedged-shaped. Its aperture is rather centered over the umbilicus and a triangular tooth projects over it and in the prolongation of a deep and slightly curved vertical suture. The final chamber is rather appressed and oval in outline. In edge view, the chambers are compressed and ovoid in shape. The ultimate chamber tends to bend over the umbilical region. In spiral view, sutures are poorly visible and weakly incised in the earlier whorls, becoming more deeply incised in the final whorl, radial to slightly curved. The chambers tend to show a rather globular outline.

Size: 400 µm in width; 450 µm in length.

**Remarks.** Berggren & Norris (1997) and Berggren *et al.* (1999) initially included *A. primitiva* in synonymy with *A. coalingensis*. Berggren *et al.* (2006) no longer include *A. primitiva* as a synonym with *A coalingensis* and now restricts it to the more triangular tests with straight incised sutures, in contract with the more robust and subquadrate tests of *A. coalingensis*.

Surprisingly, it has been found that the specimen on Fig. 23K-S (Zone E10 of ODP Sample 763B-6X-6W) and *A. primitiva* exhibit morphological resemblances. The projection of the last chamber over the umbilicus and broadly wedge-shaped outline is characteristic of *A. primitiva* (Berggren *et al.* 2006). However, this specimen does not lack an umbilical suture which is placed in the prolongation of the umbilical tooth as seen in '*D.*' *eotripartita* (Figs. 19I-P, 20A-H, 21 and 22A-H). More interestingly, the chambers show a rather sub-quadrate to sub-circular outline as seen in '*D.*' *eotripartita*, rather than the triangular chambers from *A. primitiva*. We attribute specimen *A.* cf. *A. primitiva* as a potential transition between *A. primitiva* and '*D.*' *eotripartita*.

[Insert Fig. 23 here]

## Revised stratigraphic range of Eocene *Dentoglobigerina*

An update of the stratigraphic range of Eocene *Dentoglobigerina* (Fig. 24) has been possible based on the examination of multiple middle and upper Eocene samples from multiple sites (Table 1). The following stratigraphic range has been compared with past studies such as Olsson *et al.* (2006a) and Wade *et al.* (2018a). Each selected specimen of *Dentoglobigerina* has been placed on the timescale regarding their age, species, and are annotated with a corresponding symbol and colour. All three species of Eocene *Dentoglobigerina* are present in the stratigraphic record at Zone E11 and even at Zone E10 and Zone E9 (Fig. 24). More specifically, it seems that *D. galavisi* appears in this study at the beginning of Zone E11 (42.3 Ma). It can be seen from Fig. 24 that morphological intermediates are abundant at Zone E9 where the oldest '*D.*' *eotripartita* and *D. pseudovenezuelana* specimens have both been traced back (44.1 Ma).

[Insert Fig. 24 here]

## Discussion

### The ancestor of *Dentoglobigerina*

Our study has revealed a number of morphological transitions that shed new light on the ancestry of *Dentoglobigerina*. Here we assess both of the ancestor theories proposed by Olsson *et al.* (2006a) with *Acarinina*, and Pearson & Wade (2015) and Wade *et al.* (2018a) with *Subbotina*. We find evidence of morphological intermediates and similarities between *Acarinina* and '*D.*' *eotripartita*, and likewise between *Subbotina*, *D. pseudovenezuelana* and *D. galavisi*.

***Acarinina* – '*D.*' *eotripartita* relationship.** The most obvious findings to emerge from the images of selected *Dentoglobigerina* specimens were the observed morphological similarities between Eocene '*D.*' *eotripartita* and the *Acarinina* genus. All specimens from Fig. 25 show a rather sub-quadrate to sub-circular shape, a morphological feature shared with *A. mcgowrani*, *A. primitiva* and *A. triplex* (Olsson *et al.* 1999; Berggren *et al.* 2006), which is inconsistent with the globular aspect of Eocene subbotinids (Olsson *et al.* 2006b). Additionally, the overall test size (length and width) of '*D.*' *eotripartita* specimens from Fig. 25, although they do not belong to *Acarinina* as they are not muricate, seems to correspond to what has been described for the *Acarinina mcgowrani* specimen (Fig. 22I-R), and specimens *A.* cf. *A. triplex* and *A.* cf. *A primitiva* (Fig. 23). Perhaps the most striking observation is the highly depressed spiral and horizontal sutures found in '*D.*' *eotripartita* (Figs. 19I-P, 20A-H, 21, 22A-H, 24E-G, 25B-C). Such morphological features resemble the radially to weakly curved and incised sutures found in the spiral view of *A. mcgowrani* (Figs 22I-R, 25J).

One unexpected finding was the extent to which pustules cover the umbilical and edge regions of '*D.*' *eotripartita*, as seen in acarininid forms. In particular specimens in Figs 19I-P, 20A-H, and 25B-C show rather denser and conical pustules in their umbilical region which contrast with the cancellate wall texture in their spiral view. Such characters are shared with the two specimens in Fig. 25I-J (also in Figs 22I-R and 23A-J), described by their highly pustulose and densely muricate wall texture, and differs from other '*D.*' *eotripartita* forms (Figs 19A-H, 20I-Q, 21, 22A-H, 25A, 25D-G). It is noticed that the specimen in Figs. 23K-S and 25H, which appears closely related to *A. primitiva*, does not have a muricate wall texture, suggesting again an affinity to '*D.*' *eotripartita*.



**Comparison with past studies on *Acarinina* and *Dentoglobigerina*.** Our observations are in agreement with the *Acarinina* ancestor theory erected by Olsson *et al.* (2006a) although potential spine holes have been observed in multiple specimens of '*D.*' *eotripartita* in this study (Fig. 20H, Q; Fig. 22H) and previous taxonomic work (Pearson & Wade 2015; Wade *et al.* 2018a). Hemleben & Olsson (2006) attributed *Dentoglobigerina* to an acarininid ancestor based on its wall texture, which was thought to be *Globoquadrina*-type and believed to be a descendant from the muricate-type wall texture as no evidence for spine holes were found. Despite the morphological similarities between '*D.*' *eotripartita* and *Acarinina*, this study cannot agree the wall texture assumption made on *Dentoglobigerina* by Olsson *et al.* (2006a) because evidence for a potential spine holes in '*D.*' *eotripartita* was found by Pearson & Wade (2015).

Olsson *et al.* (2006a) recognized *Acarinina* as the ancestor of *Dentoglobigerina* although no transitional specimens were proposed. Nevertheless, this study illustrated two potential morphological intermediates *A.* cf. *A. triplex* and *A.* cf. *A. primitiva* (Fig. 23, 25H-I) as discussed above, hence why these findings seem to be in agreement with the *Acarinina* ancestor theory, at least for '*D.*' *eotripartita*. The direct morphological resemblances between '*D.*' *eotripartita* and *Acarinina* compared to the uncertain presence of spine holes in *'D'* *eotripartita* seem to represent more tangible evidence tending towards the *Acarinina* ancestor rather than the subbotinid ancestor theory.

[Insert Fig. 25 here]

***Subbotina* – *D. pseudovenezuelana* – *D. galavisi* relation.** Two Eocene species *D. galavisi* and *D. pseudovenezuelana* share morphological traits with *Subbotina*, probably with *S. yeguaensis* (Figs 14, 26K-L) as implied before by Blow (1979). Overall, all specimens from Fig. 26 show a rather globular and imposing test, similarly to subbotinid forms (Olsson *et al.* 2006b), which is conflicting with the rather sub-quadrate to sub-circular shape and smaller size of acarininids described in this study. In addition, the pustulose character of both species *D. galavisi* and *D. pseudovenezuelana* seems constrained to the apertural regions contrary to '*D.*'*eotripartita* specimens that have shown a rather higher degree of pustules in the umbilical and edge views (Figs 19I-P, 20A-H, 24G, 25B-C).

The attribution of a specimen to the *Subbotina* or *Dentoglobigerina* genera is unclear and is shown by Figs 18 and 26J with a specimen named as ?*Subbotina* or ?*Dentoglobigerina*. This specimen (Figs 18, 26J) is characterized by an ultimate chamber bending over the umbilicus, similar to the *D. pseudovenezuelana* specimen in Figs 12A-J and 26C. However, the presence of a centered, regular and sharp tooth pointing centrally down the aperture as well the rather sub-circular outline of its penultimate chamber are more characteristic of *Subbotina*. The specimen shows a relatively elevated test with a penultimate chamber rather globular in outline but still more appressed than the *S. yeguaensis* specimens of Figs 14 and 26K-L.

A relationship between *Dentoglobigerina* and *S. eocaena* can be established with the specimen in Figs 16G-P and 25G, named as *Subbotina* cf. *S. eocaena*. While the more appressed ultimate chamber is characteristic of *Dentoglobigerina,* the moderate increase in chambers size, apertural irregular lip and tendency for a higher globular outline resembles *S. eocaena* as previously described by Olsson *et al.* (2006b) and Wade *et al.* (2018b).

***Subbotina* – *D. pseudovenezuelana* relationship.** One unanticipated finding was that *D. pseudovenezuelana*, instead of *D. galavisi*, show analogous morphological traits to *S. yeguaensis*. Such results have been obtained with two unusual specimens that we named *Subbotina* sp. 1 (Fig. 17). A potential transitional form between *S. yeguaensis* and *D. pseudovenezuelana* is shown in Figs 17K-T and 26I. This form is similar in outline to the specimen in Figs 17A-J and 26H but with a more appressed penultimate chamber, similar to the *D. pseudovenezuelana* specimen of Figs 12A-J and 26C, however the chambers seem to be less embraced such as it can be seen for *S. yeguaensis*. More specifically, the irregular tooth of the specimen in Figs 17K-T and 26I tapers both in the umbilical and edge views, which is a distinguishing character of *S. yeguaensis* (Olsson *et al.* 2006b).

Such assumption was also made upon three specimens that we named *S.* cf. *S. yeguaensis* (Fig. 15, Fig. 16A-F). The taxonomic attribution of the *S.* cf. *S. yeguaensis* form in Figs 15A-H and 26D to *S. yeguaensis* remains uncertain as morphological relationships can also be established with *D. pseudovenezuelana*. The tendency for pustules in the apertural region would place it within species *D. pseudovenezuelana* (Figs 12A-J, 26C), although the overall more globular shape of the test and opened aperture remembers *S. yeguaensis* (Figs 14 and 26K-L). The rather more elevated, globular outline of *S.* cf. *S. yeguaensis* forms in Figs

15I-R, 16A-F and 26E-F compared to *D. pseudovenezuelana* (Figs 12A-J and 26C) and the tooth that gradually narrows in umbilical and edge view is analogous to *S. yeguaensis* (Figs 14 and 26K-L). However, the slightly more appressed final chamber of *S.* cf. *S. yeguaensis* (Figs 15I-R, 16A-F and 26E-F) with regard to *S. yeguaensis* (Figs 14 and 26K-L) would place them within *D. pseudovenezuelana*.

***Subbotina* – *D. galavisi* relationship.** We observe a particular affinity between *D. galavisi* and *S. yeguaensis* in most of the *D. galavisi* specimens. Five out of eight forms of *D. galavisi* (Figs 6I-O, 7I-P, 8K-T and 9) show resemblances to *S. yeguaensis* based on the globular shape of their chambers and/or the presence of a thin lip (Wade *et al.* 2018a, b). Contrary to expectations, this study did not find a morphological resemblance between the *D. galavisi* specimen in Fig. 26A (also Fig. 7A-H) and *S. yeguaensis* (Figs 14 and 26K-L), in a way that the test of this specimen defines a more sub-quadrate outline (such as specimens from Figs 6A-H and 8A-H) compared to *D. galavisi* in Fig. 26B (also Fig. 9I-O), which resemble the specimen described by Olsson *et al.* (2006a) under its work on p.405, pl.13.1, fig. 12.

**Comparison with past studies on *Subbotina* and *Dentoglobigerina*.** Our study broadly supports the initial subbotinid ancestor proposed by Blow (1979) and Bolli & Saunders (1985). Blow (1979) illustrated two unusual specimens showing transitional features between *Dentoglobigerina* and *Subbotina* (Wade *et al.* 2018a) as illustrated on pl.191, figs.8-9 of Blow (1979). We do not recognise this relationship based on the two specimens illustrated by Blow (1979). Such specimens are, in fact, morphologically similar to globular subbotinid species, potentially *S. projecta* (Wade *et al.* 2018b). Nevertheless, seven potential morphological intermediates have been identified in Figs 15-18 of this study, potentially with *S. yeguaensis* or *S. eocaena*.

*D. galavisi* has long been thought to be closely related to *S. yeguaensis* (Blow 1979; Stainforth 1974; Bolli & Saunders 1985; Pearson & Wade 2015; Wade *et al.* 2018a). Blow (1979) thought *S. yeguaensis* could be a potential intermediate species between *D. galavisi* and *D. pseudovenezuelana* (Olsson *et al.* 2006b). Such assumptions seem to be in contradiction with the findings of this study, where *D. pseudovenezuelana* and *S. yeguaensis* rather show a closer relationship.

More recently, Pearson & Wade (2015) and Wade *et al.* (2018a) provided evidence for potential spine holes in the wall texture of the three Eocene *Dentoglobigerina* species, suggesting a subbotinid ancestor. Our study is in agreement with SEM images revealing spine holes in *D. galavisi* (Fig. 6G-H, 6O; Fig. 7G-H, 7O-P; Fig. 8G-J; Fig. 9H) and *D. pseudovenezuelana* (Fig. 10G-H, 9R; Fig. 11H, 11R-S; Fig. 12H-J; Fig.13G-J, 13Q-R). However, this study was not able to provide similar evidence for '*D.*' *eotripartita* because we could only find potential evidence (Fig. 20H, Q; Fig. 22H), hence weighing towards an acarininid ancestor. Pearson & Wade (2015) also illustrated one potential morphological intermediate between '*D.*' *eotripartita* and *D. galavisi* (pl.21.6a-b), however, this study identified morphological gradation between *Acarinina* and '*D.*' *eotripartita* instead.

[Insert Fig. 26 here]

**Phylogenetic implications.** On the basis of these results the potential ancestor of *Dentoglobigerina* remains questionable as such theories rely on idiosyncratic morphological analysis. However, our evidence suggests that '*D.*' *eotripartita* evolved from *Acarinina* (*A. triplex* or *A. primitiva*), as a separate lineage, based on the following evidence: (1) The identification of two potential morphological intermediates (Fig. 23) between '*D.*' *eotripartita*, *A. triplex and A. primitiva*; (2) The direct morphological resemblances between '*D.*'

*eotripartita* and *Acarinina*; (3) The higher degree of pustules in the wall texture of '*D.*' *eotripartita* in comparison to *D. pseudovenezuelana* and *D. galavisi*.

In parallel, *Subbotina* could have given rise to *D. pseudovenezuelana* followed by *D. galavisi* in a separate lineage, with *Subbotina yeguaensis* eventually, based on the following evidence: (1) Identification of spine holes in *D. galavisi* and *D. pseudovenezuelana* specimens from diverse sites and samples; (2) Potential morphological intermediates (Figs 15, 16A-F, 17, 18) between *S. yeguaensis* and *D. pseudovenezuelana*; (3) A potential morphological intermediate between *S. eocaena* and *D. pseudovenezuelana* (Figs 16G-P and 26G); (4) Globular and imposing characters of both *Subbotina* and *Dentoglobigerina* rather than the sub-quadrate to sub-circulate and small morphology of *Acarinina*; (5) The stronger analogy between *S. yeguaensis* and *D. pseudovenezuelana* than between *S. yeguaensis* and *D. galavisi*.

The potential existence of two separate lineages for *Dentoglobigerina* would imply that there were potentially two distinct genera as illustrated in Figs 27 and 28, one including the more quadrate and compact '*D.*' *eotripartita*, and another genus characterized by more globular and larger tests of *D. galavisi* and *D. pseudovenezuelana* but still remaining more appressed than for *Subbotina* individuals. A new genus has implications beyond the Eocene and impacts the phylogeny of Oligocene and Miocene forms, including zonal markers, such as *D. altispira*. Tracing the evolution and phylogeny from the mid Eocene through to the Pliocene (30 million years) is beyond the scope of this study, and further work is part of the Neogene planktonic foraminifera working group. Here we place the species *eotripartita* temporality in '*Dentoglobigerina*', pending further investigations. '*Dentoglobigerina*' are typically more compact than co-occurring *Dentoglobigerina* and distinguished from *Acarinina* by the cancellate, non-muricate wall texture. *D. pseudovenezuelana* and *D. galavisi* are still grouped under the genus *Dentoglobigerina* and the *Subbotina* ancestor theory is approved for these forms. Further investigations may reveal that the highly pustulose Oligocene forms, such as *D. sellii*, may also belong within '*Dentoglobigerina*'.

[Insert Figs 27, 28 here]

## The first occurrence in the stratigraphic record

Several studies have shown that *Dentoglobigerina* likely evolved during the middle Eocene with the ancestor *D. galavisi*. Miller *et al.* (1991) estimated its first occurrence at Zone E14/E15 whereas Olsson *et al.* (2006a) reported it at about Zone E13 and Wade *et al.* (2018a) at Zone E12. It has been advised by Wade *et al.* (2018a) that *D. galavisi* could have evolved earlier than thought, probably at Zones E11 and E10. Consequently, this study has looked at older samples ranging from Zone E9 to Zone E11. We find that Eocene *Dentoglobigerina* appears much earlier in the stratigraphic record, in Zone E9. Fig. 24 has correlated selected specimens to the stratigraphic range of past studies made by Olsson *et al.* (2006a) and Wade *et al.* (2018a) and it has been observed that '*D.*' *eotripartita* and *D. pseudovenezuelana* appear in Zone E9. *D. galavisi* appears at the beginning of Zone E11 (Fig. 24).

Consequently, this study updated the stratigraphic range of Eocene *Dentoglobigerina* (taking in account the separation of '*D.*' *eotripartita*) with its first occurrence at Zone E9 with species *D. pseudovenezuelana* and '*D.*' *eotripartita*. Olsson *et al.* (2006a) and Wade *et al.* (2018a) both recognized *D. galavisi* as the first species to have appeared and gave rise to *D. pseudovenezuelana* (in Zones E12 or E14) and later on to '*D.*' *eotripartita* (at the beginning of Zone E14). However, this study results reveal the earlier appearance of *D. pseudovenezuelana* and '*D.*' *eotripartita* compared to *D. galavisi*.

On the basis of these results, this study does now recognize two potential lineages for Eocene *Dentoglobigerina* as illustrated in Figures 27 and 28. One of the lineages would include

'*D.*' *eotripartita*, species that would have evolved from potentially *A. triplex* or *A. primitiva* at Zone E9 at around 44.1 Ma. Another lineage (*Dentoglobigerina*) would include *D. galavisi* and *D. pseudovenezuelana* species that would have evolved from a subbotinid ancestor, likely *S. yeguaensis*. This study considers that *S. yeguaensis* gave rise to *D. pseudovenezuelana* in Zone E9 at around 44.1 Ma. Later, *D. galavisi* would have evolved from *D. pseudovenezuelana* at the beginning of Zone E11 at about 42.3 Ma, hence in our work the ancestral species of *Dentoglobigerina* is *D. pseudovenezuelana* instead of *D. galavisi*.

The presence of both '*D.*' *eotripartita* and *D. pseudovenezuelana* at Zone E9 implies further work is needed to constrain their lower datum, hence the need to look at samples from Zones E7 and E8. To highlight this, we have extended dashed lines back to Zone E7b for both species on Figures 24 and 28. As *D. venezuelana* was observed in sample ODP Sample 763B-3X-5W at Zone E15, the evolution is thus older than in Wade et al. (2018) and suggests the need for updating its stratigraphic range and evaluating potential evolutionary patterns.

**The spine conservation character**

The last objective of this project was to push the research into the Miocene in order to trace the conservation of the spine character in *Dentoglobigerina* as spine holes were identified in Eocene forms. Plates of Miocene forms and their details can be found in the IODP data report Fayolle & Wade (2020).

Several studies have accumulated evidence of spine holes in Oligocene and lower Miocene *Dentoglobigerina* forms. Fox & Wade (2013) represented spine holes in the Miocene species *D. juxtabinaiensis* (Table 2) whereas Pearson & Wade (2015) illustrated spine holes in the species *D. galavisi*, *D. pseudovenezuelana*, '*D.*' *eotripartita* (Table 3), *D. taci* and *D. tapuriensis*. More recently, Wade *et al.* (2018a) accumulated evidence for *D. baroemoenenis*, *D. binaiensis* and *D. larmeui* (Table 2) but did not find such evidence in other species.

The IODP data report (Fayolle & Wade 2020) presents additional evidence of spine holes for *D. baroemoenensis* and first evidence for *D. globosa*. However, spine holes were not observed in *D. venezuelana*, *D. globularis* and *Globoquadrina dehiscens*, which seems to be in accordance with the results obtained by Wade *et al.* (2018a) and Sexton *et al.* (2006). Spine holes were reported on *D. binaiensis* by Wade *et al.* (2018a) but Fayolle and Wade (2020) did not find any.

[Insert Table 2 and 3 here]

In accordance with the present results, previous studies have made the assumption that (1) there could be two clades with convergent morphologies, one spinose and the other non-spinose, or that (2) spines could have been lost through the evolution of *Dentoglobigerina* (Pearson & Wade 2015; Wade *et al.* 2018a). Spine holes were found in species *D. galavisi* and *D. pseudovenezuelana*, similarly to Sexton *et al.* (2006), but were not securely observed in '*D.*' *eotripartita* in this study (Table 3). Pearson & Wade (2015) illustrated spine holes in '*D.*' *eotripartita* in the upper Eocene, Zone E15/E16.

On the basis of these results, it is inferred that *Dentoglobigerina* could be made of two separate clades with converging morphologies, one spinose, evolved from *Subbotina*, with *D. galavisi* and *D. pseudovenezuelana*, and one possibly non-spinose or sparsely spinose, evolved from *Acarinina*, with '*D.*' *eotripartita*. Our study supports to the existence of two separate lineages with two different ancestors and the need for placing '*D.*' *eotripartita* under a different genus from *Dentoglobigerina*. '*D.*' *tripartita* has been established as the descendant of '*D.*' *eotripartita* by Wade *et al.* (2018a), and this implies that '*D.*' *eotripartita* and '*D.*' *tripartita* would both be part of the clade '*Dentoglobigerina*'. Further investigations of Miocene species are required to determine which species also belong within '*Dentoglobigerina*' and the relationship to *Globoquadrina*.

## Conclusions

Through light microscope z-stacking and SEM analysis of Eocene planktonic foraminifera from multiple sites, we find morphological relationships have been established between *Dentoglobigerina* and *Subbotina*, and especially between *D. pseudovenezuelana* and *S. yeguaensis*. To the contrary, '*D.*' *eotripartita* seemed to show closer resemblance with *Acarinina*, potentially with *A. triplex* and *A. primitiva*. The research has also shown evidence of spine holes in the wall texture of several *D. galavisi* and *D. pseudovenezuelana* with large uncertainties remaining for '*D.*' *eotripartita*. We find that '*D.*' *eotripartita* and *D. pseudovenezuelana* appeared before *D. galavisi* in the stratigraphic record at Zone E9 (around 44.1 Ma). In comparison, *D. galavisi* was first observed at the beginning of Zone E11 (around 42.3 Ma). This study contributes to our understanding of *Dentoglobigerina* phylogeny by describing and illustrating potential morphological intermediates between *Acarinina* and *Dentoglobigerina* for the first time. Taken together, our results imply that *D. pseudovenezuelana* evolved from a subbotinid, potentially from *S. yeguaensis*. *D. pseudovenezuelana* is thus the ancestor of *Dentoglobigerina,* and gave rise to *D. galavisi* at the beginning of middle Eocene Zone E11. '*D.*' *eotripartita* evolved from an *Acarinina* ancestor in a separate lineage.

## Acknowledgments

We thank Jim Davy for assistance with Scanning Electron Microscopy and his help during the SEM preparation process; Marcin Latas for help with the z-stacking light microscope; Rehemat

Bhatia for ordering and washing Site 763 samples; Shari Hilding-Kronforst for assistance in fieldwork; and Paul Pearson for comments on an earlier version of this manuscript. This research used samples provided by the International Ocean Discovery Program (IODP) and its predecessors. BW was supported by Natural Environment Research Council grant numbers NE/G014817 and NE/P019013/1. Florent Fayolle acknowledges funding from the Geologists' Association Curry Award.

## References

**Aze, T., Ezard, T.H., Purvis, A., Coxall, H.K., Stewart, D.R., Wade, B.S. & Pearson, P.N.** 2011. A phylogeny of Cenozoic macroperforate planktonic foraminifera from fossil data. *Biological Reviews*, **86**(4), 900-927.

**Bengtson, P.** 1988. Open nomenclature. *Palaeontology*, **31**(1), 223-227.

**Berggren, W. A. & Norris, R. D.** 1997. Biostratigraphy, phylogeny and systematics of Paleocene trochospiral planktic foraminifera. *Micropaleontology*, **43**, supplement 1, 1-116.

**Berggren, W. A., Kent, D.V., Swisher, III, C.C. & Aubry, M.-P.** 1995, A revised Cenozoic geochronology and chronostratigraphy. Pp 129-212 in Berggren W.A., Kent D.V., Aubry M.-P., and Hardenbol, J. (eds.) *Geochronology, Time Scales and Global Stratigraphic Correlation*. Society for Sedimentary Geology (SEPM) Special Publication, **54**.

**Berggren, W.A. & Pearson, P.N.** 2005. Tropical to subtropical planktonic foraminiferal zonation of the Eocene and Oligocene. *Cushman Foundation Special Publication*, **41**, 29-40.

**Berggren, W.A., Pearson, P.N., Huber, B.T. & Wade, B.S.** 2006. Taxonomy, biostratigraphy, and phylogeny of Eocene Acarinina. *Atlas of Eocene Planktonic Foraminifera. Cushman Foundation Special Publication*, **41**, 257-326.

**Bermúdez, P.J.** 1961. Contribucion al estudio de las Globigerinidae de la region Caribe-Antillana (Paleocene-Reciente): Boletino Geologia (Venezuela). *Congres Geologia Venezolano, 3d, Caracas, 1959, Mem.*, **3**, 1119-1393.

**Blow & Banner, F.T.** 1962. The Mid-Tertiary (Upper Eocene to Aquitanian) Globigerinace. Pp 8-17 in Eames, F. T., and others (eds.) *Fundamentals of Mid-Tertiary Stratigraphical Correlations*. Cambridge, Cambridge University Press, **61**.

**Blow, W.H.** 1969. Late Middle Eocene to Recent planktonic foraminiferal biostratigraphy. *Proceedings of the first international conference on planktonic microfossils*. EJ Brill Leiden, **1**, 199-422.

**Blow, W.H.** 1979. *The Cainozoic Globigerinida*. Brill Archive, Atlas **3**, 1413pp

**Bolli, H.M.** 1957. The genera *Globigerina* and *Globorotaria* in Paleocene-Lower Eocene Lizard Spring Formation of Trinidad. *BWI Bulletin of the United States National Museum*, **215**, 61-81.

**Bolli, H.M., & Saunders, J.B.** 1985. Oligocene to Holocene low latitude planktonic foraminifera. Pp 155-262 in Bolli, H.M., Saunders, J.B., and Perch-Nielsen, K. (eds.) *Plankton Stratigraphy*. Cambridge University Press, Cambridge.

**Brönnimann, P. & Resig, J.** 1971. A Neogene globigerinacean biochronologic time-scale of the southwestern Pacific. *Initial Reports of the Deep Sea Drilling Project*, **7**(2), 1235-1469.

**Brotzen, F. & Pozaryska, K.** 1961. Foraminifères du Paléocène et de l'Éocène inférieur en Pologne septentrionale; remarques paléogéographiques. *Revue de Micropaléontologie*, ***4***(3), 155-166.

**Cande, S.C. & Kent, D.V.** 1995. Revised calibration of the geomagnetic polarity timescale for the Late Cretaceous and Cenozoic. *Journal of Geophysical Research: Solid Earth*, **100**(B4), 6093-6095.

**Carpenter, W.B., Parker, W.K. & Jones, T.R.** 1862. *Introduction to the study of the Foraminifera*. Ray society publications, London, 139pp.

**Coxall, H.K.** 2000. *Hantkeninid planktonic foraminifera and Eocene palaeoceanographic change*. PhD thesis, University of Bristol, 254pp.

**d'Orbigny, A.** 1826. Tableau methodique de la classe des Foraminiféres. *Ann. Sci. Nat*, **7**, 245-314.

**Fayolle, F. & Wade, B.S.** 2020. Data report: Miocene planktonic foraminifera *Dentoglobigerina* and *Globoquadrina* from IODP Sites U1489 and U1490 (Expedition 363) in Rosenthal, Y., Holbourn, A.E., Kulhanek, D.K., and the Expedition 363 Scientists, Western Pacific Warm Pool. Proceedings of the International Ocean Discovery Program, 363: College Station, TX (International Ocean Discovery Program). https://doi.org/10.14379/iodp.proc.363.203.2020

**Finlay, H.J.** 1947. New Zealand Foraminifera: Key species in stratigraphy – No. 5. *New Zealand Journal of Science and Technology*, **28**, 259-292.

**Firth, J.V., Eldrett, J.S., Harding, I.C., Coxall, H.K. & Wade, B.S.** 2013. Integrated biomagnetochronology for the Palaeogene of ODP Hole 647A: implications for correlating palaeoceanographic events from high to low latitudes. *Geological Society, London, Special Publications*, **373**(1), 29-78.

**Fleisher, R. L.** 1974. Cenozoic planktonic foraminifera and biostratigraphy, Arabian Sea, Deep Sea Drilling Project, Leg 23A. *Initial Reports of the Deep Sea Drilling Project*, ***23***, 1001-1072.

**Gümbel, C.W.** 1868, Beiträge zur Foraminiferenfauna dernordalpinen, älteren Eocängebilde oder der Kressenberger Nummulitenschichten. *Abhandlungen der K. Bayerische Akademie der Wissenschaften*, Cl. II, **10**, 579-730.

**Fox, L.R. & Wade, B.S.** 2013. Systematic taxonomy of early–middle Miocene planktonic foraminifera from the equatorial Pacific Ocean: Integrated Ocean Drilling Program, Site U1338. *The Journal of Foraminiferal Research*, **43**(4), 374-405.

**Hemleben, C., Spindler, M. & Anderson, O.R.** 1989. *Modern planktonic foraminifera*. Springer, New York , 363pp.

**Hemleben, C., Mühlen, D., Olsson, R.K & Berggren, W.A.** 1991. Surface texture and the first occurrence of spines in planktonic foraminifera from the early Tertiary. *Geologisches Jahrbuch, 128*(A), 117-146.

**Hemleben, C. & Olsson, R.K.** 2006. Wall textures of Eocene planktonic foraminifera. Pp 47-66 in Pearson, P.N., Olsson, R.K., Huber, B.T., Hemleben Ch., and Berggren, W.A. (eds.) *Atlas of Eocene Planktonic Foraminifera*. Cushman Foundation for Foraminiferal Research Special Publication, **41**.

**Huber, B.T.** 1991. *Paleocene and Early Neogene Planktonic Foraminifer Biostratigraphy of Sites 738 and 744, Kerguelen Plateau (Southern Indian Ocean)*. Pp 427-449 in Barron, J., Larsen, B., and others (eds.) *Proceedings of the Ocean Drilling Program.* Scientific Results, College Station, TX, **119**.

**Khalilov, D.M.** 1956. O pelagicheskoy faune foraminifer Paleogenovykh otlozheniy Azerbaydzhana. *Trudy Instituta Geologii, Akademiya Nauk Azerbaydzhanskoy SSR,* **17**, 234-255.

**Koch, R.** 1926. Mitteltertiäre Foraminiferen aus Bulongan, Ost-Borneo. *Eclogae Geologicae Helvetiae*, **19**, 722-751.

**Krasheninnikov, V.A. & Hoskins, R.H.** 1973. Late Cretaceous, Paleogene and Neogene planktonic foraminifera. *Initial Reports of the Deep Sea Drilling Project*, **20**, 105-203.

**Krasheninnikov, V.A. & Plaufmann, U.** 1978. Zonal stratigraphy of Neogene deposits of the eastern part of the Atlantic Ocean by means of planktonic foraminifers, Leg 41 Deep Sea Drilling Project. *Lancelot, Y., Seibold, E., et al., Init. Repts. DSDP*, **41**, 613-657.

**Krasheninnikov, V.A., & Basov, I.A.** 1983. *Cenozoic planktonic foraminifers of the Falkland Plateau and Argentine Basin, Deep Sea Drilling Project Leg 71.* Pp 821-858 in Ludwig, W. J., Krasheninnikov, V. A., and others (eds.) *Initial Reports of the Deep Sea Drilling Project.* U.S. Government Printing Office, Washington, D.C., **71**.

**Miller, K.G., Wright, J.D. & Fairbanks, R.G.** 1991. Unlocking the ice house: Oligocene-Miocene oxygen isotopes, eustasy, and margin erosion. *Journal of Geophysical Research: Solid Earth*, **96**(B4), 6829-6848.

**Olsson, R.K., Berggren, W.A., Hemleben, C.I. & Huber, B.T.** 1999. Atlas of Paleocene planktonic foraminifera. *Smithsonian contributions to Paleobiology*, 252pp.

**Olsson, R.K., Hemleben, C. & Pearson, P.N.** 2006a. *Taxonomy, biostratigraphy and phylogeny of Eocene Dentoglobigerina*. Pp 401-412 in Pearson, P.N., Olsson, R.K., Huber, B.T., Hemleben Ch., and Berggren, W.A. (eds.) *Atlas of Eocene planktonic foraminifera.* Cushman Foundation Special Publication, **41**.

**Olsson, R.K., Hemleben, C., Huber, B.T. & Berggren, W.A.** 2006b. *Taxonomy, biostratigraphy, and phylogeny of Eocene Globigerina, Globoturborotalita, Subbotina, and Turborotalita*. Pp 11-168 in Pearson, P.N., Olsson, R.K., Huber, B.T., Hemleben Ch., and Berggren, W.A. (eds.) *Atlas of Eocene planktonic foraminifera.* Cushman Foundation Special Publication, **41**.

**Pälike, H., Lyle, M., Nishi, H., Raffi, I., Gamage, K., Klaus, A. & Expedition 320/321 Scientists** 2010. *Proceedings of the Integrated Ocean Drilling Program*, 320-321.

**Pearson, P.N., Shackleton, N.J. & Hall, M.A.** 1993. Stable isotope paleoecology of middle Eocene planktonic foraminifera and multi-species isotope stratigraphy, DSDP Site 523, South Atlantic. *The Journal of Foraminiferal Research*, **23**(2), 123-140.

**Pearson, P.N. & Palmer, M.R.** 1999. Middle Eocene seawater pH and atmospheric carbon dioxide concentrations. *Science*, **284**(5421), 1824-1826.

**Pearson, P.N., Ditchfield, P.W., Singano, J., Harcourt-Brown, K.G., Nicholas, C.J., Olsson, R.K., Shackleton, N.J. & Hall, M.A.** 2001. Warm tropical sea surface temperatures in the Late Cretaceous and Eocene epochs. *Nature*, **413**(6855), 481-487.

**Pearson, P.N., Olsson, R.K., Huber, B.T., Hemleben, C. & Berggren, W.A.** 2006. *Atlas of eocene planktonic foraminifera.* Cushman Foundation for Foraminiferal Research Special Publication, Fredericksburg, USA.

**Pearson, P. N., & Berggren, W. A.** 2006. *Taxonomy, biostratigraphy, and phylogeny of Morozovelloides n. gen*. Pp 343-376 in Pearson, P.N., Olsson, R.K., Huber, B.T., Hemleben Ch., and Berggren, W.A. (eds.) *Atlas of Eocene Planktonic Foraminifera.* Cushman Foundation for Foraminiferal Research, Special Publication, **41**.

**Pearson, P.N. & Wade, B.S.** 2015. Systematic taxonomy of exceptionally well-preserved planktonic foraminifera from the Eocene/Oligocene boundary of Tanzania. *Cushman Foundation Special Publication*, **45**, 1-85.

**Plummer, H.J.** 1926. Foraminifera of the Midway Formation in Texas. *University of Texas Bulletin*, **2644**, 1-206.

**Poole, C.R. & Wade, B.S.** 2019. Systematic taxonomy of the Trilobatus sacculifer plexus and descendant *Globigerinoidesella fistulosa* (planktonic foraminifera). *Journal of Systematic Palaeontology*, 17(23), 1989-2030.

**Rosenthal, Y., Holbourn, A.E., Kulhanek, D.K., Aiello, I.W., Babila, T.L., Bayon, G., Beaufort, L., Bova, S.C., Chun, J.H., Dang, H. & Drury, A.J.** 2018. *International Ocean Discovery Program*, **363**.

**Sexton, P.F., Wilson, P.A. & Pearson, P.N.** 2006. Palaeoecology of late middle Eocene planktic foraminifera and evolutionary implications. *Marine Micropaleontology*, **60**(1), 1-16.

**Speijer, R.P., Pälike, H., Hollis, C.J., Hooker, J.J. & Ogg, J.G.** 2020. *The Paleogene period.* Pp 1087-1140 in Ogg, J.G. (eds.) *Geologic Time Scale 2020.* Elsevier.

**Spezzaferri, S. & Silva, I.P.** 1991. Oligocene planktonic foraminiferal biostratigraphy and paleoclimatic interpretation from Hole 538A, DSDP Leg 77, Gulf of Mexico. *Palaeogeography, Palaeoclimatology, Palaeoecology*, **83**(1-3), 217-263.

**Stainforth, R.M.** 1974. Nomenclature of some large Eo-Oligocene globigerinas. Contributions to the geology and paleobiology of the Caribbean and adjacent areas. *Verhandlungen der Naturforschenden Gesellschaft in Basel*, **84**, 256-263.

**Subbotina, N.N.** 1953. Iskopaemye foraminifery SSSR (Globigerinidy, Khantkeninınidy i Globorotaliidy)[Fossil foraminifera of the USSR, Globigerinidae, Hantkeninidae and Globorotaliidae]. *Trudy Vsesoyuznogo Neftyanogo Nauchno-Issledovatel'skogo Geologo-Razvedochnogo Instituta* (*VNIGRI*), **76**, 1-296.

**Wade, B. S., Kroon, D., & Norris, R. D.** 2001. Orbitally forced climate change in late mid-Eocene time at Blake Nose (Leg 171B): Evidence from stable isotopes in foraminifera. *Geological Society, London, Special Publications*, **183**(1), 273-291.

**Wade, B.S.** 2004. Planktonic foraminiferal biostratigraphy and mechanisms in the extinction of *Morozovella* in the late middle Eocene. *Marine Micropaleontology*, **51**(1-2), 23-38.

**Wade, B.S., Pearson, P.N., Berggren, W.A. & Pälike, H.** 2011. Review and revision of Cenozoic tropical planktonic foraminiferal biostratigraphy and calibration to the geomagnetic polarity and astronomical time scale. *Earth-Science Reviews*, **104**(1-3), 111-142.

**Wade, B.S., Pearson, P.N., Olsson, R.K., Fraass, A.J., Leckie, R.M. & Hemleben, C.** 2018a. *Taxonomy, biostratigraphy, and phylogeny of Oligocene and Lower Miocene Dentoglobigerina and Globoquadrina*. Pp 331-384 in Olsson, R.K., Pearson, P.N., Huber, B.T. and Berggren, W.A. (eds.) *Atlas of Oligocene planktonic foraminifera.* Cushman Foundation for Foraminiferal Research Special Publication, ***46***.

**Wade, B.S., Olsson, R.K., Pearson, P.N., Edgar, K.M. & Premoli Silva, I.** 2018b. *Taxonomy, biostratigraphy, and phylogeny of Oligocene Subbotina*. Pp 307-330 in Olsson, R.K., Pearson, P.N., Huber, B.T. and Berggren, W.A. (eds.) *Atlas of Oligocene planktonic foraminifera. Cushman Foundation for Foraminiferal Research* Special Publication, **46**.

**Weinzierl, L.L., & Applin, E.R.** 1929. The Claiborne Formation on the Coastal Domes. *Journal of Paleontology*, **3**, 384- 410.



**Table captions**.

**Table 1.** Biostratigraphic, location and preservation details of selected Eocene samples along with their sites and age. The age timescale is given in millions of years (Ma) and is calibrated to both Cande & Kent (1995) and GTS2020 (Speijer *et al.* 2020). See Table 4 in the Supplementary Online Materials for age references. 'W. *et al.* (2011)' stands for Wade *et al.* (2011), 'C&K' stands for Cande & Kent and 'PF' for planktonic foraminifera.

**Table 2.** Accumulated evidence for the presence of spines holes in the wall texture of Miocene *Dentoglobigerina* forms and its descendant *Globoquadrina dehiscens*. In comparison with previous work made on Oligocene and Miocene forms of *Dentoglobigerina* (Fox & Wade 2013; Wade *et al.* 2018a). Blank box means the relevant species was not observed in the study.

**Table 3 .** Accumulated evidence for the presence of spines holes in the wall texture of Eocene *Dentoglobigerina* forms. In comparison with previous work made on Eocene forms of *Dentoglobigerina* (Sexton *et al.* 2006; Olsson *et al.* 2006a; Pearson & Wade 2015). Blank box means the relevant species was not observed in the study.



**Figure Captions**

**Figure 1.** Chronology of the phylogenetic and taxonomic work accomplished on Eocene *Dentoglobigerina* since 1957. The upper box relates the changes at Family level and the lower box the changes at Genus level.

**Figure 2.** Schematic diagram of the two ancestor theories for the genus *Dentoglobigerina* including SEMs of *Dentoglobigerina*, *Acarinina* and *Subbotina* and the accumulated wall texture evidence: the *Acarinina* ancestor theory according to Olsson *et al.* (2006) and the *Subbotina* ancestor theory according to Wade *et al.* (2018a) and Pearson & Wade (2015). The spine holes are highlighted by white or black circles. **(A)** *A. mcgowrani* (Berggren *et al.* 2006: 293, pl. 9.13, figs 13-14); **(B)** *D. galavisi* (Olsson *et al.* 2006a: 405: pl. 13.1, figs 12 & 16); **(C)** *D. eotripartita* (Olsson *et al.* 2006a: 409, pl. 13.3, fig. 12); **(D)** *D. pseudovenezuelana* (Olsson *et al.* 2006a: 407, pl. 13.2, figs 3-4); **(E)** *S. yeguaensis* (Olsson *et al.* 2006b: 152, pl. 6.18, fig. 10 & 16); **(F)** *D. galavisi* (Pearson & Wade 2015: 55, fig. 15.7a-7b); **(G)** *D. pseudovenezuelana*

(Pearson & Wade 2015: 59, fig. 17.6a & 6d); **(H)** *D. eotripartita* (Pearson & Wade 2015: 67, fig. 21.4a & 4e). The zonation is from Wade *et al.* (2011) and the polarity time scale is from Cande & Kent (1995). Note that '*D. pseudo.*' is the chosen abbreviation for *D. pseudovenezuelana*.

**Figure 3.** Location map showing sites from this study from the Eocene (black star symbols) and Miocene (black dot symbols) time intervals.

**Figure 4.** The three states of preservation in planktonic foraminiferal test and their wall texture based on z-stacker and SEM images. **(A, B, C)** Good preservation state of a Miocene *D. binaiensis* test from IODP sample U1489D-27X-CC available in Fayolle & Wade (2020). In SEM, the pore and pore intersection are clearly visible, smooth and unfilled both in test and wall texture images. In z-stacker light, the test is translucent, and the pores are visible especially in spiral view. **(D, E, F)** Fair preservation state of an Eocene *D. pseudovenezuelana* test from ODP sample 865C-3H-5 (see Fig. 12K-S). The pore and pore intersections are clearly visible but partially infilled and affected by recrystallisation in some areas, but true spine holes are identifiable. In z-stacker light, the test is opaque and white whereas in SEM light, the aperture is identifiable, and pores are well preserved. **(G, H, I)** Poor preservation state of an Eocene *D. galavisi* test from ODP sample 763B-6X-5W (see Fig. 8I-O). In SEM, the pores and pore intersections are obscured, and the test is affected in all parts making it hard to discern any wall texture feature. In the z-stacker light microscope, the test is opaque. White circles denote evidence of spine holes.

**Figure 5.** Our approach to assessing morphological features analogous to spine holes and splitting them into two categories: 'Evidence of spine holes' and 'No evidence of spine holes'.

**(A)** two large and well-rounded spine holes in the wall texture of a *Dentoglobigerina pseudovenezuelana* specimen from ODP Sample 865C-7H-3 (Fig. 13J); **(B)** one slit shaped and enlarged spine hole in the wall texture of a Subbotina sp. 1 specimen from ODP Sample 865C-7H-3 (Fig.17T); **(C)** a large and well-rounded spine hole in the wall texture (fair preservation) of a *Dentoglobigerina galavisi* specimen from ODP Sample 865C-4H-6 (Fig. 6O); **(D)** three slightly slit shaped spine holes in the wall texture of a *Dentoglobigerina galavisi* specimen from ODP Sample 1263B-7H-5W (Fig. 9H); **(E)** one potential and slightly slit-like spine hole in the wall texture of a '*D.*' *eotripartita* specimen from ODP Sample 865C-4H-2 (Fig. 20Q); **(F)** one potential and slit-like spine hole in the wall texture of a '*D.*' *eotripartita* specimen from ODP Sample 865C-4H-2 (Fig. 20H); **(G)** one potential, slit-like and elongated spine hole in the wall texture of a '*D.*' *eotripartita* specimen from ODP Sample 865C-7H-3 (Fig. 22H). White circles denote 'Evidence of spine holes' and dashed white circles denote potential spine holes that do not classify for 'Evidence of spine holes'.

**Figure 6.** *Dentoglobigerina galavisi* **(NHMUK PM PF XXXXX, A-H)**, ODP Sample 1052B-12H-5, 3-6 cm, middle Eocene Zone E13, Blake Nose, western North Atlantic Ocean: Z-stacker images of **(A)** umbilical view, **(B)** edge view, **(C)** spiral view; SEM images of **(D)** umbilical view, **(E)** edge view, **(F)** spiral view; Wall texture SEM images of **(G)** edge view, **(H)** spiral view. Evidence of spine holes. Scale bars: 100 µm (whole specimens) and 10 µm (close-up images). *Dentoglobigerina galavisi* **(NHMUK PM PF XXXXX, I-O)**, ODP Sample 865C-4H-6, 63-65 cm, middle Eocene Zone E13, Allison Guyot, western Pacific Ocean: Z-stacker images of **(I)** umbilical view, **(J)** edge view, **(K)** spiral view; SEM images of **(L)** umbilical view, edge view not obtained, **(M)** spiral view; Wall texture SEM images of **(N)** umbilical view and **(O)** spiral view. Evidence of a spine hole. Scale bars: 100 µm (whole specimens) and 10 µm (close-up images). White circles denote evidence of spine holes.

**Figure 7.** *Dentoglobigerina galavisi* **(NHMUK PM PF XXXXX, A-H)**, ODP Sample 763B-2X-5W, 120-122 cm, upper Eocene Zone E16, Exmouth Plateau, Indian Ocean: Z-stacker images of **(A)** umbilical view, **(B)** edge view, **(C)** spiral view; SEM images of **(D)** umbilical view, **(E)** edge view, **(F)** spiral view; Wall texture SEM images of **(G)** edge view, **(H)** spiral view. Evidence of spine holes. Scale bars: 100 µm (whole specimens) and 10 µm (close-up images). *Dentoglobigerina galavisi* **(NHMUK PM PF XXXXX, I-P)**, ODP Sample 763B-4X-3W, 46-48 cm, upper Eocene Zone E15, Exmouth Plateau, Indian Ocean: Z-stacker images of **(I)** umbilical view, **(J)** edge view, **(K)** spiral view; SEM images of **(L)** umbilical view, **(M)** edge view, **(N)** spiral view; Wall texture SEM images of **(O)** umbilical view, **(P)** spiral view. Evidence of spine holes. Scale bars: 100 µm (whole specimens) and 10 µm (close-up images). White circles denote evidence of spine holes.

**Figure 8.** *Dentoglobigerina galavisi* **(NHMUK PM PF XXXXX, A-J)**, ODP Sample 763B-4X-3W, 46-48 cm, upper Eocene Zone E15, Exmouth Plateau, Indian Ocean: Z-stacker images of **(A)** umbilical view, **(B)** edge view, **(C)** spiral view; SEM images of **(D)** umbilical view, **(E)** edge view, **(F)** spiral view; Wall texture SEM images of **(G)** umbilical view, **(H)** edge view, **(I)** edge view, **(J)** spiral view. Evidence of spine holes. Scale bars: 100 µm (whole specimens) and 10 µm (close-up images). *Dentoglobigerina galavisi* **(NHMUK PM PF XXXXX, K-T)**, ODP Sample 763B-5X-2W, 55-57 cm, upper Eocene Zone E14, Exmouth Plateau, Indian Ocean: Z-stacker images of **(K)** umbilical view, **(L)** edge view, **(M)** spiral view; SEM images of **(N)** umbilical view, **(O)** edge view, **(P)** spiral view; Wall texture SEM images of **(Q)** umbilical view, **(R)** umbilical view, **(S)** spiral view, **(T)** spiral view. No evidence of spine holes.

Scale bars: 100 µm (whole specimens) and 10 µm (close-up images). White circles denote evidence of spine holes.

**Figure 9**. *Dentoglobigerina galavisi* **(NHMUK PM PF XXXXX, A-H)**, ODP Sample 1263B-7H-5W, 138-140 cm, middle Eocene Zone E13, Walvis Ridge eastern South Atlantic Ocean: Z-stacker images of **(A)** umbilical view, **(B)** edge view, **(C)** spiral view; SEM images of **(D)** umbilical view, **(E)** edge view, **(F)** spiral view; Wall texture SEM images of **(G)** umbilical view, **(H)** spiral view. Evidence of spine holes. Scale bars: 100 µm (whole specimens) and 10 µm (close-up images). *Dentoglobigerina galavisi* **(NHMUK PM PF XXXXX, I-O)**, ODP Sample 763B-6X-5W, 42-44 cm, middle Eocene Zone E11, Exmouth Plateau, Indian Ocean: Z-stacker images of **(I)** umbilical view, **(J)** edge view, **(K)** spiral view; SEM images of **(L)** umbilical view, **(M)** edge view, **(N)** spiral view; Wall texture SEM image of **(O)** spiral view. No evidence of spine holes. Scale bars: 100 µm (whole specimens) and 10 µm (close-up image). White circles denote evidence of spine holes.

**Figure 10**. *Dentoglobigerina pseudovenezuelana* **(NHMUK PM PF XXXXX, A-I)**, ODP Sample 1052B-10H-6, 13-16 cm, upper Eocene Zone E14, Blake Nose, western North Atlantic Ocean: Z-stacker images of **(A)** umbilical view, **(B)** edge view, **(C)** spiral view; SEM images of **(D)** umbilical view, **(E)** edge view, **(F)** spiral view; Wall texture SEM image of **(G)** umbilical view, **(H)** edge view and **(I)** spiral view. Evidence of spine holes. Scale bars: 100 µm (whole specimens) and 10 µm (close-up images). *Dentoglobigerina pseudovenezuelana* **(NHMUK PM PF XXXXX, J-R)**, ODP Sample 1052B-10H-6, 13-16 cm, upper Eocene Zone E14, Blake Nose, western North Atlantic Ocean: Z-stacker images of **(J)** umbilical view, **(K)** edge view, **(L)** spiral view; SEM images of **(M)** umbilical view, **(N)** edge view, **(O)** spiral view; Wall texture SEM image of **(P)** umbilical view, **(Q)** edge view and **(R)** spiral view. No evidence of

spine holes. Scale bars: 100 µm (whole specimens) and 10 µm (close-up images). White circles denote evidence of spine holes.

**Figure 11.** *Dentoglobigerina pseudovenezuelana* **(NHMUK PM PF XXXXX, A-J)**, ODP Sample 1263B-8H-5W, 139-141 cm, middle Eocene Zone E13, eastern South Atlantic Ocean: Z-stacker images of **(A)** umbilical view, **(B)** edge view, **(C)** spiral view; SEM images of **(D)** umbilical view, **(E)** edge view, **(F)** spiral view; Wall texture SEM image of **(G)** umbilical view, **(H)** umbilical view, **(I)** edge view, **(J)** spiral view. Evidence of spine holes. Scale bars: 100 µm (whole specimens) and 10 µm (close-up images). *Dentoglobigerina pseudovenezuelana* **(NHMUK PM PF XXXXX, K-S)**, ODP Sample 865C-3H-5, 110-112 cm, upper Eocene Zone E15, Allison Guyot, western Pacific Ocean: Z-stacker images of **(K)** umbilical view, **(L)** edge view, **(M)** spiral view; SEM images of **(N)** umbilical view, **(O)** edge view, **(P)** spiral view; Wall texture SEM image of **(Q)** umbilical view, **(R)** edge view and **(S)** spiral view. Evidence of spine holes. Scale bars: 100 µm (whole specimens) and 10 µm (close-up images). White circles denote evidence of spine holes.

**Figure 12.** *Dentoglobigerina pseudovenezuelana* **(NHMUK PM PF XXXXX, A-J)**, ODP Sample 865C-3H-6, 46-48 cm, upper Eocene Zone E15, Allison Guyot, western Pacific Ocean: Z-stacker images of **(A)** umbilical view, **(B)** edge view, **(C)** spiral view; SEM images of **(D)** umbilical view, **(E)** edge view, **(F)** spiral view; Wall texture SEM image of **(G)** umbilical view (pustulose tooth), **(H)** umbilical view, **(I)** edge view, **(J)** spiral view. Evidence of spine holes. Scale bars: 100 µm (whole specimens) and 10 µm (close-up images). *Dentoglobigerina pseudovenezuelana* (**NHMUK PM PF XXXXX, K-T**), ODP Sample 865C-3H-6, 46-48 cm, upper Eocene Zone E15, Allison Guyot, western Pacific Ocean: Z-stacker images of (**K**) umbilical view, (**L**) edge view, (**M**) spiral view; SEM images of (**N**) umbilical view, (**O**) edge view, (**P**) spiral view; Wall texture SEM image of (**Q**) umbilical view, (**R**) edge view, (**S**) spiral

view, (**T**) spiral view. No evidence of spine holes. Scale bars: 100 µm (whole specimens) and 10 µm (close-up images). White circles denote evidence of spine holes.

**Figure 13.** *Dentoglobigerina pseudovenezuelana* **(NHMUK PM PF XXXXX, A-K)**, ODP Sample 865C-7H-3, 110-11 cm, middle Eocene Zone E9, Allison Guyot, western Pacific Ocean: Z-stacking images of **(A)** umbilical view, **(B)** edge view, **(C)** spiral view; SEM images of **(D)** umbilical view, **(E)** edge view, **(F)** spiral view; Wall texture SEM image of **(G)** umbilical view, **(H)** edge view, **(I, J)** spiral view, **(K)** edge view (pustules in the apertural region). Evidence of spine holes. Scale bars: 100 µm (whole specimens) and 10 µm (close-up images). *Dentoglobigerina pseudovenezuelana* **(NHMUK PM PF XXXXX, L-R)**, ODP Sample 763B-5X-2W, 55-57 cm, upper Eocene Zone E14, Exmouth Plateau, Indian Ocean: Z-stacking images of **(L)** umbilical view, **(M)** edge view, **(N)** spiral view; SEM images of **(O)** umbilical view, edge view not obtained, **(P)** spiral view; Wall texture SEM image of **(Q)** umbilical view, **(R)** spiral view. Evidence of spine holes. Scale bars: 100 µm (whole specimens) and 10 µm (close-up images). White circles denote evidence of spine holes.

**Figure 14.** *Subbotina yeguaensis* **(NHMUK PM PF XXXXX, A-H)**, ODP Sample 763B-6X-5W, 42-44 cm, middle Eocene Zone E11, Exmouth Plateau, Indian Ocean: Z-stacker images of **(A)** umbilical view, **(B)** edge view, **(C)** spiral view; SEM images of **(D)** umbilical view, **(E)** edge view, **(F)** spiral view; Wall texture SEM image of **(G)** umbilical view, **(H)** umbilical view. Evidence of spine holes. Scale bars: 100 µm (whole specimens) and 10 µm (close-up images). *Subbotina yeguaensis* **(NHMUK PM PF XXXXX, I-Q)**, ODP Sample 763B-6X-5W, 42-44 cm, middle Eocene Zone E11, Exmouth Plateau, Indian Ocean: Z-stacker images of **(I)** umbilical view, **(J)** edge view, **(K)** spiral view; SEM images of **(L)** umbilical view, **(M)** edge view, **(N)** spiral view; Wall texture SEM image of **(O)** umbilical view, **(P)** edge view, **(Q)** spiral

view. Evidence of spine holes. Scale bars: 100 µm (whole specimens) and 10 µm (close-up images). White circles denote evidence of spine holes.

**Figure 15.** *Subbotina* cf. *S. yeguaensis* **(NHMUK PM PF XXXXX, A-F)**, ODP Sample 1263B-8H-5W, 139-141 cm, middle Eocene Zone E13, Walvis Ridge, eastern Atlantic Ocean: Z-stacker images of **(A)** umbilical view, **(B)** edge view, **(C)** spiral view; SEM images of **(D)** umbilical view, **(E)** edge view, **(F)** spiral view; Wall texture SEM image of **(G)** umbilical view, **(H)** spiral view. No evidence of spine holes. Scale bars: 100 µm (whole specimens) and 10 µm (close-up images). *Subbotina* cf. *S. yeguaensis* **(NHMUK PM PF XXXXX, I-R)**, ODP Sample 865C-3H-6, 46-48 cm, upper Eocene Zone E15, Allison Guyot, western Pacific Ocean: Z-stacker images of **(I)** umbilical view, **(J)** edge view, **(K)** spiral view; SEM images of **(L)** umbilical view, **(M)** edge view, **(N)** spiral view; Wall texture SEM image of **(O)** umbilical view, **(P)** edge view, **(Q)** edge view, **(R)** spiral view. Evidence of spine holes. Scale bars: 100 µm (whole specimens) and 10 µm (close-up images). White circles denote evidence of spine holes.

**Figure 16.** *Subbotina* cf. *S. yeguaensis* **(NHMUK PM PF XXXXX, A-F)**, ODP Sample 865C-4H-6, 63-65 cm, middle Eocene Zone E13, Allison Guyot, western Pacific Ocean: Z-stacker images of **(A)** umbilical view, **(B)** edge view, **(C)** spiral view; SEM images of **(D)** umbilical view, edge view not obtained, **(E)** spiral view; Wall texture SEM image of **(F)** spiral view. Evidence of spine holes. Scale bars: 100 µm (whole specimens) and 10 µm (close-up image). *Subbotina* cf. *S. eocaena* **(NHMUK PM PF XXXXX, G-P)**, ODP Sample 763B-6X-6W, 53-55 cm, middle Eocene Zone E10, Exmouth Plateau, Indian Ocean: Z-stacker images of **(G)** umbilical view, **(H)** edge view, **(I)** spiral view; SEM images of **(J)** umbilical view, **(K)** edge view, **(L)** spiral view; Wall texture SEM images of **(M)** umbilical view, (N) the tooth in

umbilical view, **(O)** edge view, **(P)** spiral view. Evidence of spine holes. Scale bars: 100 µm (whole specimens) and 10 µm (close-up images). White circles denote evidence of spine holes.

**Figure 17.** *Subbotina* sp. 1 **(NHMUK PM PF XXXXX, A-J)**, ODP Sample 865C-7H-3, 110-112 cm, middle Eocene Zone E9, Allison Guyot, western Pacific Ocean: Z-stacker images of **(A)** umbilical view, **(B)** edge view, **(C)** spiral view; SEM images of **(D)** umbilical view, **(E)** edge view, **(F)** spiral view; Wall texture SEM image of **(G)** edge view, **(H)** edge view, **(I)** spiral view, **(J)** spiral view. Evidence of spine holes. Scale bars: 100 µm (whole specimens) and 10 µm (close-up images). *Subbotina* sp. 1 **(NHMUK PM PF XXXXX, K-T)**, ODP Sample 865C-7H-3, 110-112 cm, middle Eocene Zone E9, Allison Guyot, western Pacific Ocean: Z-stacker images of **(K)** umbilical view, **(L)** edge view, **(M)** spiral view; SEM images of **(N)** umbilical view, **(O)** edge view, **(P)** spiral view; Wall texture SEM image of **(Q)** umbilical view, **(R)** edge view, **(S)** edge view, **(T)** spiral view. Evidence of spine holes. Scale bars: 100 µm (whole specimens) and 10 µm (close-up images). White circles denote evidence of spine holes.

**Figure 18.** ?*Subbotina* or ?*Dentoglobigerina* **(NHMUK PM PF XXXXX, A-H)**, ODP Sample 865C-7H-3, 110-112 cm, middle Eocene Zone E9, Allison Guyot, western Pacific Ocean: Z-stacker images of **(A)** umbilical view, **(B)** edge view, **(C)** spiral view; SEM images of **(D)** umbilical view, **(E)** edge view, **(F)** spiral view; Wall texture SEM image of **(G)** umbilical view, **(H)** edge view. Evidence of spine holes. Scale bars: 100 µm (whole specimens) and 10 µm (close-up images). White circles denote evidence of spine holes.

**Figure 19.** '*Dentoglobigerina*' *eotripartita* **(NHMUK PM PF XXXXX, A-H)**, Sample BW10-M1-2, upper Eocene, Zone E16, Shubuta Clay, Wayne County, Mississippi: Z-stacker images of **(A)** umbilical view, **(B)** edge view, **(C)** spiral view; SEM images of **(D)** umbilical view, **(E)**

edge view, **(F)** spiral view; Wall texture SEM images of **(G)** umbilical view, **(H)** spiral view. No evidence of spine holes. Scale bars: 100 µm (whole specimens) and 10 µm (close-up images). '*Dentoglobigerina*' *eotripartita* **(NHMUK PM PF XXXXX, I-P)**, ODP Sample 865C-3H-5, 110-112 cm, upper Eocene Zone E15, Allison Guyot, western Pacific Ocean: Z-stacking images of **(I)** umbilical view, **(J)** edge view, **(K)** spiral view; SEM images of **(L)** umbilical view, **(M)** edge view, **(N)** spiral view; Wall texture SEM images of **(O)** umbilical view, **(P)** spiral view. No evidence of spine holes. Scale bars: 100 µm (whole specimens) and 10 µm (close-up images).

**Figure 20**. '*Dentoglobigerina*' *eotripartita* **(NHMUK PM PF XXXXX, A-H)**, ODP Sample 865C-4H-2, 110-112 cm, upper Eocene Zone E14, Allison Guyot, western Pacific Ocean: Z-stacker images of **(A)** umbilical view, **(B)** edge view, **(C)** spiral view; SEM images of **(D)** umbilical view, **(E)** edge view, **(F)** spiral view; Wall texture SEM images of **(G)** umbilical view, **(H)** spiral view. White dashed circle denotes evidence of a potential spine holes. Scale bars: 100 µm (whole specimens) and 10 µm (close-up images). '*Dentoglobigerina*' *eotripartita* **(NHMUK PM PF XXXXX, I-Q)**, ODP Sample 865C-4H-2, 110-112 cm, upper Eocene Zone E14, Allison Guyot, western Pacific Ocean: Z-stacker images of **(I)** umbilical view, **(J)** edge view, **(K)** spiral view; SEM images of **(L)** umbilical view, **(M)** edge view, **(N)** spiral view; Wall texture SEM images of **(O)** umbilical view, **(P)** edge view, **(Q)** spiral view. White dashed circle denotes evidence of a potential spine holes. Scale bars: 100 µm (whole specimens) and 10 µm (close-up images).

**Figure 21**. '*Dentoglobigerina*' *eotripartita* **(NHMUK PM PF XXXXX, A-H)**, ODP Sample 865C-4H-6, 63-65 cm, middle Eocene Zone E13, Allison Guyot, western Pacific Ocean: Z-stacker images of **(A)** umbilical view, **(B)** edge view, **(C)** spiral view; SEM images of **(D)**

umbilical view, **(E)** edge view, **(F)** spiral view; Wall texture SEM images **(G)** spiral view, **(H)** spiral view. No evidence of spine holes. Scale bars: 100 µm (whole specimens) and 10 µm (close-up images). '*Dentoglobigerina*' *eotripartita* **(NHMUK PM PF XXXXX, I-P)**, ODP Sample 865C-7H-3, 110-112 cm, middle Eocene Zone E9, Allison Guyot, western Pacific Ocean: Z-stacker images of **(I)** umbilical view, **(J)** edge view, **(K)** spiral view; SEM images of **(L)** umbilical view, **(M)** edge view, **(N)** spiral view; Wall texture SEM images of **(O)** umbilical view, **(P)** spiral view. No evidence of spine holes. Scale bars: 100 µm (whole specimens) and 10 µm (close-up images).



**Figure 22.** '*Dentoglobigerina*' *eotripartita* **(NHMUK PM PF XXXXX, A-H)**, ODP Sample 865C-7H-3, 110-112 cm, middle Eocene Zone E9, Allison Guyot, western Pacific Ocean: Z-stacker images of **(A)** umbilical view, **(B)** edge view, **(C)** spiral view; SEM images of **(D)** umbilical view, **(E)** edge view, **(F)** spiral view; Wall texture SEM images of **(G)** umbilical view, **(H)** spiral view. White dashed circle denotes evidence of a potential spine holes. Scale bars: 100 µm (whole specimens) and 10 µm (close-up images). *Acarinina mcgowrani* (**NHMUK PM PF XXXXX, I-R)**, ODP Sample 865C-8H-3, 70-72 cm, middle Eocene Zone E9, Allison Guyot, western Pacific Ocean: Z-stacker images of **(I)** umbilical view, **(J)** edge view, **(K)** spiral view; SEM images of **(L)** umbilical view, **(M)** edge view, **(N)** spiral view; Wall texture SEM image of **(O)** umbilical view, **(P)** umbilical view, **(Q)** edge view, **(R)** spiral view. No evidence of spine holes. Scale bars: 100 µm (whole specimens) and 10 µm (close-up images).

**Figure 23.** *Acarinina* cf. *A. triplex* **(NHMUK PM PF XXXXX, A-J)**, ODP Sample 865C-8H-3, 70-72 cm, middle Eocene Zone E9, Allison Guyot, western Pacific Ocean: Z-stacker images of **(A)** umbilical view, **(B)** edge view, **(C)** spiral view; SEM images of **(D)** umbilical view, **(E)**

edge view, **(F)** spiral view; Wall texture SEM image of **(G)** pustules in umbilical view, **(H)** edge view, **(I)** edge view, **(J)** spiral view. No evidence of spine holes. Scale bars: 100 µm (whole specimens) and 10 µm (close-up images). *Acarinina* cf. *A. primitiva* **(NHMUK PM PF XXXXX, K-S)**, ODP Sample 763B-6X-6W, 53-55 cm, middle Eocene Zone E10, Exmouth Plateau, Indian Ocean: Z-stacker images of **(K)** umbilical view, **(L)** edge view, **(M)** spiral view; SEM images of **(N)** umbilical view, **(O)** edge view, **(P)** spiral view; Wall texture SEM images of **(Q)** edge view, **(R)** spiral view, **(S)** tooth image in umbilical view. No evidence of spine holes. Scale bars: 100 µm (whole specimens) and 10 µm (close-up images).

**Figure 24.** Updated stratigraphic range of Eocene *Dentoglobigerina* and comparison with Olsson *et al*. (2006a) and Wade *et al.* (2018a) using the Planktonic Foraminiferal Zonation of the Eocene by Berggren & Pearson (2005) and Wade *et al.* (2011). **(A)** green triangles for selected specimens of *D. galavisi*; **(B)** blue circles for specimens of '*Dentoglobigerina*' *eotripartita*; **(C)** red squares for specimens of *D. pseudovenezuelana*; **(D)** purple diamonds for morphological intermediates between *Dentoglobigerina* and *Subbotina*; (E) orange pentagons for morphological intermediates between '*Dentoglobigerina*' and *Acarinina*; (F) grey stars for *S. yeguaensis*; (G) the grey trapeze for *Subbotina* cf. *S. eocaena*; (H) the orange square for *A. mcgowrani*. 'D.' refers to '*Dentoglobigerina*'.

**Figure 25.** SEM images of '*D.*' *eotripartita* specimens and morphological intermediates with *Acarinina* to infer morphological similarities between the two taxa: **(A)** NHMUK PM PF XXXXX – Fig. 18A-H, Shubuta FM, Zone E16; **(B)** NHMUK PM PF XXXXX – Fig. 18I-P, Allison Guyot, western Pacific Ocean, Zone E15; **(C)** NHMUK PM PF XXXXX – Fig. 19A-H, Allison Guyot, western Pacific Ocean, Zone E14; **(D)** NHMUK PM PF XXXXX – Fig. 19I-Q, Allison Guyot, western Pacific Ocean, Zone E14; **(E)** NHMUK PM PF XXXXX – Fig. 20A-

H, Allison Guyot, western Pacific Ocean, Zone E13; **(F)** NHMUK PM PF XXXXX – Fig. 20I-P, Allison Guyot, western Pacific Ocean, Zone E9; **(G)** NHMUK PM PF XXXXX – Fig. 21A-H, Allison Guyot, western Pacific Ocean, Zone E9; **(H)** NHMUK PM PF XXXXX – Fig. 22K-S, Exmouth Plateau, Indian Ocean, Zone E10; **(I)** NHMUK PM PF XXXXX – Fig. 22A-J, Allison Guyot, western Pacific Ocean, Zone E9; **(J)** NHMUK PM PF XXXXX – Figure 21I-R Allison Guyot, western Pacific Ocean, Zone E9. Green box = Acarinina genus; red box = morphological intermediates; blue box = '*Dentoglobigerina*' genus.

**Figure 26.** SEM images of *D. pseudovenezuelana*, *D. galavisi*, *S. yeguaensis* and morphological intermediates with *Subbotina*: **(A)** NHMUK PM PF XXXXX – Fig. 6A-H, Exmouth Plateau, Indian Ocean, Zone E15; **(B)** NHMUK PM PF XXXXX – Fig. 8I-O, Exmouth Plateau, Indian Ocean, Zone E11; **(C)** NHMUK PM PF XXXXX – Fig. 11A-J, Allison Guyot, western Pacific Ocean, Zone E15; **(D)** NHMUK PM PF XXXXX – Fig. 14A-H, Walvis Ridge eastern Atlantic Ocean, Zone E13; **(E)** NHMUK PM PF XXXXX – Fig. 14I-R, Allison Guyot, western Pacific Ocean, Zone E15; **(F)** NHMUK PM PF XXXXX – Figure 15A-F, Allison Guyot, western Pacific Ocean, Zone E13; **(G)** NHMUK PM PF XXXXX – Fig. 15G-P, Exmouth Plateau, Indian Ocean, Zone E10; **(H)** NHMUK PM PF XXXXX – Fig. 16A-J, Allison Guyot, western Pacific Ocean, Zone E9; **(I)** NHMUK PM PF XXXXX – Fig. 16K-T, Allison Guyot, western Pacific Ocean, Zone E9; **(J)** NHMUK PM PF XXXXX – Fig. 17, Allison Guyot, western Pacific Ocean, Zone E9; **(K)** NHMUK PM PF XXXXX – Fig. 13A-H, Exmouth Plateau, Indian Ocean, Zone E11; **(L)** NHMUK PM PF XXXXX – Fig. 13I-Q, Exmouth Plateau, Indian Ocean, Zone E11. Green box = *Subbotina yeguaensis*; red box = morphological intermediates; blue box = *Dentoglobigerina* genus.

**Figure 27.** Proposed phylogenetic relationships between *Dentoglobigerina*, *Acarinina* and

*Subbotina* and comparison with previous relationships proposed by Olsson *et al.* (2006a) and Wade *et al.* (2018a); use of the Planktonic Foraminiferal Zonation of Wade *et al.* (2011). Illustration of the supposedly spinose and non-spinose lineages of *Dentoglobigerina*. Question marks are placed where the evolutionary pattern between two taxa remains hypothetical. Dashed lines indicate uncertain stratigraphic ranges. 'Dento.' = *Dentoglobigerina* and 'D.' = '*Dentoglobigerina*'.

**Figure 28.** The two proposed lineages, including SEMs of selected specimens of *Dentoglobigerina*, *Acarinina*, *Subbotina* and potential intermediate specimens. The zonation is from Wade *et al.* (2011). The dashed lines represent hypothetical extensions of the stratigraphic range of taxa to earlier ages. The polarity time scale is from Cande & Kent (1995). White circles denote evidence of spine holes.

| Leg/ Field trip | Site/ Hole | Core/ Type/ Section | Interval (cm) | Depth (mbsf) | PF Zone | Preser-vation | C&K Age (Ma) | GTS2020 Age (Ma) |
|---|---|---|---|---|---|---|---|---|
| **105** | 647A | 35R-2 | 24-27 | 329.04 | E15 | Good | 34.35 | 34.70 |
| **105** | 647A | 36R-1 | 19-22 | 339.45 | E15 | Good | 34.4 | 34.75 |
| **122** | 763B | 2X-5W | 120-122 | 198.46 | E16 | Fair | 34 | 34.25 |
| **122** | 763B | 3X-5W | 145-147 | 208.25 | E16 | Fair | 34.1 | 34.3 |
| **122** | 763B | 4X-3W | 46-48 | 217.46 | E15 | Fair | 35 | 35.35 |
| **122** | 763B | 5X-2W | 55-57 | 222.3 | E14 | Good | 37.5 | 37.5 |
| **122** | 763B | 6X-5W | 42-44 | 234.74 | E11 | Fair | 42.3 | 41.9 |
| **122** | 763B | 6X-6W | 53-55 | 236.49 | E10 | Poor | 42.8 | 42.8 |
| **143** | 865C | 3H-5 | 110-112 | 18.9 | E15 | Fair | 34.8 | 35.25 |
| **143** | 865C | 3H-6 | 46-48 | 20.4 | E15 | Fair | 35.2 | 35.5 |
| **143** | 865C | 4H-2 | 110-112 | 22.50-32 | E14 | Fair | 37.6 | 37.53 |
| **143** | 865C | 4H-6 | 63-65 | 29.90 | E13 | Fair | 39.7 | 39.7 |
| **143** | 865C | 5H-6 | 70-72 | 40-41.5 | E11 | Poor | 41.4 | 41.1 |
| **143** | 865C | 7H-3 | 110-112 | 54.80 | E9 | Fair | 44.1 | 43.5 |
| **143** | 865C | 8H-3 | 70-72 | 63.40 | E9 | Fair | 44.3 | 43.9 |
| **171B** | 1052B | 10H-6 | 13-16 | 79.75 | E14 | Fair | 37.55 | 37.55 |
| **171B** | 1052B | 12H-5 | 3-6 | 97.05 | E13 | Fair | 38.11 | 38.11 |
| **208** | 1263B | 7H-5W | 138-140 | 103.00 | E13 | Fair | 38.1 | 38.1 |
| **208** | 1263B | 8H-5W | 139-141 | 112.50 | E13 | Poor | 39.2 | 39.2 |
| **208** | 1263B | 9H-5W | 139-141 | 122.00 | E11 | Fair | 41.5 | 41.2 |
| **Shubuta Formation** | BW10 | M1-2 | | | E16 | Fair | 33.8 | 34.1 |

**Table 1.** Biostratigraphic, location and preservation details of selected Eocene samples along with their sites and age. The age timescale is given in millions of years (Ma) and is calibrated to both Cande & Kent (1995) and GTS2020 (Speijer et al. 2020). See Table 4 in the Supplementary Online Materials for age references. 'W. et al. (2011)' stands for Wade et al. (2011), 'C&K' stands for Cande & Kent and 'PF' for planktonic foraminifera.

| Genera | This study | Fox & Wade (2013) | Wade *et al.* (2018a) |
|---|---|---|---|
| ***Globoquadrina* (descendant)** | | Evidence of spine holes? | |
| ***dehiscens*** | No | No | No |
| ***Dentoglobigerina*** | | Evidence of spine holes? | |
| ***altispira*** | | No | |
| ***baroemoenensis*** | Yes | No | Yes |
| ***binaiensis*** | No | No | Yes |
| ***globosa*** | Yes | No | No |
| ***globularis*** | No | | No |
| ***juxtabinaiensis*** | | Yes | |
| ***larmeui*** | | | Yes |
| ***tripartita*** | No | No | No |
| ***sellii*** | | | No |
| ***venezuelana*** | No | No | No |

**Table 2.** Accumulated evidence for the presence of spines holes in the wall texture of Miocene *Dentoglobigerina* forms and its descendant *Globoquadrina dehiscens*. In comparison with previous work made on Oligocene and Miocene forms of *Dentoglobigerina* (Fox & Wade 2013; Wade *et al.* 2018a). Blank box means the relevant species was not observed in the study.

| **Genera** | **This study** | **Sexton *et al.* (2006)** | **Olsson *et al.* (2006a)** | **Pearson & Wade (2015)** |
|---|---|---|---|---|
| ***Dentoglobigerina*** | | Evidence of spine holes? | | |
| ***galavisi*** | Yes | Yes | No | Yes |
| ***pseudovenezuelana*** | Yes | Yes | No | Yes |
| ***'Dentoglobigerina'*** | | Evidence of spine holes? | | |
| ***eotripartita*** | No | | No | Yes |

**Table 3.** Accumulated evidence for the presence of spines holes in the wall texture of Eocene *Dentoglobigerina* forms. In comparison with previous work made on Eocene forms of *Dentoglobigerina* (Sexton *et al.* 2006; Olsson *et al.* 2006a; Pearson & Wade 2015). Blank box means the relevant species was not observed in the study.

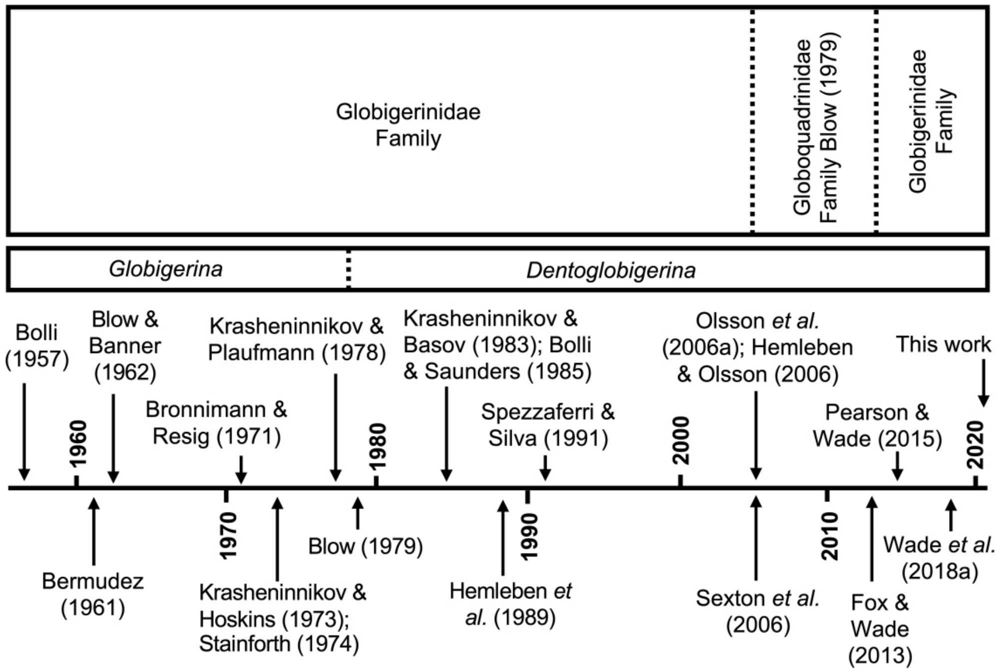


**Figure 1.** Chronology of the phylogenetic and taxonomic work accomplished on Eocene *Dentoglobigerina* since 1957. The upper box relates the changes at Family level and the lower box the changes at Genus level.

172x118mm (600 x 600 DPI)

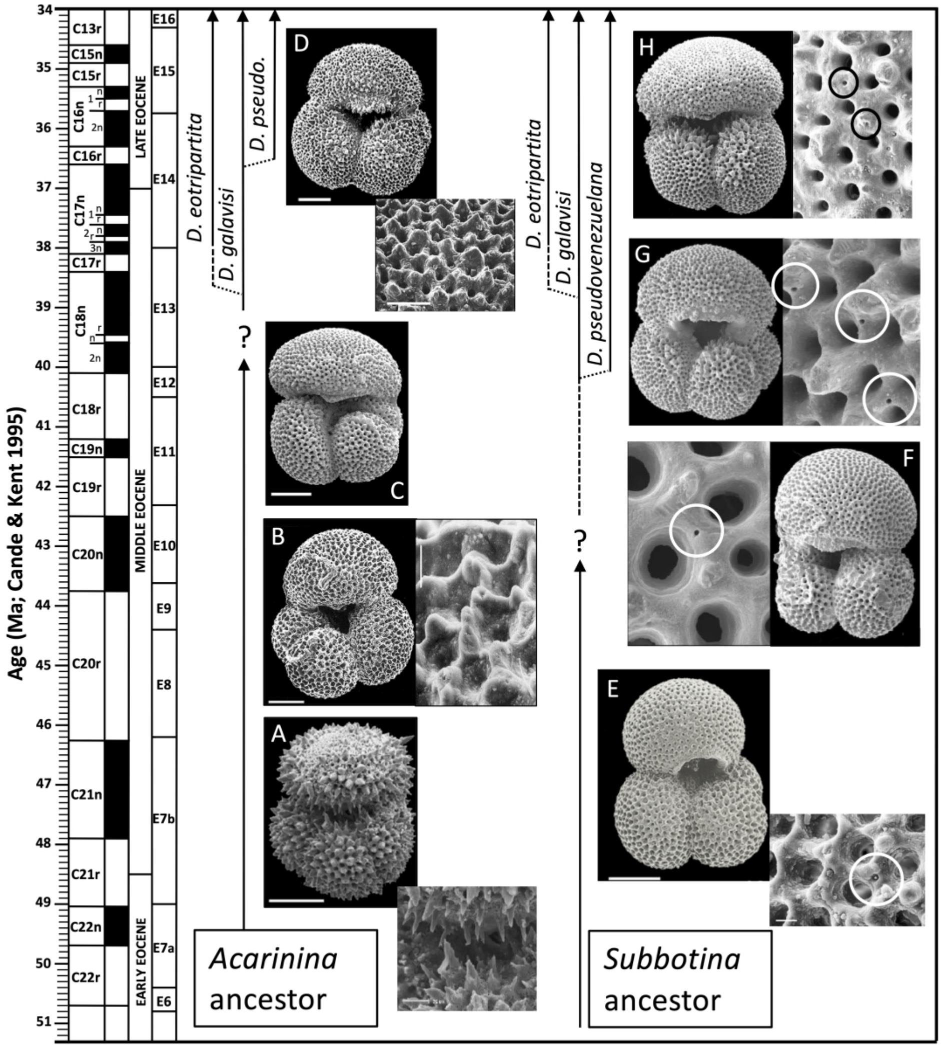


**Figure 2.** Schematic diagram of the two ancestor theories for the genus *Dentoglobigerina* including SEMs of *Dentoglobigerina*, *Acarinina* and *Subbotina* and the accumulated wall texture evidence: the *Acarinina* ancestor theory according to Olsson *et al.* (2006) and the *Subbotina* ancestor theory according to Wade *et al.* (2018a) and Pearson & Wade (2015). The spine holes are highlighted by white or black circles. **(A)** *A. mcgowrani* (Berggren *et al.* 2006: 293, pl. 9.13, figs 13-14); **(B)** *D. galavisi* (Olsson *et al.* 2006a: 405: pl. 13.1, figs 12 & 16); **(C)** *D. eotripartita* (Olsson *et al.* 2006a: 409, pl. 13.3, fig. 12); **(D)** *D. pseudovenezuelana* (Olsson *et al.* 2006a: 407, pl. 13.2, figs 3-4); **(E)** *S. yeguaensis* (Olsson *et al.* 2006b: 152, pl. 6.18, fig. 10 & 16); **(F)** *D. galavisi* (Pearson & Wade 2015: 55, fig. 15.7a-7b); **(G)** *D. pseudovenezuelana* (Pearson & Wade 2015: 59, fig. 17.6a & 6d); **(H)** *D. eotripartita* (Pearson & Wade 2015: 67, fig. 21.4a & 4e). The zonation is from Wade *et al.* (2011) and the polarity time scale is from Cande & Kent (1995). Note that '*D. pseudo.*' is the chosen abbreviation for *D. pseudovenezuelana*.

171x189mm (600 x 600 DPI)

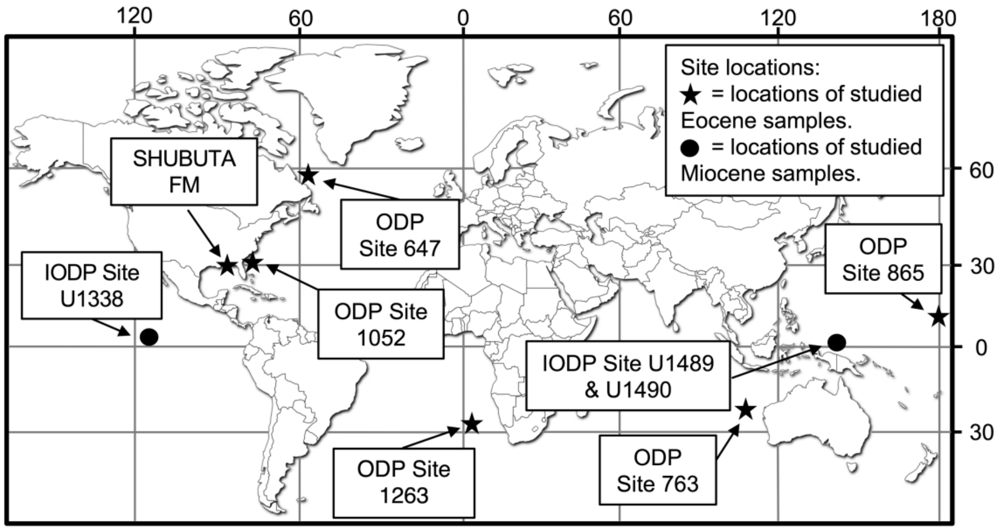


**Figure 3.** Location map showing sites from this study from the Eocene (black star symbols) and Miocene (black dot symbols) time intervals.

172x101mm (600 x 600 DPI)

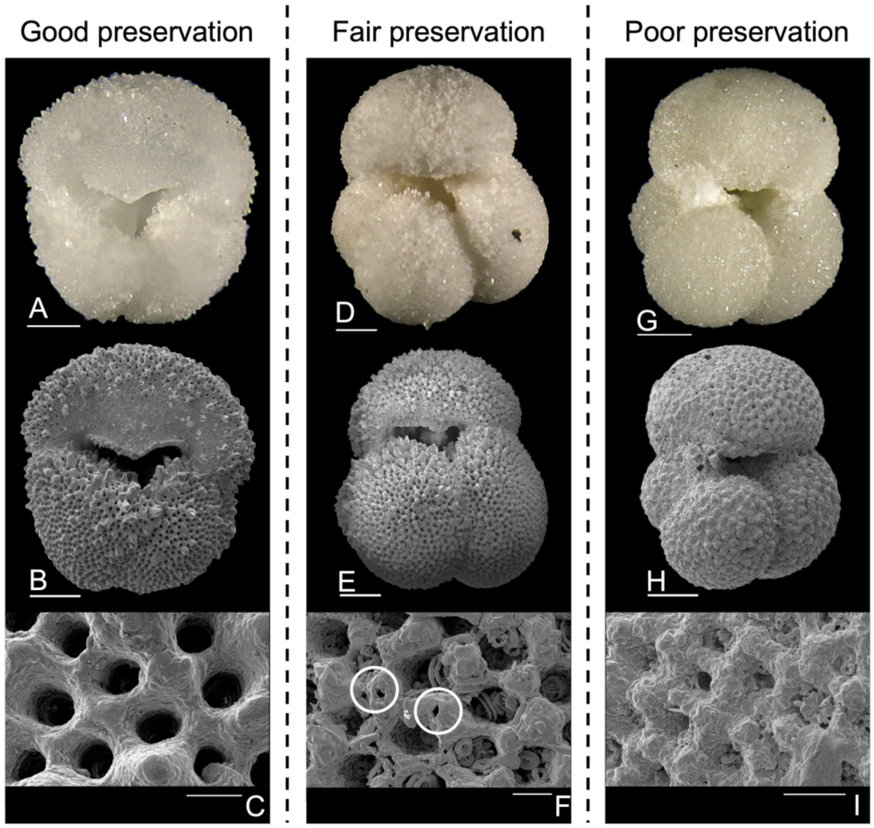


**Figure 4.** The three states of preservation in planktonic foraminiferal test and their wall texture based on z-stacker and SEM images. **(A, B, C)** Good preservation state of a Miocene *D. binaiensis* test from IODP sample U1489D-27X-CC available in Fayolle & Wade (2020). In SEM, the pore and pore intersection are clearly visible, smooth and unfilled both in test and wall texture images. In z-stacker light, the test is translucent, and the pores are visible especially in spiral view. **(D, E, F)** Fair preservation state of an Eocene *D. pseudovenezuelana* test from ODP sample 865C-3H-5 (see Fig. 12K-S). The pore and pore intersections are clearly visible but partially infilled and affected by recrystallisation in some areas, but true spine holes are identifiable. In z-stacker light, the test is opaque and white whereas in SEM light, the aperture is identifiable, and pores are well preserved. **(G, H, I)** Poor preservation state of an Eocene *D. galavisi* test from ODP sample 763B-6X-5W (see Fig. 8I-O). In SEM, the pores and pore intersections are obscured, and the test is affected in all parts making it hard to discern any wall texture feature. In the z-stacker light microscope, the test is opaque. White circles denote evidence of spine holes.

172x155mm (300 x 300 DPI)

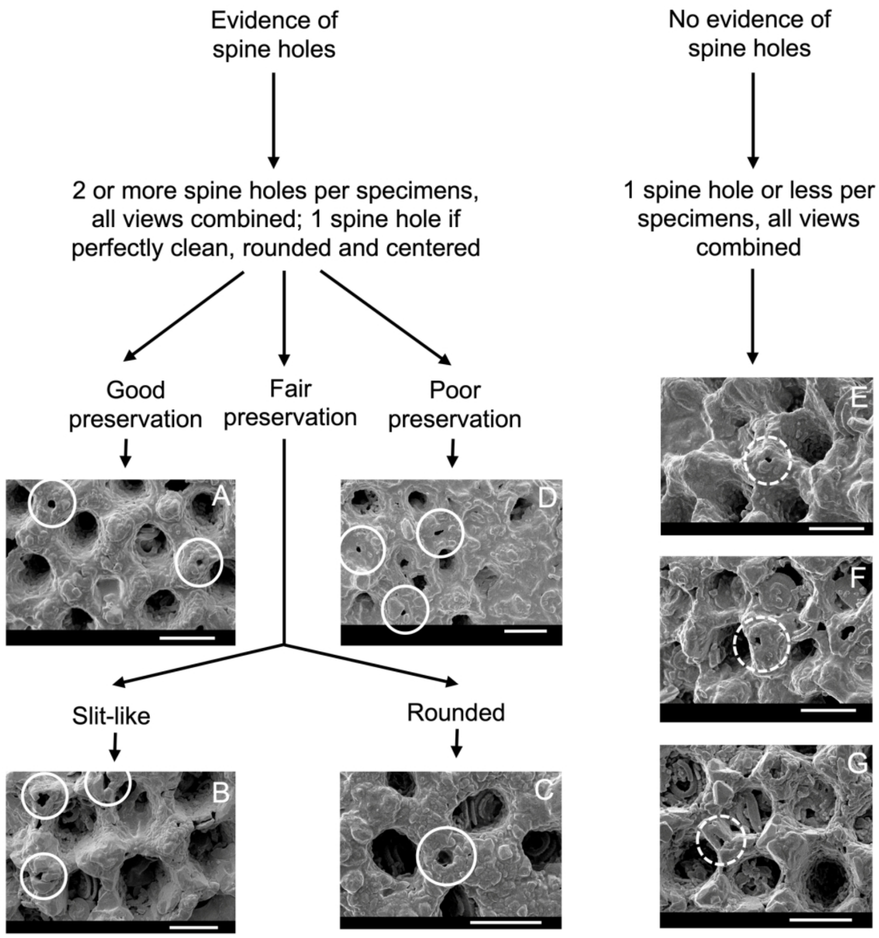


**Figure 5.** Our approach to assessing morphological features analogous to spine holes and splitting them into two categories: 'Evidence of spine holes' and 'No evidence of spine holes'. **(A)** two large and well-rounded spine holes in the wall texture of a *Dentoglobigerina pseudovenezuelana* specimen from ODP Sample 865C-7H-3 (Fig. 13J); **(B)** one slit shaped and enlarged spine hole in the wall texture of a *Subbotina* sp. 1 specimen from ODP Sample 865C-7H-3 (Fig.17T); **(C)** a large and well-rounded spine hole in the wall texture (fair preservation) of a *Dentoglobigerina galavisi* specimen from ODP Sample 865C-4H-6 (Fig. 6O); **(D)** three slightly slit shaped spine holes in the wall texture of a *Dentoglobigerina galavisi* specimen from ODP Sample 1263B-7H-5W (Fig. 9H); **(E)** one potential and slightly slit-like spine hole in the wall texture of a '*D.*' *eotripartita* specimen from ODP Sample 865C-4H-2 (Fig. 20Q); **(F)** one potential and slit-like spine hole in the wall texture of a '*D.*' *eotripartita* specimen from ODP Sample 865C-4H-2 (Fig. 20H); **(G)** one potential, slit-like and elongated spine hole in the wall texture of a '*D.*' *eotripartita* specimen from ODP Sample 865C-7H-3 (Fig. 22H). White circles denote 'Evidence of spine holes' and dashed white circles denote potential spine holes that do not classify for 'Evidence of spine holes'.

172x171mm (300 x 300 DPI)

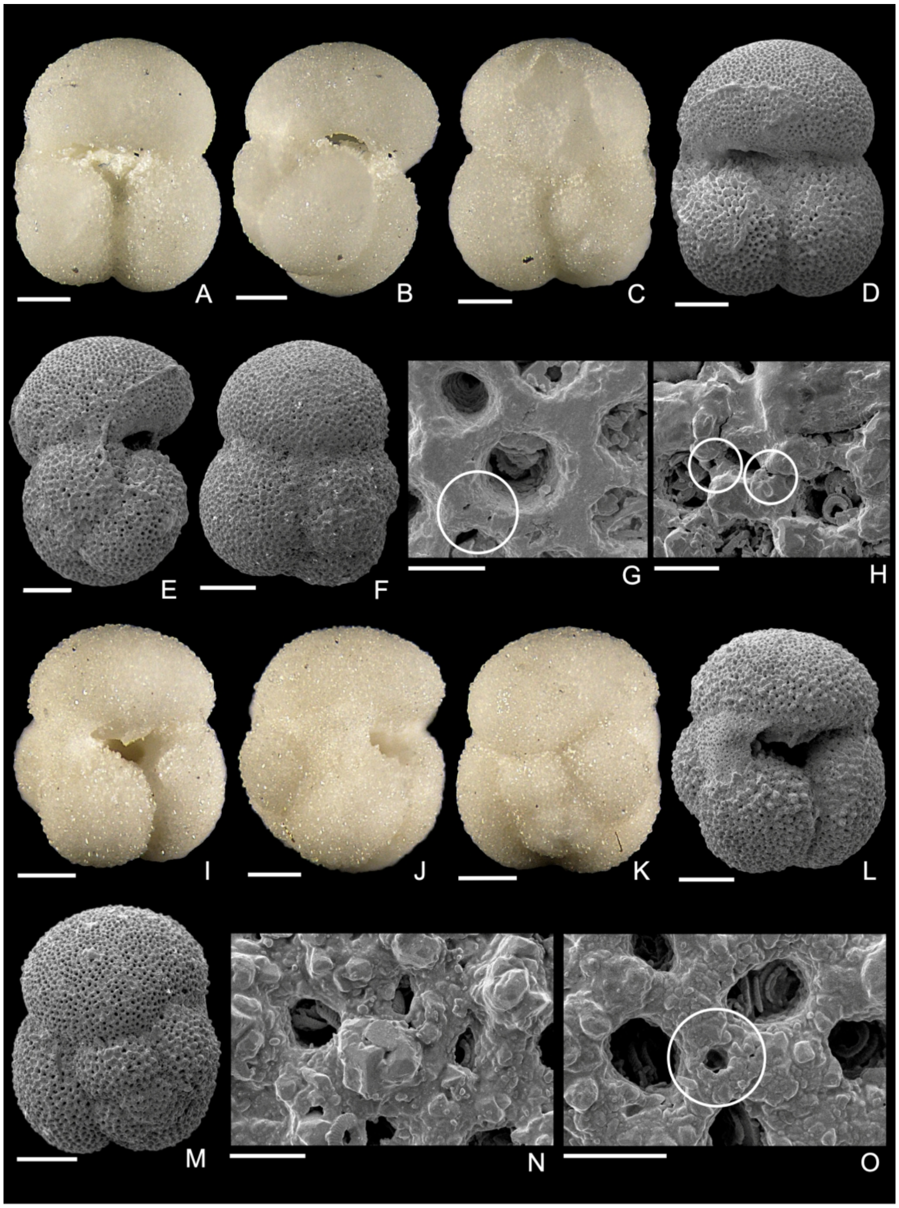


**Figure 6.** *Dentoglobigerina galavisi* **(NHMUK PM PF XXXXX, A-H)** , ODP Sample 1052B-12H-5, 3-6 cm, middle Eocene Zone E13, Blake Nose, western North Atlantic Ocean: Z-stacker images of **(A)** umbilical view, **(B)** edge view, **(C)** spiral view; SEM images of **(D)** umbilical view, **(E)** edge view, **(F)** spiral view; Wall texture SEM images of **(G)** edge view, **(H)** spiral view. Evidence of spine holes. Scale bars: 100 μm (whole specimens) and 10 μm (close-up images). *Dentoglobigerina galavisi* **(NHMUK PM PF XXXXX, I-O)**, ODP Sample 865C-4H-6, 63-65 cm, middle Eocene Zone E13, Allison Guyot, western Pacific Ocean: Z-stacker images of **(I)** umbilical view, **(J)** edge view, **(K)** spiral view; SEM images of **(L)** umbilical view, edge view not obtained, **(M)** spiral view; Wall texture SEM images of **(N)** umbilical view and **(O)** spiral view. Evidence of a spine hole. Scale bars: 100 μm (whole specimens) and 10 μm (close-up images). White circles denote evidence of spine holes.

172x231mm (300 x 300 DPI)

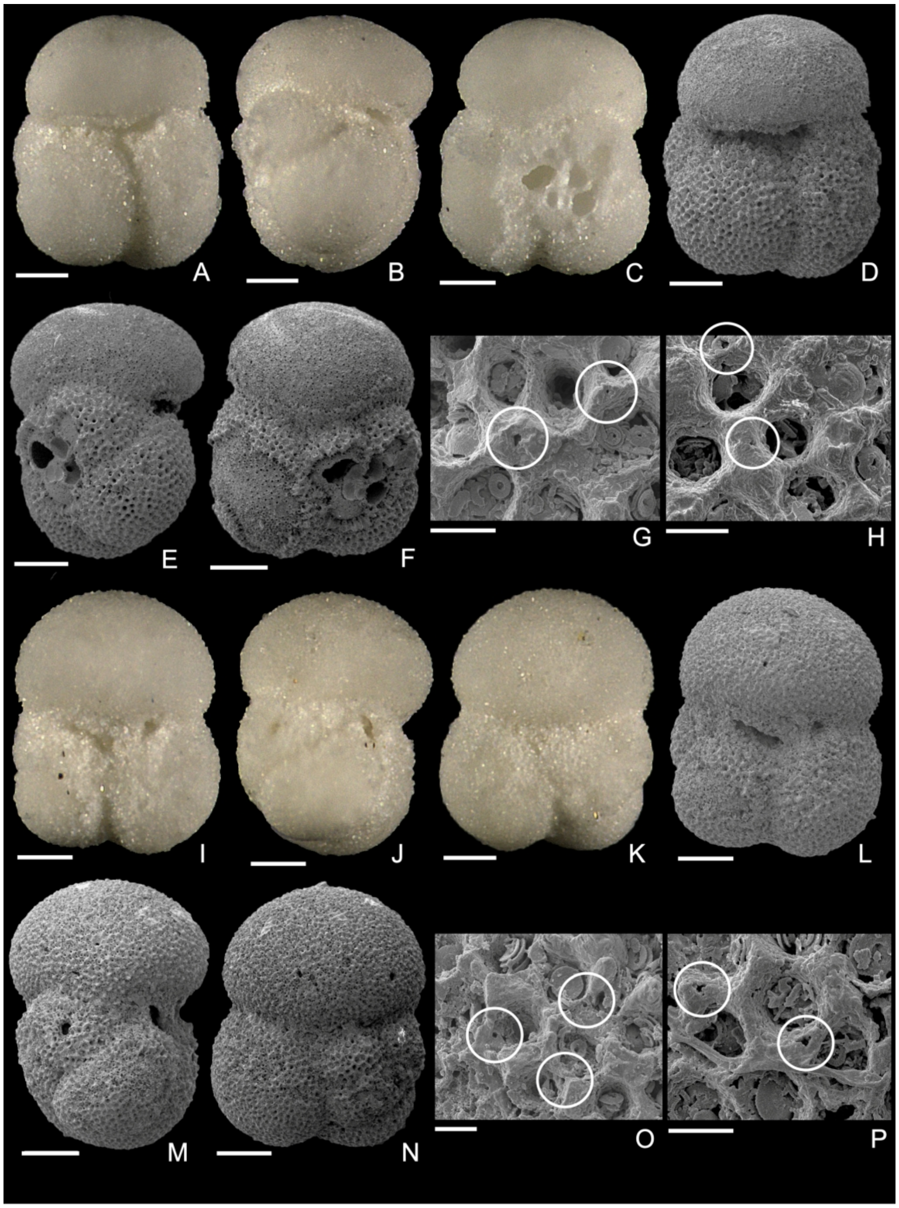


**Figure 7.** *Dentoglobigerina galavisi* **(NHMUK PM PF XXXXX, A-H)**, ODP Sample 763B-2X-5W, 120-122 cm, upper Eocene Zone E16, Exmouth Plateau, Indian Ocean: Z-stacker images of **(A)** umbilical view, **(B)** edge view, **(C)** spiral view; SEM images of **(D)** umbilical view, **(E)** edge view, **(F)** spiral view; Wall texture SEM images of **(G)** edge view, **(H)** spiral view. Evidence of spine holes. Scale bars: 100 µm (whole specimens) and 10 µm (close-up images). *Dentoglobigerina galavisi* **(NHMUK PM PF XXXXX, I-P)**, ODP Sample 763B-4X-3W, 46-48 cm, upper Eocene Zone E15, Exmouth Plateau, Indian Ocean: Z-stacker images of **(I)** umbilical view, **(J)** edge view, **(K)** spiral view; SEM images of **(L)** umbilical view, **(M)** edge view, **(N)** spiral view; Wall texture SEM images of **(O)** umbilical view, **(P)** spiral view. Evidence of spine holes. Scale bars: 100 µm (whole specimens) and 10 µm (close-up images). White circles denote evidence of spine holes.

172x231mm (300 x 300 DPI)

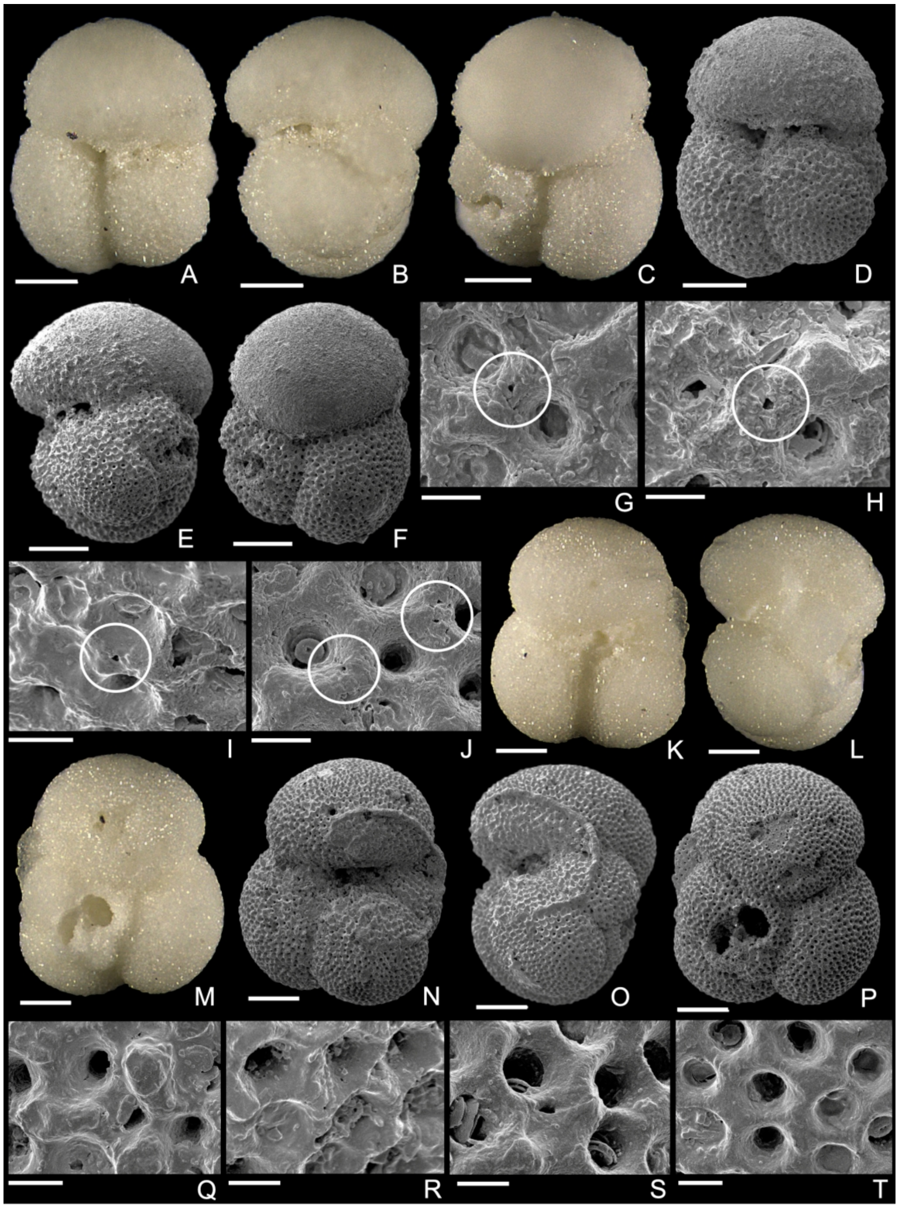


**Figure 8.** *Dentoglobigerina galavisi* **(NHMUK PM PF XXXXX, A-J)**, ODP Sample 763B-4X-3W, 46-48 cm, upper Eocene Zone E15, Exmouth Plateau, Indian Ocean: Z-stacker images of **(A)** umbilical view, **(B)** edge view, **(C)** spiral view; SEM images of **(D)** umbilical view, **(E)** edge view, **(F)** spiral view; Wall texture SEM images of **(G)** umbilical view, **(H)** edge view, **(I)** edge view, **(J)** spiral view. Evidence of spine holes. Scale bars: 100 µm (whole specimens) and 10 µm (close-up images). *Dentoglobigerina galavisi* **(NHMUK PM PF XXXXX, K-T)**, ODP Sample 763B-5X-2W, 55-57 cm, upper Eocene Zone E14, Exmouth Plateau, Indian Ocean: Z-stacker images of **(K)** umbilical view, **(L)** edge view, **(M)** spiral view; SEM images of **(N)** umbilical view, **(O)** edge view, **(P)** spiral view; Wall texture SEM images of **(Q)** umbilical view, **(R)** umbilical view, **(S)** spiral view, **(T)** spiral view. No evidence of spine holes. Scale bars: 100 µm (whole specimens) and 10 µm (close-up images). White circles denote evidence of spine holes.

172x231mm (300 x 300 DPI)

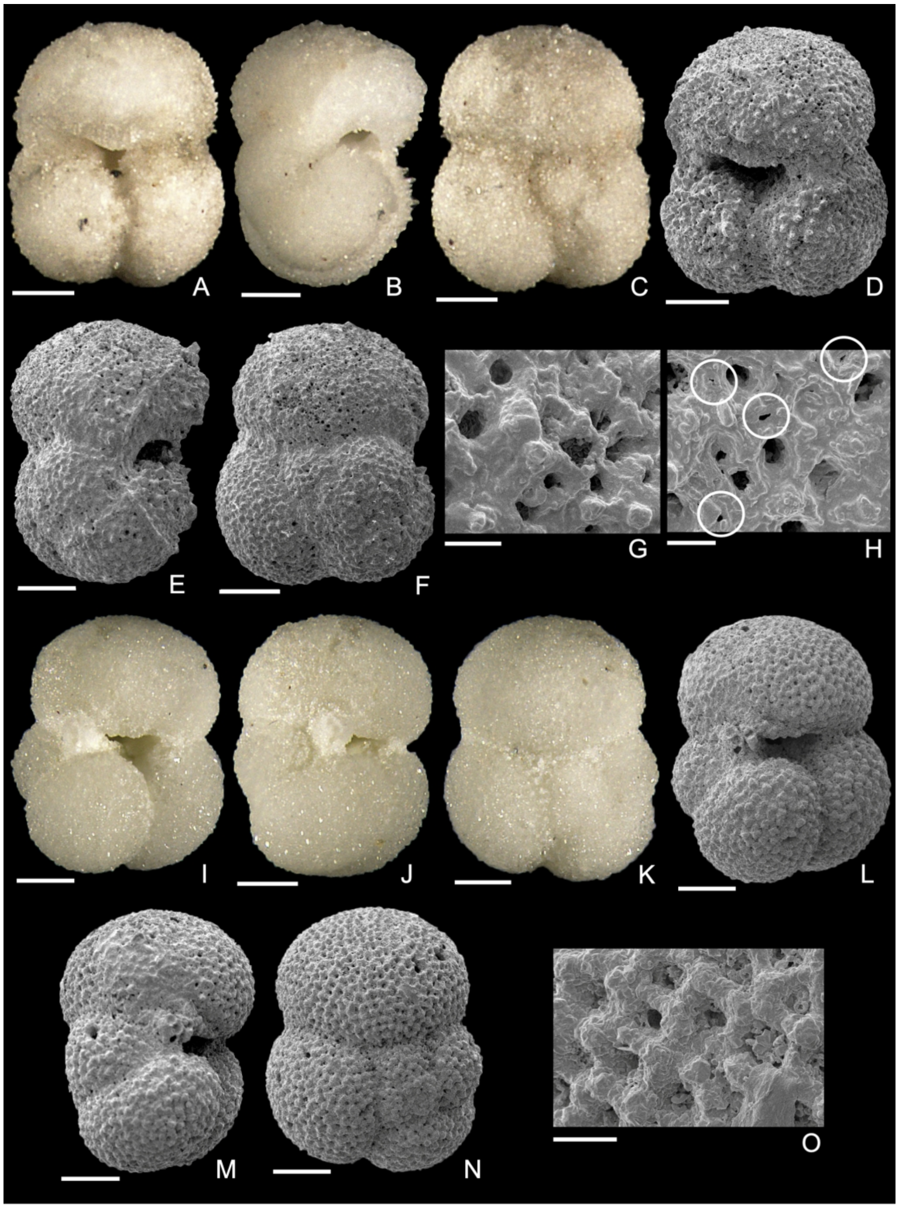


**Figure 9.** *Dentoglobigerina galavisi* **(NHMUK PM PF XXXXX, A-H)**, ODP Sample 1263B-7H-5W, 138-140 cm, middle Eocene Zone E13, Walvis Ridge eastern South Atlantic Ocean: Z-stacker images of **(A)** umbilical view, **(B)** edge view, **(C)** spiral view; SEM images of **(D)** umbilical view, **(E)** edge view, **(F)** spiral view; Wall texture SEM images of **(G)** umbilical view, **(H)** spiral view. Evidence of spine holes. Scale bars: 100 µm (whole specimens) and 10 µm (close-up images). *Dentoglobigerina galavisi* **(NHMUK PM PF XXXXX, I-O)**, ODP Sample 763B-6X-5W, 42-44 cm, middle Eocene Zone E11, Exmouth Plateau, Indian Ocean: Z-stacker images of **(I)** umbilical view, **(J)** edge view, **(K)** spiral view; SEM images of **(L)** umbilical view, **(M)** edge view, **(N)** spiral view; Wall texture SEM image of **(O)** spiral view. No evidence of spine holes. Scale bars: 100 µm (whole specimens) and 10 µm (close-up image). White circles denote evidence of spine holes.

172x231mm (300 x 300 DPI)

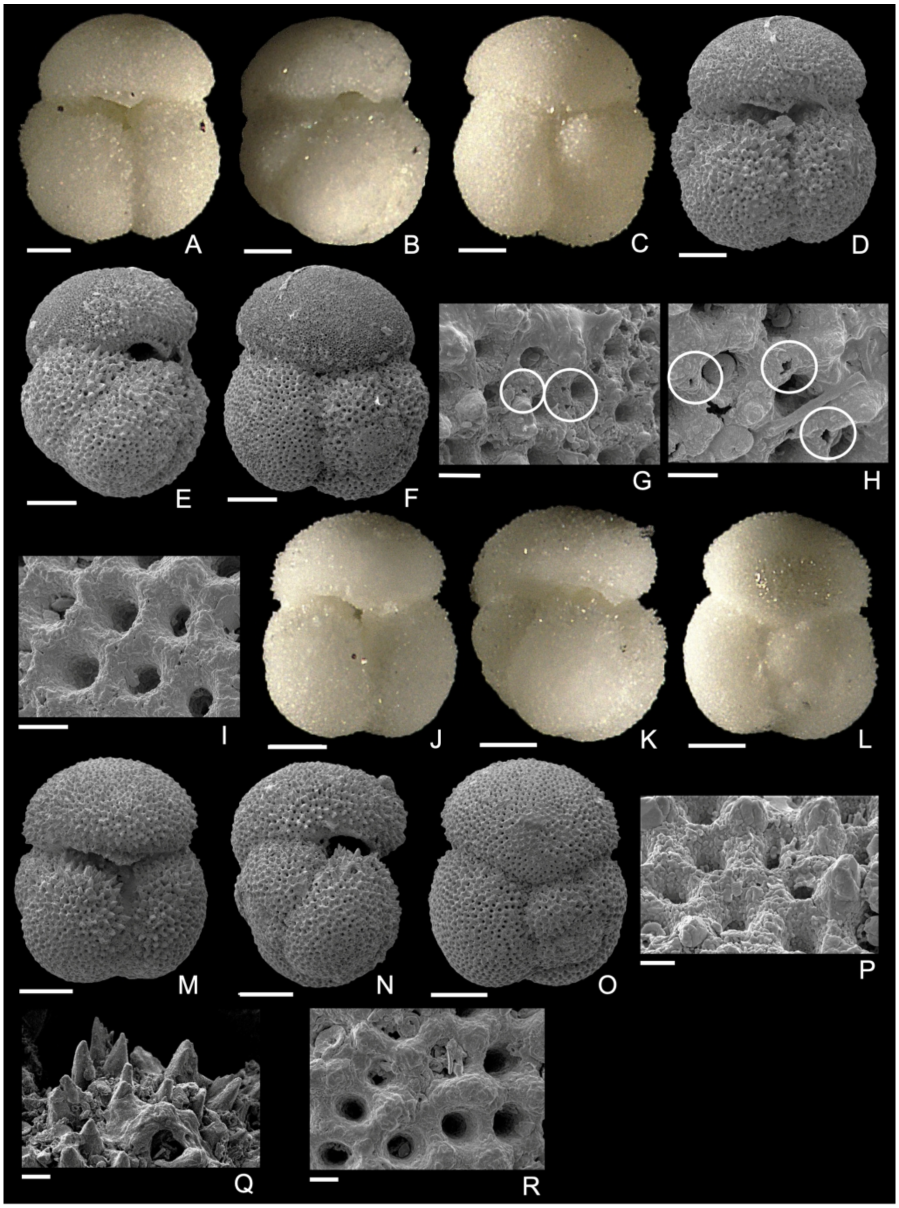


**Figure 10.** *Dentoglobigerina pseudovenezuelana* **(NHMUK PM PF XXXXX, A-I)**, ODP Sample 1052B-10H-6, 13-16 cm, upper Eocene Zone E14, Blake Nose, western North Atlantic Ocean: Z-stacker images of **(A)** umbilical view, **(B)** edge view, **(C)** spiral view; SEM images of **(D)** umbilical view, **(E)** edge view, **(F)** spiral view; Wall texture SEM image of **(G)** umbilical view, **(H)** edge view and **(I)** spiral view. Evidence of spine holes. Scale bars: 100 µm (whole specimens) and 10 µm (close-up images). *Dentoglobigerina pseudovenezuelana* **(NHMUK PM PF XXXXX, J-R)**, ODP Sample 1052B-10H-6, 13-16 cm, upper Eocene Zone E14, Blake Nose, western North Atlantic Ocean: Z-stacker images of **(J)** umbilical view, **(K)** edge view, **(L)** spiral view; SEM images of **(M)** umbilical view, **(N)** edge view, **(O)** spiral view; Wall texture SEM image of **(P)** umbilical view, **(Q)** edge view and **(R)** spiral view. No evidence of spine holes. Scale bars: 100 µm (whole specimens) and 10 µm (close-up images). White circles denote evidence of spine holes.

172x231mm (300 x 300 DPI)

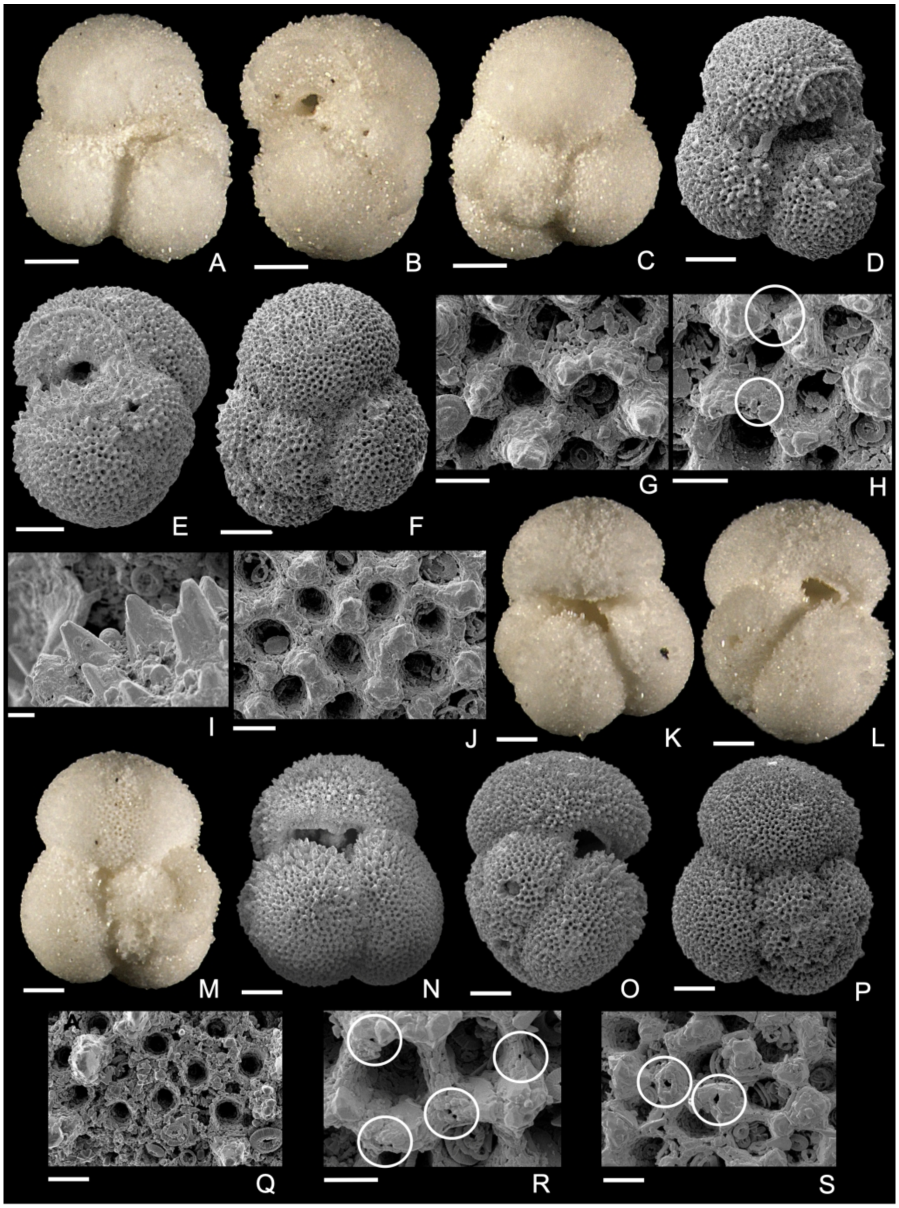


**Figure 11.** *Dentoglobigerina pseudovenezuelana* **(NHMUK PM PF XXXXX, A-J)**, ODP Sample 1263B-8H-5W, 139-141 cm, middle Eocene Zone E13, eastern South Atlantic Ocean: Z-stacker images of **(A)** umbilical view, **(B)** edge view, **(C)** spiral view; SEM images of **(D)** umbilical view, **(E)** edge view, **(F)** spiral view; Wall texture SEM image of **(G)** umbilical view, **(H)** umbilical view, **(I)** edge view, **(J)** spiral view. Evidence of spine holes. Scale bars: 100 µm (whole specimens) and 10 µm (close-up images). *Dentoglobigerina pseudovenezuelana* **(NHMUK PM PF XXXXX, K-S)**, ODP Sample 865C-3H-5, 110-112 cm, upper Eocene Zone E15, Allison Guyot, western Pacific Ocean: Z-stacker images of **(K)** umbilical view, **(L)** edge view, **(M)** spiral view; SEM images of **(N)** umbilical view, **(O)** edge view, **(P)** spiral view; Wall texture SEM image of **(Q)** umbilical view, **(R)** edge view and **(S)** spiral view. Evidence of spine holes. Scale bars: 100 µm (whole specimens) and 10 µm (close-up images). White circles denote evidence of spine holes.

172x232mm (300 x 300 DPI)

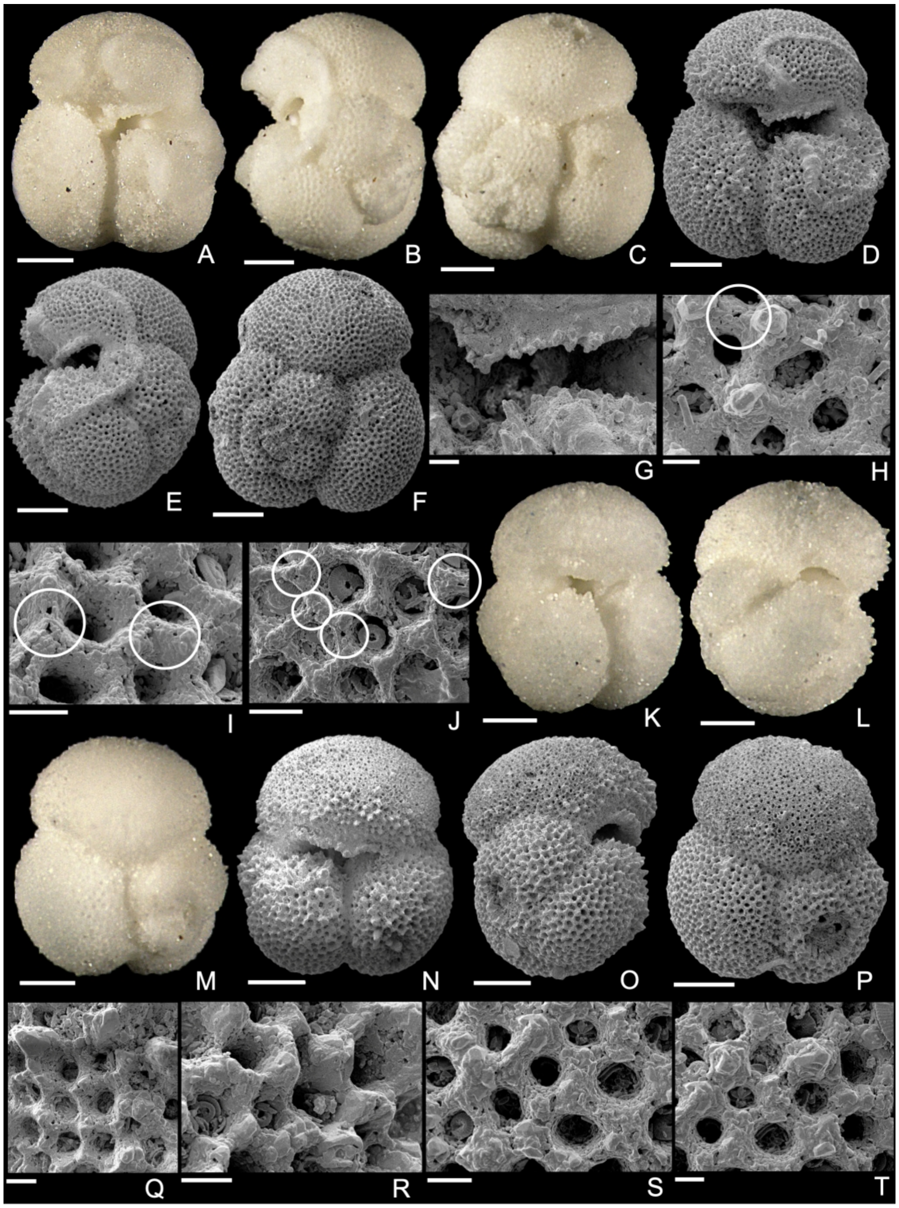


**Figure 12.** *Dentoglobigerina pseudovenezuelana* **(NHMUK PM PF XXXXX, A-J)**, ODP Sample 865C-3H-6, 46-48 cm, upper Eocene Zone E15, Allison Guyot, western Pacific Ocean: Z-stacker images of **(A)** umbilical view, **(B)** edge view, **(C)** spiral view; SEM images of **(D)** umbilical view, **(E)** edge view, **(F)** spiral view; Wall texture SEM image of **(G)** umbilical view (pustulose tooth), **(H)** umbilical view, **(I)** edge view, **(J)** spiral view. Evidence of spine holes. Scale bars: 100 µm (whole specimens) and 10 µm (close-up images). *Dentoglobigerina pseudovenezuelana* **(NHMUK PM PF XXXXX, K-T)**, ODP Sample 865C-3H-6, 46-48 cm, upper Eocene Zone E15, Allison Guyot, western Pacific Ocean: Z-stacker images of **(K)** umbilical view, **(L)** edge view, **(M)** spiral view; SEM images of **(N)** umbilical view, **(O)** edge view, **(P)** spiral view; Wall texture SEM image of **(Q)** umbilical view, **(R)** edge view, **(S)** spiral view, **(T)** spiral view. No evidence of spine holes. Scale bars: 100 µm (whole specimens) and 10 µm (close-up images). White circles denote evidence of spine holes.

172x232mm (300 x 300 DPI)

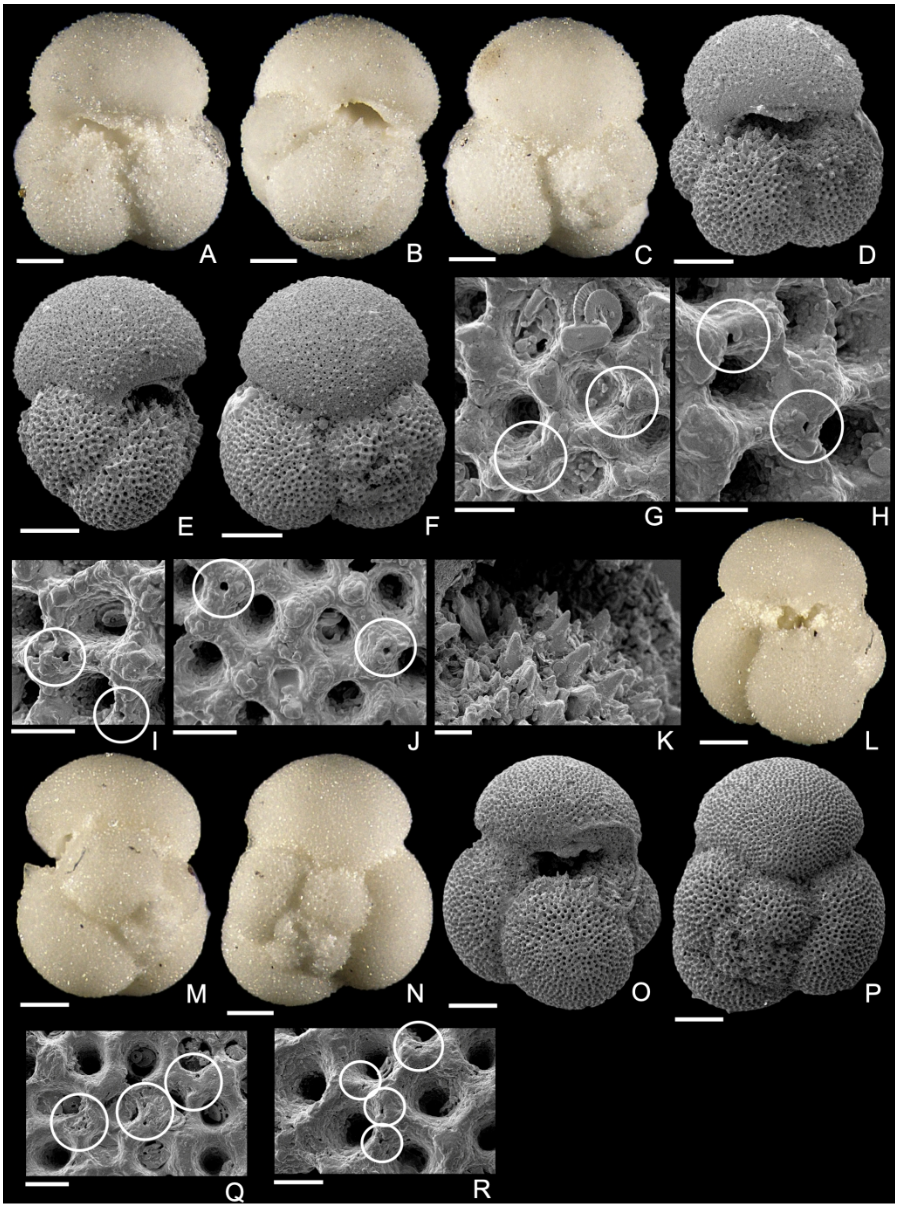


**Figure 13.** *Dentoglobigerina pseudovenezuelana* **(NHMUK PM PF XXXXX, A-K)**, ODP Sample 865C-7H-3, 110-11 cm, middle Eocene Zone E9, Allison Guyot, western Pacific Ocean: Z-stacking images of **(A)** umbilical view, **(B)** edge view, **(C)** spiral view; SEM images of **(D)** umbilical view, **(E)** edge view, **(F)** spiral view; Wall texture SEM image of **(G)** umbilical view, **(H)** edge view, **(I, J)** spiral view, **(K)** edge view (pustules in the apertural region). Evidence of spine holes. Scale bars: 100 µm (whole specimens) and 10 µm (close-up images). *Dentoglobigerina pseudovenezuelana* **(NHMUK PM PF XXXXX, L-R)**, ODP Sample 763B-5X-2W, 55-57 cm, upper Eocene Zone E14, Exmouth Plateau, Indian Ocean: Z-stacking images of **(L)** umbilical view, **(M)** edge view, **(N)** spiral view; SEM images of **(O)** umbilical view, edge view not obtained, **(P)** spiral view; Wall texture SEM image of **(Q)** umbilical view, **(R)** spiral view. Evidence of spine holes. Scale bars: 100 µm (whole specimens) and 10 µm (close-up images). White circles denote evidence of spine holes.

172x232mm (300 x 300 DPI)

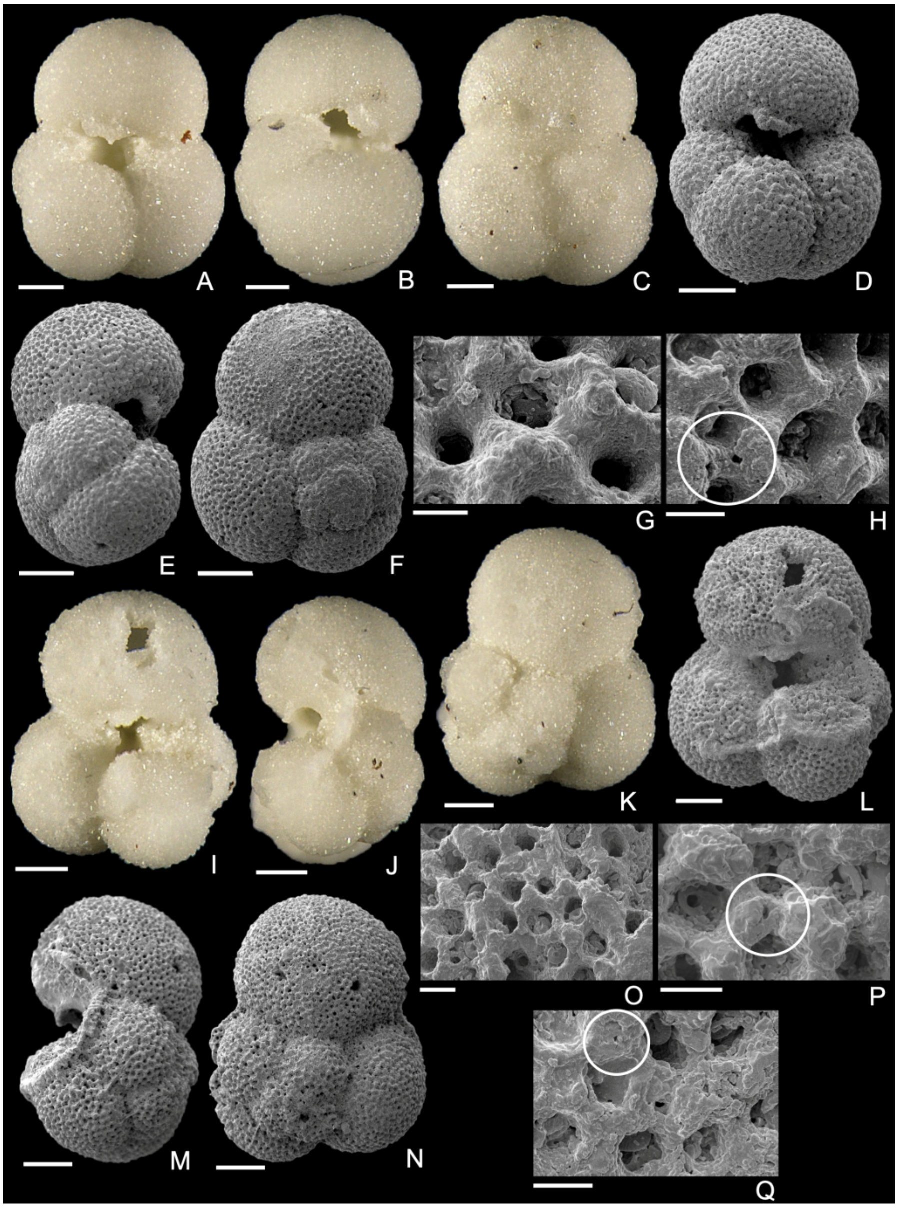


**Figure 14.** *Subbotina yeguaensis* **(NHMUK PM PF XXXXX, A-H)**, ODP Sample 763B-6X-5W, 42-44 cm, middle Eocene Zone E11, Exmouth Plateau, Indian Ocean: Z-stacker images of **(A)** umbilical view, **(B)** edge view, **(C)** spiral view; SEM images of **(D)** umbilical view, **(E)** edge view, **(F)** spiral view; Wall texture SEM image of **(G)** umbilical view, **(H)** umbilical view. Evidence of spine holes. Scale bars: 100 µm (whole specimens) and 10 µm (close-up images). *Subbotina yeguaensis* **(NHMUK PM PF XXXXX, I-Q)**, ODP Sample 763B-6X-5W, 42-44 cm, middle Eocene Zone E11, Exmouth Plateau, Indian Ocean: Z-stacker images of **(I)** umbilical view, **(J)** edge view, **(K)** spiral view; SEM images of **(L)** umbilical view, **(M)** edge view, **(N)** spiral view; Wall texture SEM image of **(O)** umbilical view, **(P)** edge view, **(Q)** spiral view. Evidence of spine holes. Scale bars: 100 µm (whole specimens) and 10 µm (close-up images). White circles denote evidence of spine holes.

172x232mm (300 x 300 DPI)

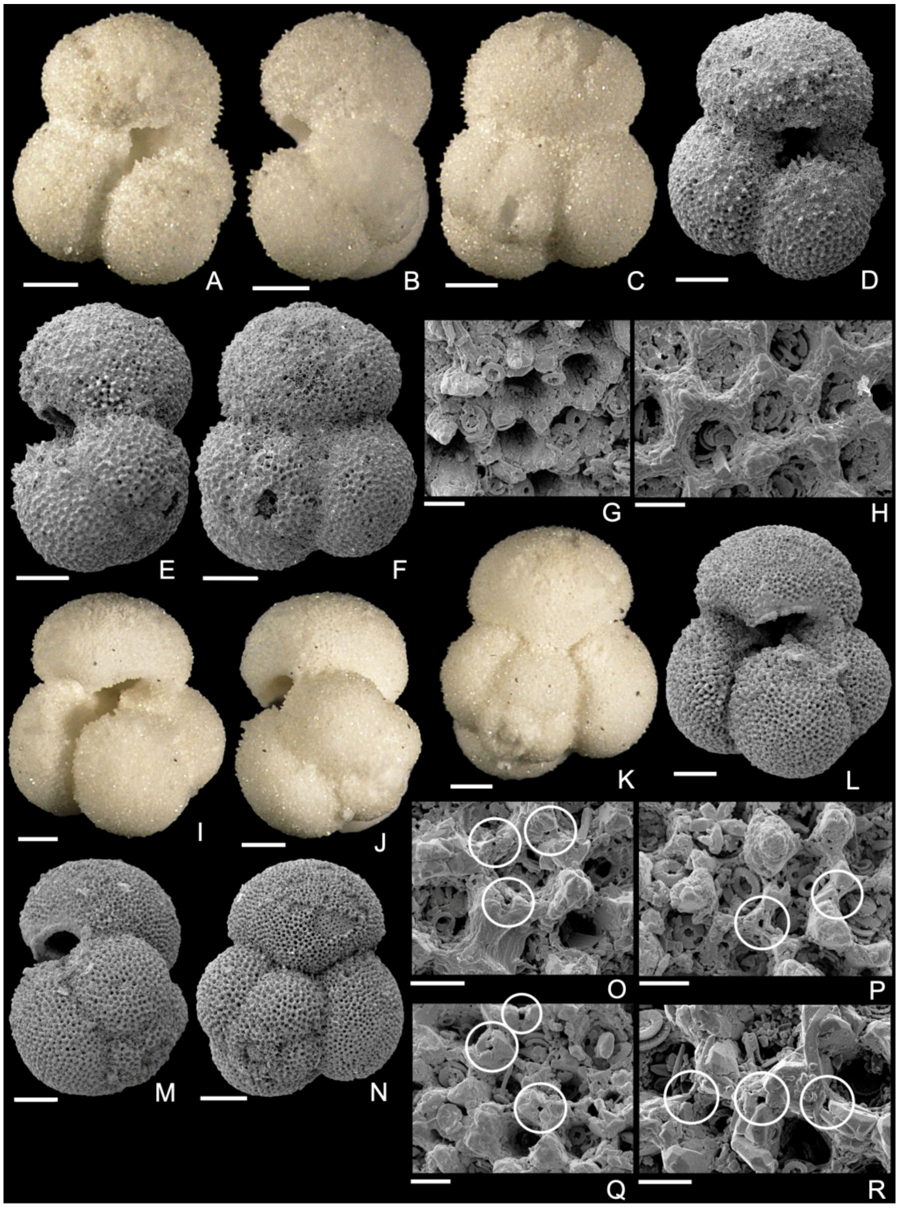


**Figure 15.** *Subbotina* cf. *S. yeguaensis* **(NHMUK PM PF XXXXX, A-F)**, ODP Sample 1263B-8H-5W, 139-141 cm, middle Eocene Zone E13, Walvis Ridge, eastern Atlantic Ocean: Z-stacker images of **(A)** umbilical view, **(B)** edge view, **(C)** spiral view; SEM images of **(D)** umbilical view, **(E)** edge view, **(F)** spiral view; Wall texture SEM image of **(G)** umbilical view, **(H)** spiral view. No evidence of spine holes. Scale bars: 100 μm (whole specimens) and 10 μm (close-up images). *Subbotina* cf. *S. yeguaensis* **(NHMUK PM PF XXXXX, I-R)**, ODP Sample 865C-3H-6, 46-48 cm, upper Eocene Zone E15, Allison Guyot, western Pacific Ocean: Z-stacker images of **(I)** umbilical view, **(J)** edge view, **(K)** spiral view; SEM images of **(L)** umbilical view, **(M)** edge view, **(N)** spiral view; Wall texture SEM image of **(O)** umbilical view, **(P)** edge view, **(Q)** edge view, **(R)** spiral view. Evidence of spine holes. Scale bars: 100 μm (whole specimens) and 10 μm (close-up images). White circles denote evidence of spine holes.

172x232mm (300 x 300 DPI)

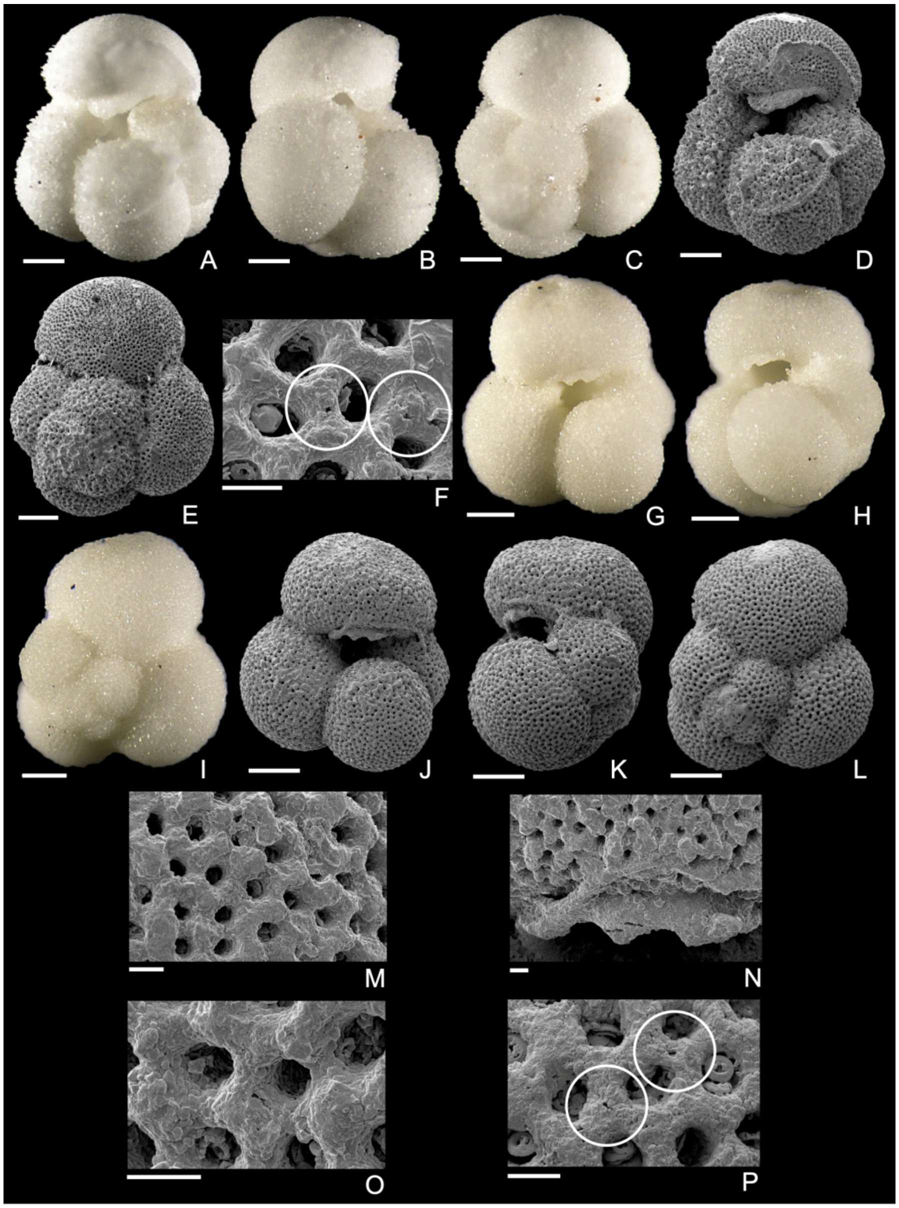


**Figure 16.** *Subbotina* cf. *S. yeguaensis* **(NHMUK PM PF XXXXX, A-F)**, ODP Sample 865C-4H-6, 63-65 cm, middle Eocene Zone E13, Allison Guyot, western Pacific Ocean: Z-stacker images of **(A)** umbilical view, **(B)** edge view, **(C)** spiral view; SEM images of **(D)** umbilical view, edge view not obtained, **(E)** spiral view; Wall texture SEM image of **(F)** spiral view. Evidence of spine holes. Scale bars: 100 μm (whole specimens) and 10 μm (close-up image). *Subbotina* cf. *S. eocaena* **(NHMUK PM PF XXXXX, G-P)**, ODP Sample 763B-6X-6W, 53-55 cm, middle Eocene Zone E10, Exmouth Plateau, Indian Ocean: Z-stacker images of **(G)** umbilical view, **(H)** edge view, **(I)** spiral view; SEM images of **(J)** umbilical view, **(K)** edge view, **(L)** spiral view; Wall texture SEM images of **(M)** umbilical view, **(N)** the tooth in umbilical view, **(O)** edge view, **(P)** spiral view. Evidence of spine holes. Scale bars: 100 μm (whole specimens) and 10 μm (close-up images). White circles denote evidence of spine holes.

172x232mm (300 x 300 DPI)

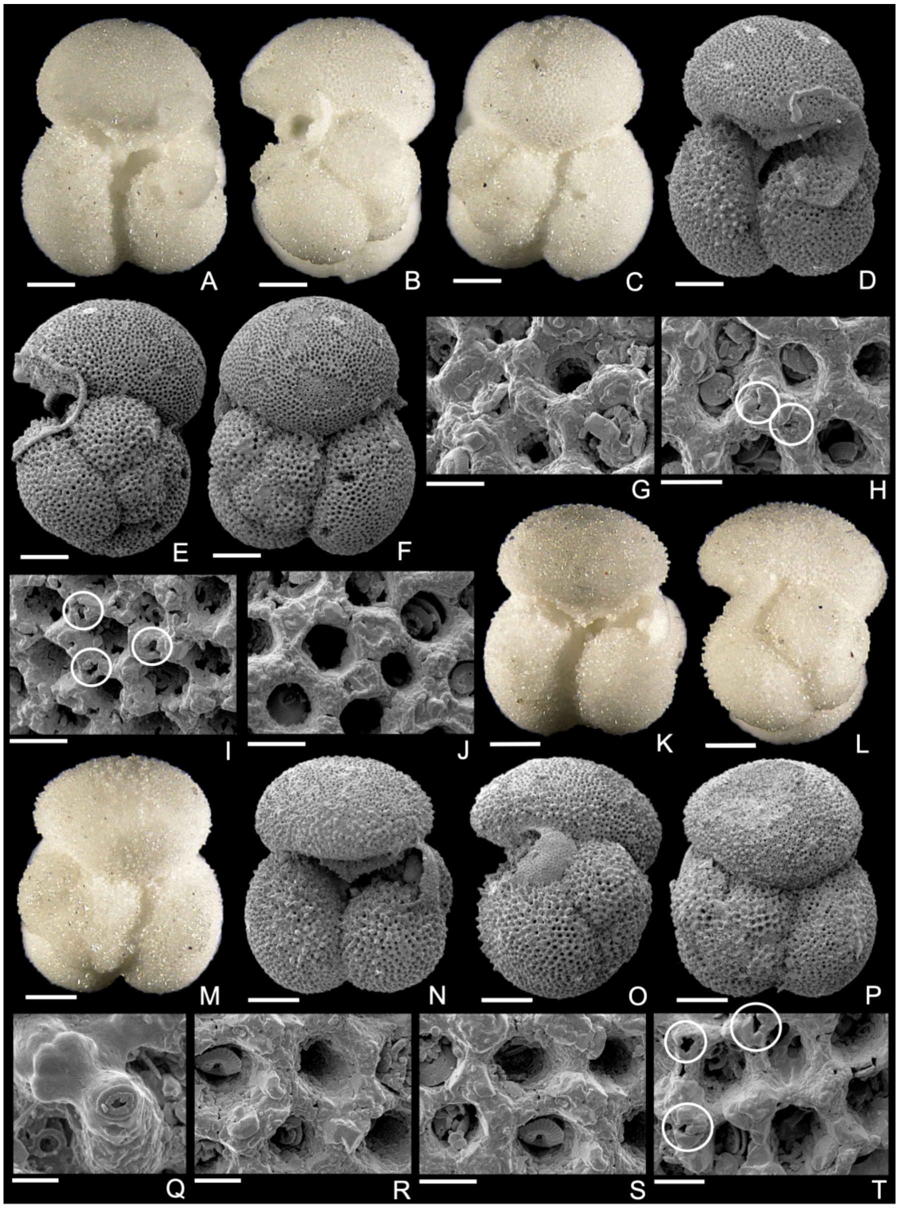


**Figure 17.** *Subbotina* sp. 1 **(NHMUK PM PF XXXXX, A-J)**, ODP Sample 865C-7H-3, 110-112 cm, middle Eocene Zone E9, Allison Guyot, western Pacific Ocean: Z-stacker images of **(A)** umbilical view, **(B)** edge view, **(C)** spiral view; SEM images of **(D)** umbilical view, **(E)** edge view, **(F)** spiral view; Wall texture SEM image of **(G)** edge view, **(H)** edge view, **(I)** spiral view, **(J)** spiral view. Evidence of spine holes. Scale bars: 100 µm (whole specimens) and 10 µm (close-up images). *Subbotina* sp. 1 **(NHMUK PM PF XXXXX, K-T)**, ODP Sample 865C-7H-3, 110-112 cm, middle Eocene Zone E9, Allison Guyot, western Pacific Ocean: Z-stacker images of **(K)** umbilical view, **(L)** edge view, **(M)** spiral view; SEM images of **(N)** umbilical view, **(O)** edge view, **(P)** spiral view; Wall texture SEM image of **(Q)** umbilical view, **(R)** edge view, **(S)** edge view, **(T)** spiral view. Evidence of spine holes. Scale bars: 100 µm (whole specimens) and 10 µm (close-up images). White circles denote evidence of spine holes.

172x232mm (300 x 300 DPI)

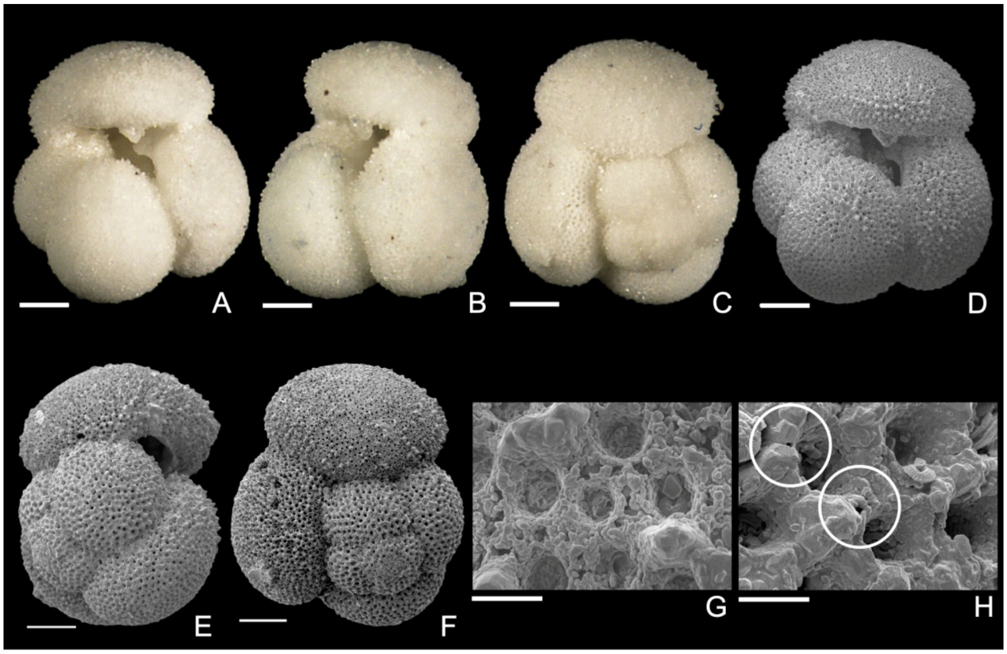


**Figure 18.** ?*Subbotina* or ?*Dentoglobigerina* **(NHMUK PM PF XXXXX, A-H)**, ODP Sample 865C-7H-3, 110-112 cm, middle Eocene Zone E9, Allison Guyot, western Pacific Ocean: Z-stacker images of **(A)** umbilical view, **(B)** edge view, **(C)** spiral view; SEM images of **(D)** umbilical view, **(E)** edge view, **(F)** spiral view; Wall texture SEM image of **(G)** umbilical view, **(H)** edge view. Evidence of spine holes. Scale bars: 100 μm (whole specimens) and 10 μm (close-up images). White circles denote evidence of spine holes.

172x111mm (300 x 300 DPI)

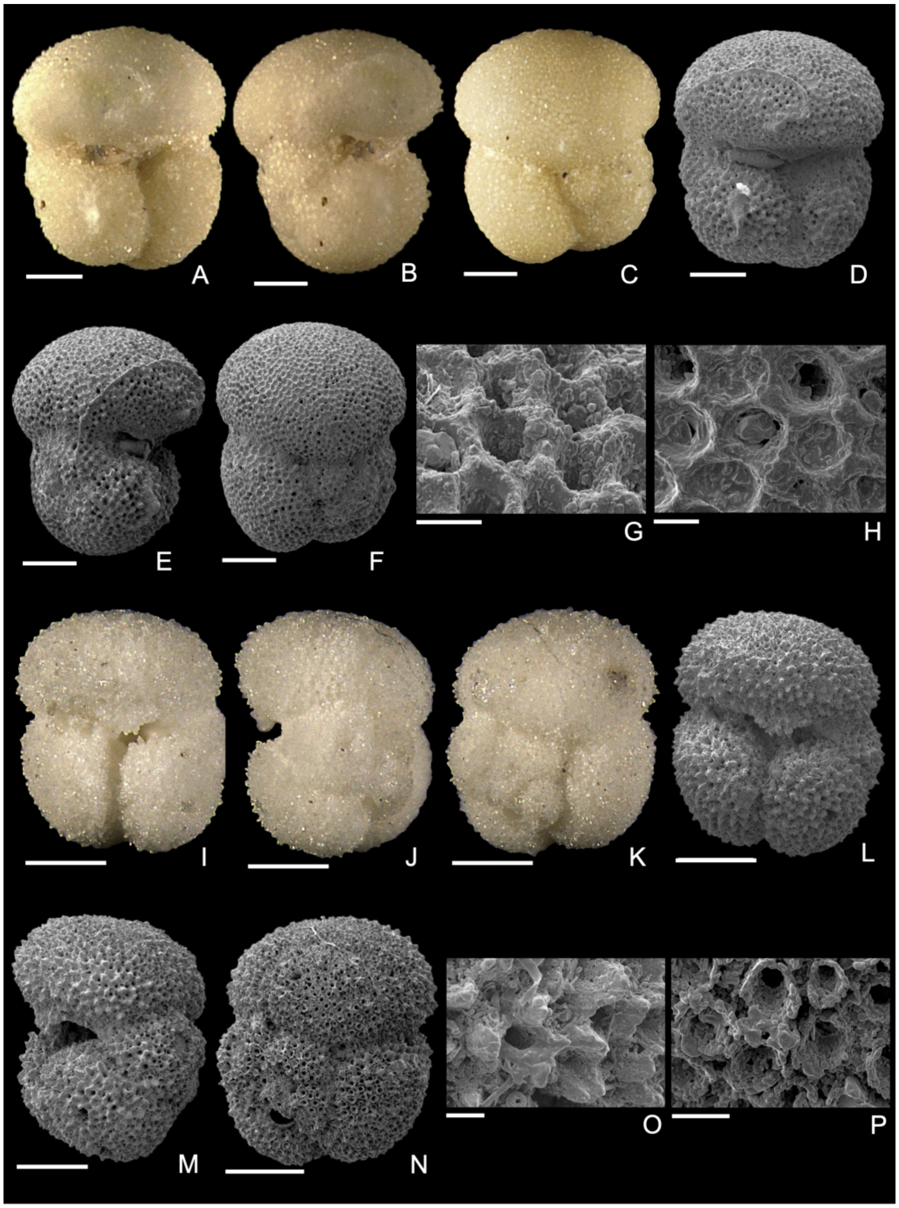


**Figure 19.** '*Dentoglobigerina*' *eotripartita* **(NHMUK PM PF XXXXX, A-H)**, Sample BW10-M1-2, upper Eocene, Zone E16, Shubuta Clay, Wayne County, Mississippi: Z-stacker images of **(A)** umbilical view, **(B)** edge view, **(C)** spiral view; SEM images of **(D)** umbilical view, **(E)** edge view, **(F)** spiral view; Wall texture SEM images of **(G)** umbilical view, **(H)** spiral view. No evidence of spine holes. Scale bars: 100 μm (whole specimens) and 10 μm (close-up images). '*Dentoglobigerina*' *eotripartita* **(NHMUK PM PF XXXXX, I-P)**, ODP Sample 865C-3H-5, 110-112 cm, upper Eocene Zone E15, Allison Guyot, western Pacific Ocean: Z-stacking images of **(I)** umbilical view, **(J)** edge view, **(K)** spiral view; SEM images of **(L)** umbilical view, **(M)** edge view, **(N)** spiral view; Wall texture SEM images of **(O)** umbilical view, **(P)** spiral view. No evidence of spine holes. Scale bars: 100 μm (whole specimens) and 10 μm (close-up images).

172x232mm (300 x 300 DPI)

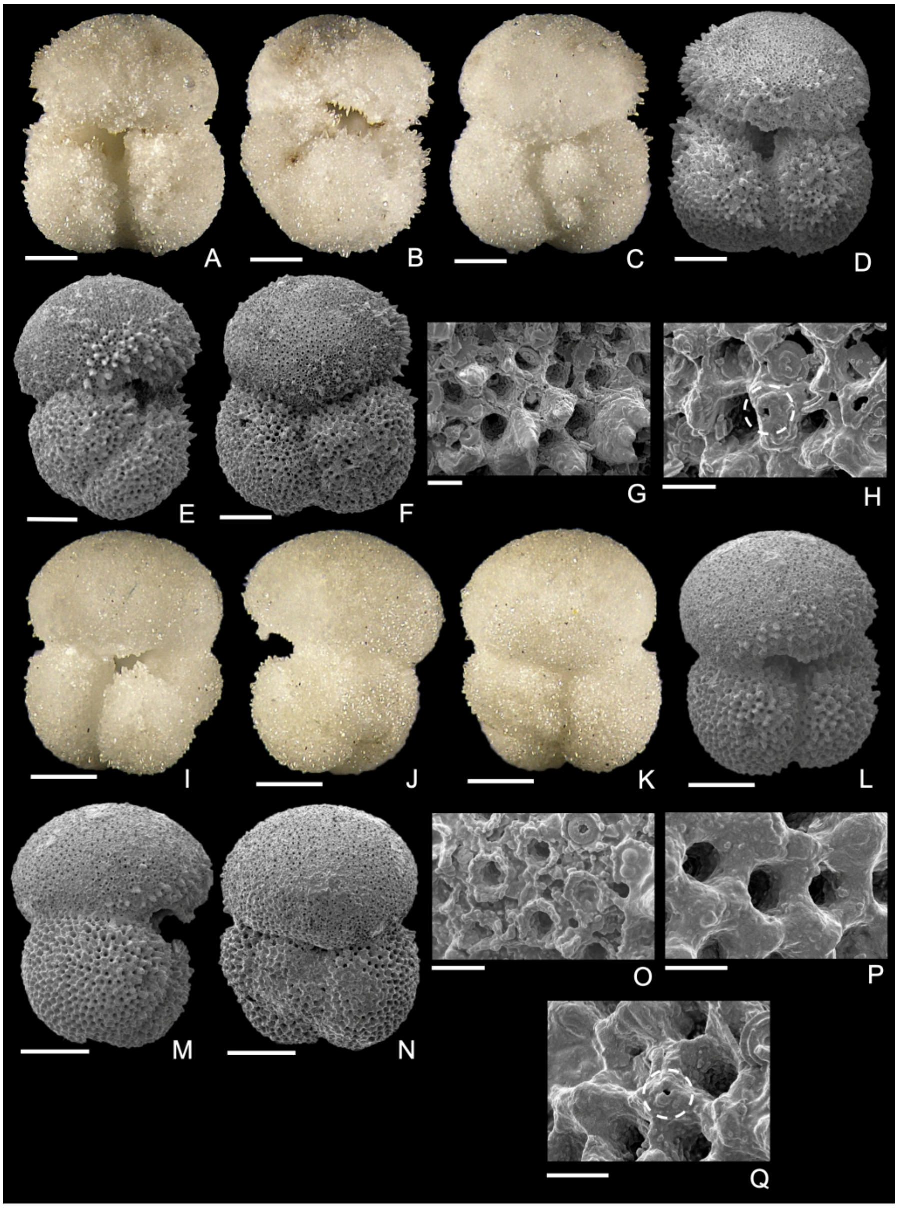


**Figure 20.** '*Dentoglobigerina*' *eotripartita* **(NHMUK PM PF XXXXX, A-H)**, ODP Sample 865C-4H-2, 110-112 cm, upper Eocene Zone E14, Allison Guyot, western Pacific Ocean: Z-stacker images of **(A)** umbilical view, **(B)** edge view, **(C)** spiral view; SEM images of **(D)** umbilical view, **(E)** edge view, **(F)** spiral view; Wall texture SEM images of **(G)** umbilical view, **(H)** spiral view. White dashed circle denotes evidence of a potential spine holes. Scale bars: 100 μm (whole specimens) and 10 μm (close-up images). '*Dentoglobigerina*' *eotripartita* **(NHMUK PM PF XXXXX, I-Q)**, ODP Sample 865C-4H-2, 110-112 cm, upper Eocene Zone E14, Allison Guyot, western Pacific Ocean: Z-stacker images of **(I)** umbilical view, **(J)** edge view, **(K)** spiral view; SEM images of **(L)** umbilical view, **(M)** edge view, **(N)** spiral view; Wall texture SEM images of **(O)** umbilical view, **(P)** edge view, **(Q)** spiral view. White dashed circle denotes evidence of a potential spine hole. Scale bars: 100 μm (whole specimens) and 10 μm (close-up images).

172x232mm (300 x 300 DPI)

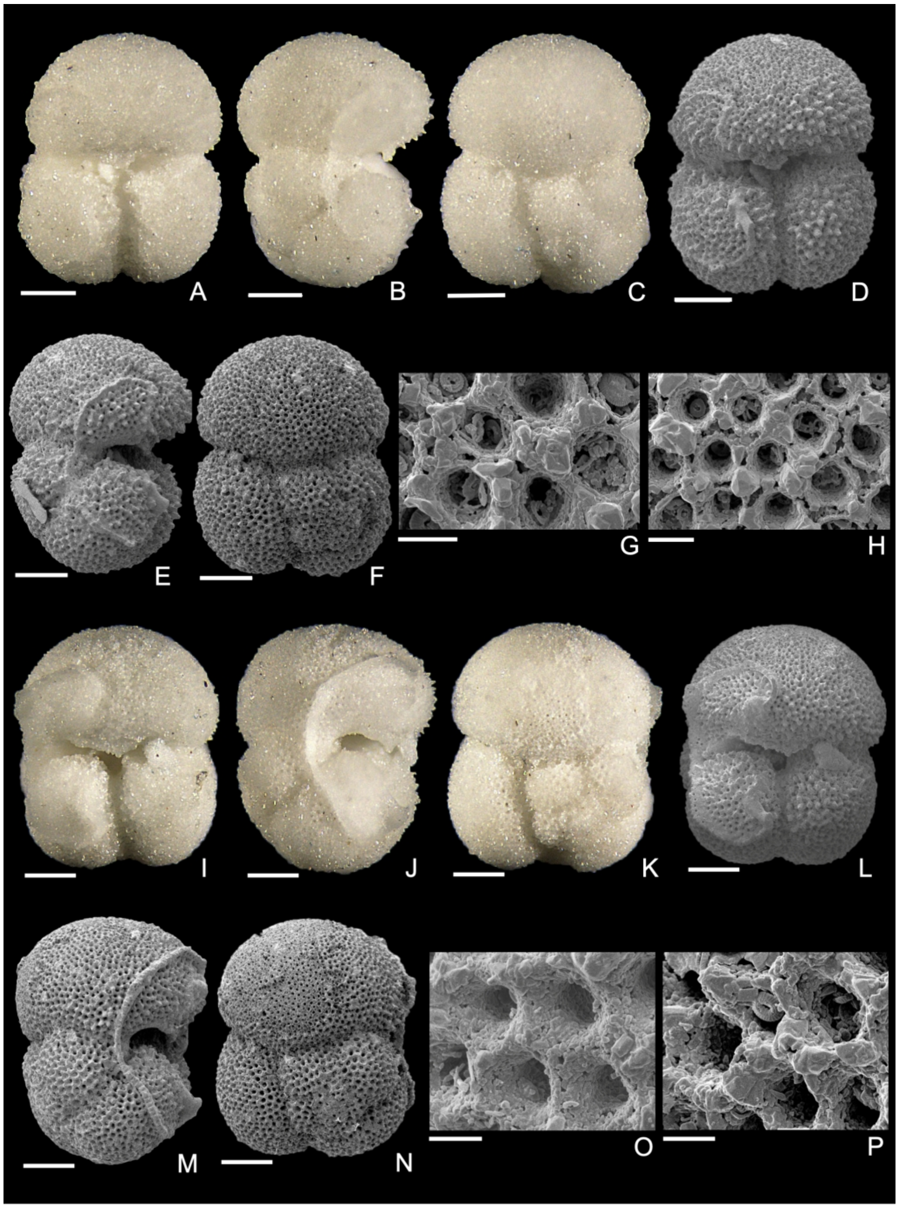


**Figure 21.** '*Dentoglobigerina*' *eotripartita* **(NHMUK PM PF XXXXX, A-H)**, ODP Sample 865C-4H-6, 63-65 cm, middle Eocene Zone E13, Allison Guyot, western Pacific Ocean: Z-stacker images of **(A)** umbilical view, **(B)** edge view, **(C)** spiral view; SEM images of **(D)** umbilical view, **(E)** edge view, **(F)** spiral view; Wall texture SEM images **(G)** spiral view, **(H)** spiral view. No evidence of spine holes. Scale bars: 100 µm (whole specimens) and 10 µm (close-up images). '*Dentoglobigerina*' *eotripartita* **(NHMUK PM PF XXXXX, I-P)**, ODP Sample 865C-7H-3, 110-112 cm, middle Eocene Zone E9, Allison Guyot, western Pacific Ocean: Z-stacker images of **(I)** umbilical view, **(J)** edge view, **(K)** spiral view; SEM images of **(L)** umbilical view, **(M)** edge view, **(N)** spiral view; Wall texture SEM images of **(O)** umbilical view, **(P)** spiral view. No evidence of spine holes. Scale bars: 100 µm (whole specimens) and 10 µm (close-up images).

172x232mm (300 x 300 DPI)

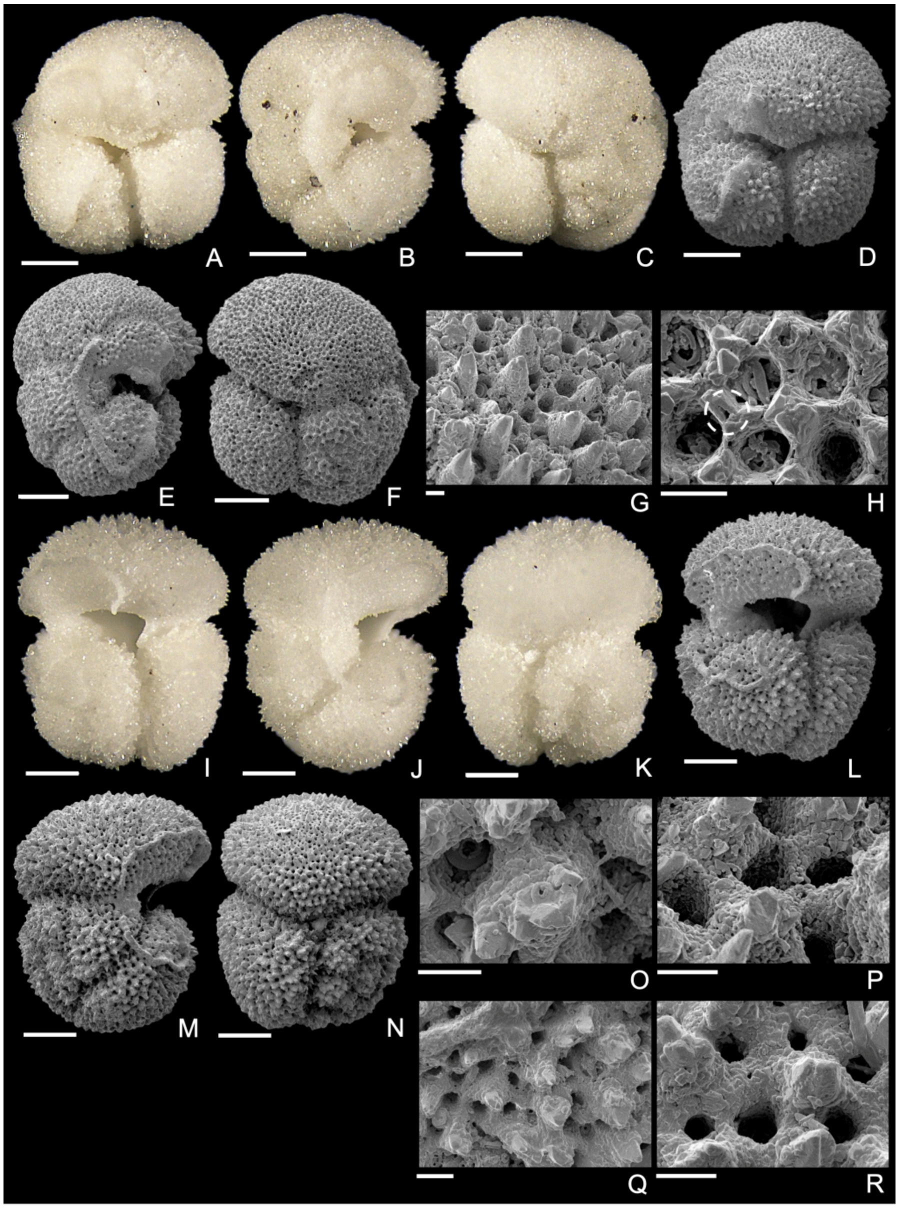


**Figure 22.** '*Dentoglobigerina*' *eotripartita* **(NHMUK PM PF XXXXX, A-H)**, ODP Sample 865C-7H-3, 110-112 cm, middle Eocene Zone E9, Allison Guyot, western Pacific Ocean: Z-stacker images of **(A)** umbilical view, **(B)** edge view, **(C)** spiral view; SEM images of **(D)** umbilical view, **(E)** edge view, **(F)** spiral view; Wall texture SEM images of **(G)** umbilical view, **(H)** spiral view. White dashed circle denotes evidence of a potential spine hole. Scale bars: 100 µm (whole specimens) and 10 µm (close-up images). *Acarinina mcgowrani* **(NHMUK PM PF XXXXX, I-R)**, ODP Sample 865C-8H-3, 70-72 cm, middle Eocene Zone E9, Allison Guyot, western Pacific Ocean: Z-stacker images of **(I)** umbilical view, **(J)** edge view, **(K)** spiral view; SEM images of **(L)** umbilical view, **(M)** edge view, **(N)** spiral view; Wall texture SEM image of **(O)** umbilical view, **(P)** umbilical view, **(Q)** edge view, **(R)** spiral view. No evidence of spine holes. Scale bars: 100 µm (whole specimens) and 10 µm (close-up images).

172x232mm (300 x 300 DPI)

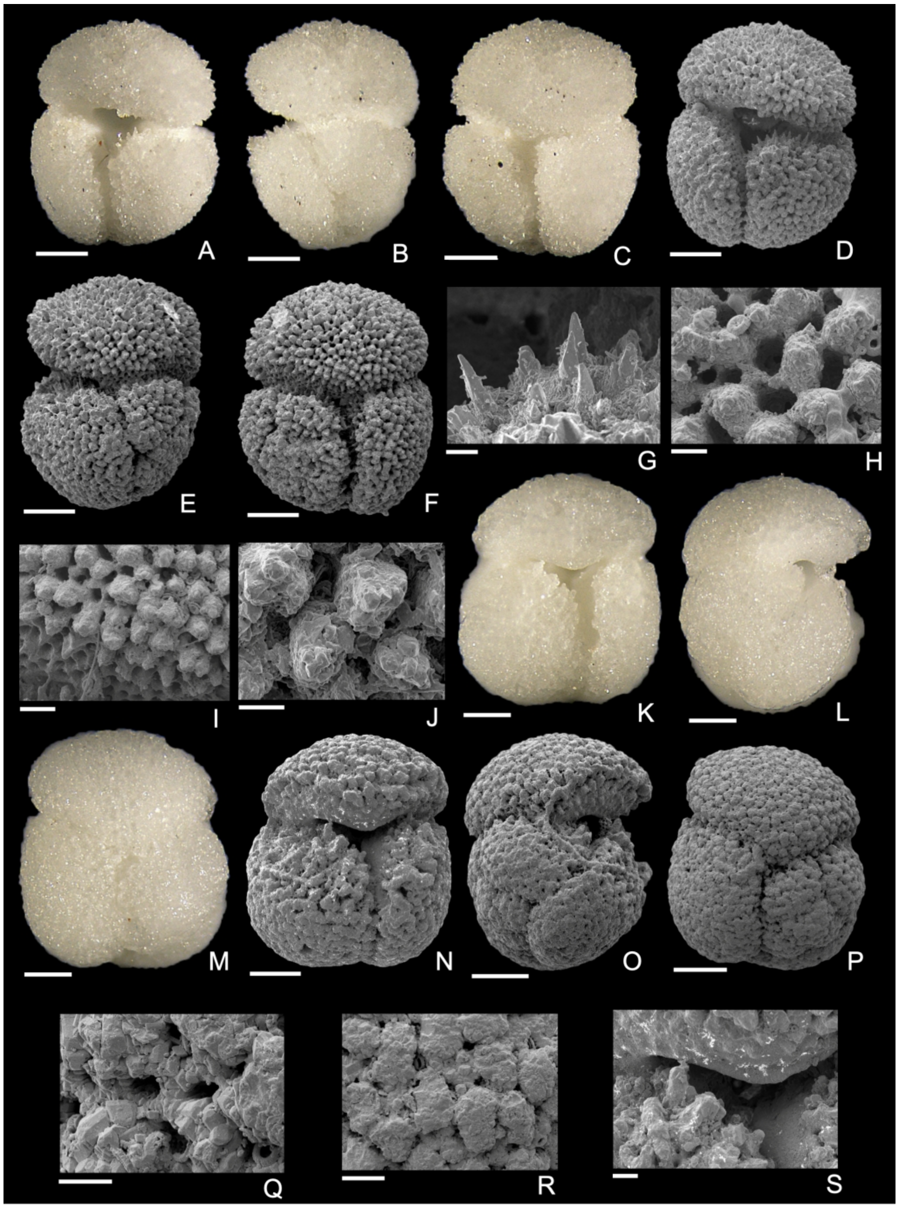


**Figure 23.** *Acarinina* cf. *A. triplex* **(NHMUK PM PF XXXXX, A-J)**, ODP Sample 865C-8H-3, 70-72 cm, middle Eocene Zone E9, Allison Guyot, western Pacific Ocean: Z-stacker images of **(A)** umbilical view, **(B)** edge view, **(C)** spiral view; SEM images of **(D)** umbilical view, **(E)** edge view, **(F)** spiral view; Wall texture SEM image of **(G)** pustules in umbilical view, **(H)** edge view, **(I)** edge view, **(J)** spiral view. No evidence of spine holes. Scale bars: 100 µm (whole specimens) and 10 µm (close-up images). *Acarinina* cf. *A. primitiva* **(NHMUK PM PF XXXXX, K-S)**, ODP Sample 763B-6X-6W, 53-55 cm, middle Eocene Zone E10, Exmouth Plateau, Indian Ocean: Z-stacker images of **(K)** umbilical view, **(L)** edge view, **(M)** spiral view; SEM images of **(N)** umbilical view, **(O)** edge view, **(P)** spiral view; Wall texture SEM images of **(Q)** edge view, **(R)** spiral view, **(S)** tooth image in umbilical view. No evidence of spine holes. Scale bars: 100 µm (whole specimens) and 10 µm (close-up images).

172x232mm (300 x 300 DPI)

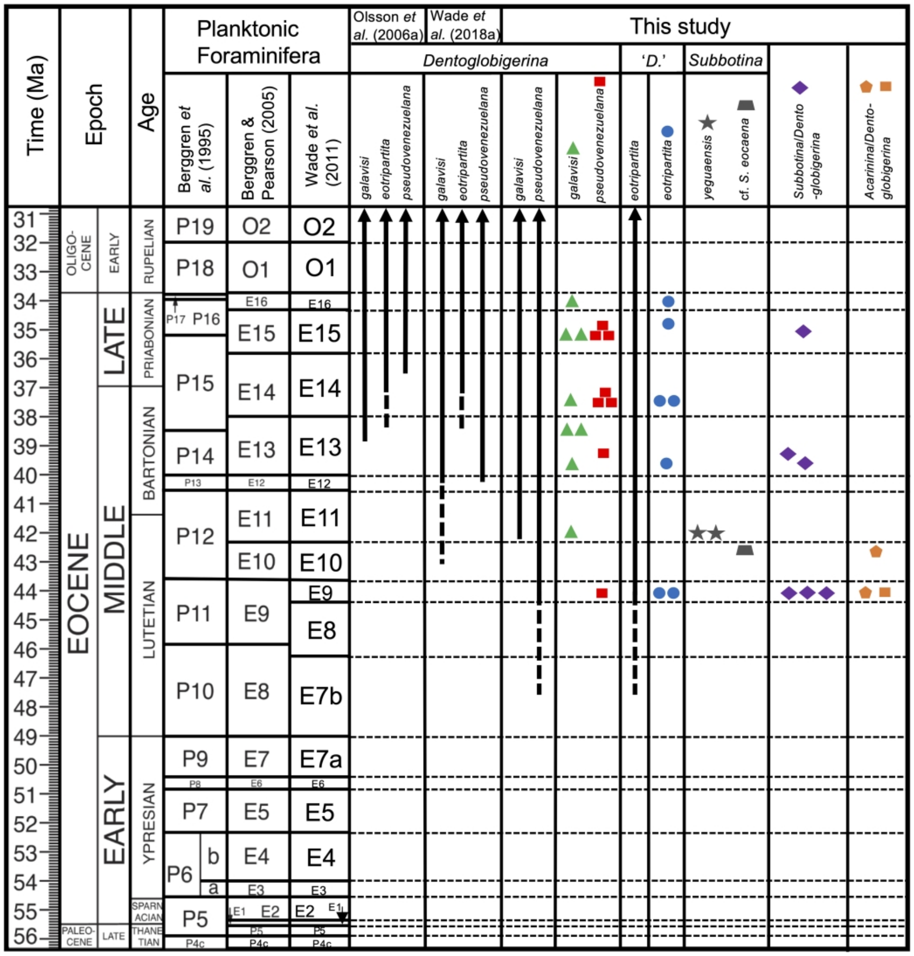


**Figure 24.** Updated stratigraphic range of Eocene *Dentoglobigerina* and comparison with Olsson *et al.* (2006a) and Wade *et al.* (2018a) using the Planktonic Foraminiferal Zonation of the Eocene by Berggren & Pearson (2005) and Wade *et al.* (2011). **(A)** green triangles for selected specimens of *D. galavisi*; **(B)** blue circles for specimens of '*Dentoglobigerina*' eotripartita; **(C)** red squares for specimens of *D. pseudovenezuelana*; **(D)** purple diamonds for morphological intermediates between *Dentoglobigerina* and *Subbotina*; **(E)** orange pentagons for morphological intermediates between '*Dentoglobigerina*' and Acarinina; **(F)** grey stars for *S. yeguaensis*; **(G)** the grey trapeze for *Subbotina* cf. *S. eocaena*; **(H)** the orange square for *A. mcgowrani*. '*D.*' refers to '*Dentoglobigerina*'.

172x176mm (600 x 600 DPI)

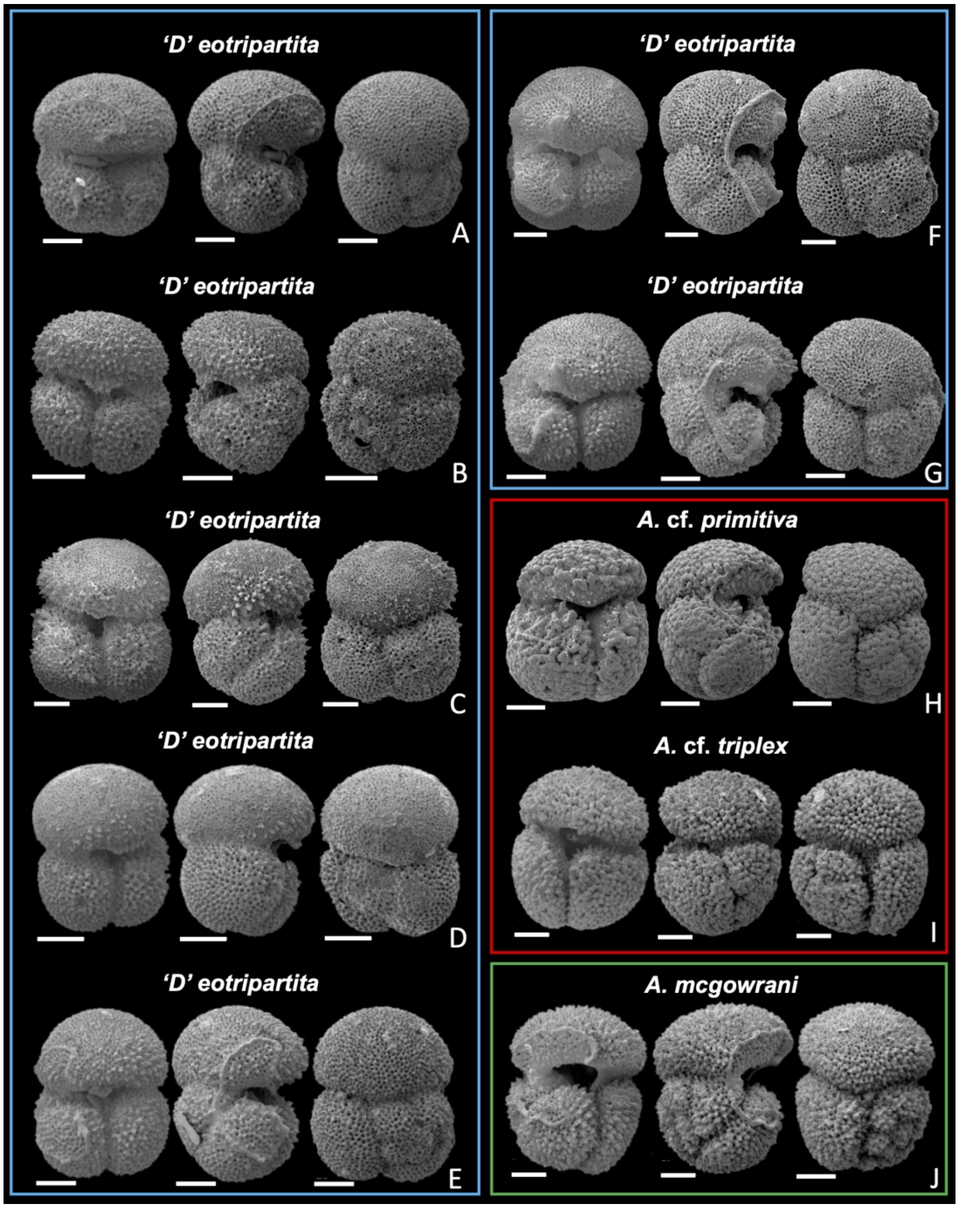


**Figure 25.** SEM images of '*D.*' *eotripartita* specimens and morphological intermediates with *Acarinina* to infer morphological similarities between the two taxa: **(A)** NHMUK PM PF XXXXX – Fig. 18A-H, Shubuta FM, Zone E16; **(B)** NHMUK PM PF XXXXX – Fig. 18I-P, Allison Guyot, western Pacific Ocean, Zone E15; **(C)** NHMUK PM PF XXXXX – Fig. 19A-H, Allison Guyot, western Pacific Ocean, Zone E14; **(D)** NHMUK PM PF XXXXX – Fig. 19I-Q, Allison Guyot, western Pacific Ocean, Zone E14; **(E)** NHMUK PM PF XXXXX – Fig. 20A-H, Allison Guyot, western Pacific Ocean, Zone E13; **(F)** NHMUK PM PF XXXXX – Fig. 20I-P, Allison Guyot, western Pacific Ocean, Zone E9; **(G)** NHMUK PM PF XXXXX – Fig. 21A-H, Allison Guyot, western Pacific Ocean, Zone E9; **(H)** NHMUK PM PF XXXXX – Fig. 22K-S, Exmouth Plateau, Indian Ocean, Zone E10; **(I)** NHMUK PM PF XXXXX – Fig. 22A-J, Allison Guyot, western Pacific Ocean, Zone E9; **(J)** NHMUK PM PF XXXXX – Figure 21I-R Allison Guyot, western Pacific Ocean, Zone E9. Green box = *Acarinina* genus; red box = morphological intermediates; blue box = '*Dentoglobigerina*' genus.

172x217mm (300 x 300 DPI)

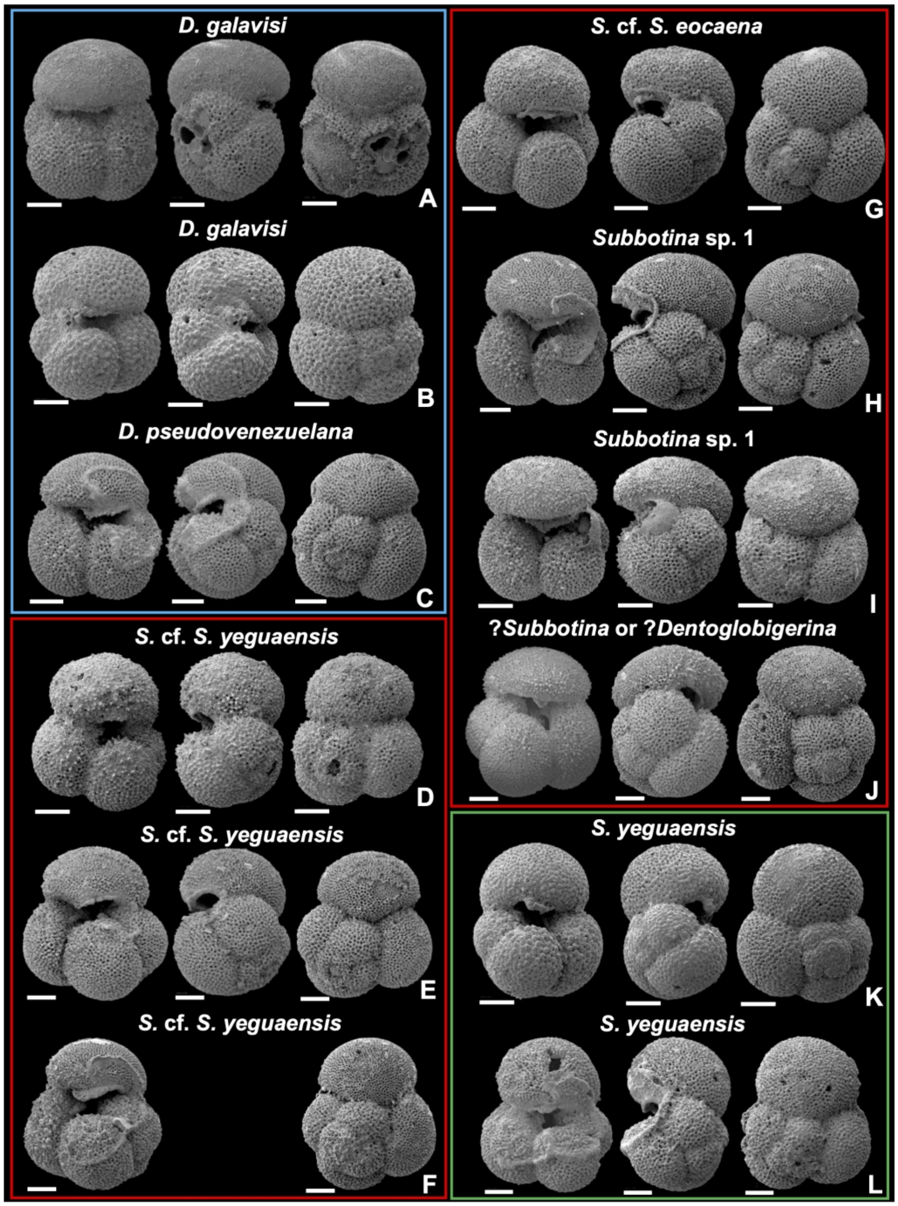


**Figure 26.** SEM images of *D. pseudovenezuelana*, *D. galavisi*, *S. yeguaensis* and morphological intermediates with *Subbotina*: **(A)** NHMUK PM PF XXXXX – Fig. 6A-H, Exmouth Plateau, Indian Ocean, Zone E15; **(B)** NHMUK PM PF XXXXX – Fig. 8I-O, Exmouth Plateau, Indian Ocean, Zone E11; **(C)** NHMUK PM PF XXXXX – Fig. 11A-J, Allison Guyot, western Pacific Ocean, Zone E15; **(D)** NHMUK PM PF XXXXX – Fig. 14A-H, Walvis Ridge eastern Atlantic Ocean, Zone E13; **(E)** NHMUK PM PF XXXXX – Fig. 14I-R, Allison Guyot, western Pacific Ocean, Zone E15; **(F)** NHMUK PM PF XXXXX – Figure 15A-F, Allison Guyot, western Pacific Ocean, Zone E13; **(G)** NHMUK PM PF XXXXX – Fig. 15G-P, Exmouth Plateau, Indian Ocean, Zone E10; **(H)** NHMUK PM PF XXXXX – Fig. 16A-J, Allison Guyot, western Pacific Ocean, Zone E9; **(I)** NHMUK PM PF XXXXX – Fig. 16K-T, Allison Guyot, western Pacific Ocean, Zone E9; **(J)** NHMUK PM PF XXXXX – Fig. 17, Allison Guyot, western Pacific Ocean, Zone E9; **(K)** NHMUK PM PF XXXXX – Fig. 13A-H, Exmouth Plateau, Indian Ocean, Zone E11; **(L)** NHMUK PM PF XXXXX – Fig. 13I-Q, Exmouth Plateau, Indian Ocean, Zone E11. Green box = *Subbotina yeguaensis*; red box = morphological intermediates; blue box = *Dentoglobigerina* genus.

172x232mm (300 x 300 DPI)

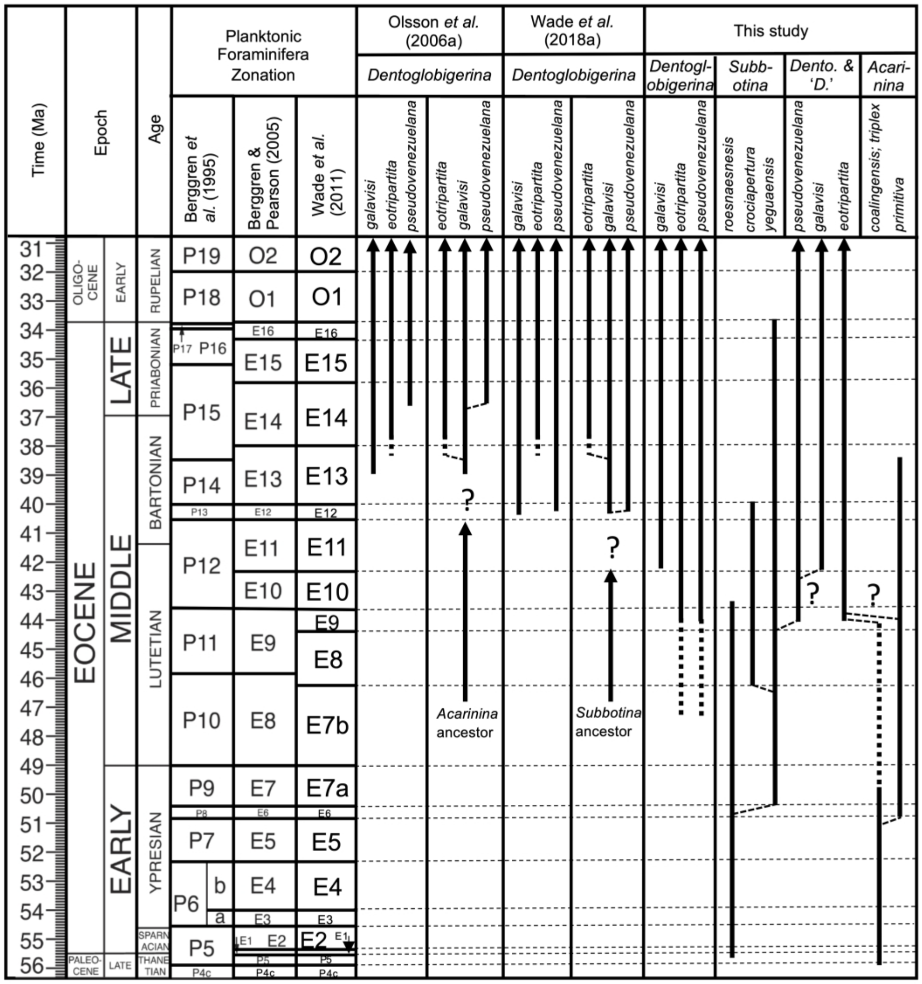


**Figure 27.** Proposed phylogenetic relationships between *Dentoglobigerina*, *Acarinina* and *Subbotina* and comparison with previous relationships proposed by Olsson *et al.* (2006a) and Wade *et al.* (2018a); use of the Planktonic Foraminiferal Zonation of Wade *et al.* (2011). Illustration of the supposedly spinose and non-spinose lineages of *Dentoglobigerina*. Question marks are placed where the evolutionary pattern between two taxa remains hypothetical. Dashed lines indicate uncertain stratigraphic ranges. '*Dento.*' = *Dentoglobigerina* and '*D.*' = '*Dentoglobigerina*'.

172x181mm (600 x 600 DPI)

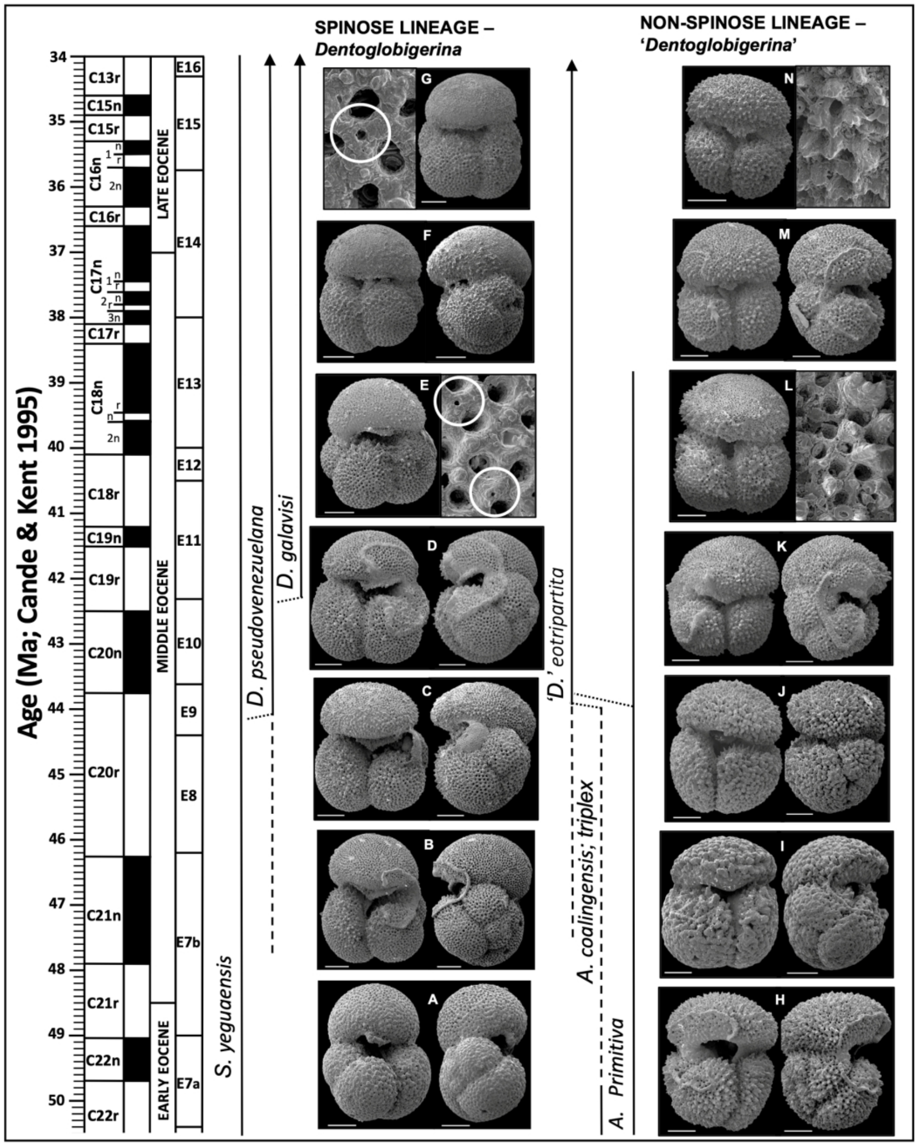


**Figure 28.** The two proposed lineages, including SEMs of selected specimens of *Dentoglobigerina*, *Acarinina*, *Subbotina* and potential intermediate specimens. The zonation is from Wade *et al.* (2011). The dashed lines represent hypothetical extensions of the stratigraphic range of taxa to earlier ages. The polarity time scale is from Cande & Kent (1995). White circles denote evidence of spine holes.

172x212mm (300 x 300 DPI)

## Supplementary online material

### Table captions

**Table 4.** Age references for studied sites. 'C&K' stands for Cande & Kent.

**Table 5.** Taxonomic name, pustulose and spinose characters of selected specimens of *Dentoglobigerina* and morphological intermediates for each sites of the Eocene interval. 'W. *et al.* (2011)' stands for Wade *et al.* (2011) and '*Dento*' for *Dentoglobigerina*.

**Table 6.** Table showing the taxonomic name, pustulose and spinose characters of recognized *Subbotina* and *Dentoglobigerina* specimens for each sites of the Eocene interval. 'W. *et al.* (2011)' stands for Wade *et al.* (2011).

**Table 7.** Picking size of selected specimens obtained for each samples of the Eocene and Miocene intervals.

### Figure captions

**Figure 29.** *Dentoglobigerina venezuelana* **(NHMUK PM PF XXXXX, A-G)**, ODP Sample 763B-3X-5W, 145-147 cm, upper Eocene Zone E15, central Exmouth Plateau off the coast of north Western Australia: Z-stacking images of **(A)** umbilical view, **(B)** edge view, **(C)** spiral view; SEM images of **(D)** umbilical view, **(E)** edge view not obtained, **(F)** spiral view; Wall texture SEM image of **(G)** umbilical view. No evidence of spine holes. Scale bars: 100 µm (whole specimens) and 10 µm (close-up image). *Subbotina corpulenta* **(NHMUK PM PF**

**XXXXX, H-N)**, ODP Sample 1263B-7H-5W, 138-140 cm, middle Eocene Zone E13, below the crest of a North-South-trending segment of Walvis Ridge off the coast of Africa in the Eastern Atlantic Ocean: Z-stacker images of **(H)** umbilical view, **(I)** edge view, **(J)** spiral view; SEM images of **(K)** umbilical view, **(L)** edge view, **(M)** spiral view; Wall texture SEM image of **(N)** umbilical view. Evidence of spine holes. Scale bars: 100 µm (whole specimens) and 10 µm (close-up image).

**Figure 30.** *Subbotina crociapertura* **(NHMUK PM PF XXXXX, A-F)**, ODP Sample 1263B-9H-5W, 139-141 cm, middle Eocene Zone E11, below the crest of a North-South-trending segment of Walvis Ridge off the coast of Africa in the Eastern Atlantic Ocean: Z-stacker images of **(A)** umbilical view, **(B)** edge view, **(C)** spiral view; SEM images of **(D)** umbilical view, edge view not obtained, **(E)** spiral view; Wall texture SEM image of **(F)** umbilical view. No evidence of spine holes. Scale bars: 100 µm (whole specimens) and 10 µm (close-up image). *Subbotina crociapertura* **(NHMUK PM PF XXXXX, G-O)**, ODP Sample 865C-5H-6, 70-72 cm, middle Eocene Zone E11, Allison Guyot, Mid-Pacific Mountains in the Western Pacific Ocean: Z-stacker images of **(G)** umbilical view, **(H)** edge view, **(I)** spiral view; SEM images of **(J)** umbilical view, **(K)** edge view, **(L)** spiral view; Wall texture SEM images of **(M)** umbilical view, **(N)** edge view, **(O)** spiral view. Evidence of spine holes. Scale bars: 100 µm (whole specimens) and 10 µm (close-up images).

**Figure 31.** *Subbotina eocaena* **(NHMUK PM PF XXXXX, A-H)**, ODP 647A-35R-2, 24-27 cm, upper Eocene, Zone E15, south of Greenland in the deep-water masses of the southern Labrador Sea: Z-stacker images of **(A)** umbilical view, **(B)** edge view, **(C)** spiral view; SEM images of **(D)** umbilical view, **(E)** edge view not obtained, **(F)** spiral view; Wall texture SEM images of **(G)** edge view, **(H)** spiral view. Evidence of spine holes. Scale bars: 100 µm (whole

specimens) and 10 µm (close-up images). *Subbotina eocaena* **(NHMUK PM PF XXXXX, I-P)**, ODP 647A-35R-2, 24-27 cm, upper Eocene, Zone E15, south of Greenland in the deep-water masses of the southern Labrador Sea: Z-stacker images of **(I)** umbilical view, **(J)** edge view, **(K)** spiral view; SEM images of **(L)** umbilical view, **(M)** edge view not obtained, **(N)** spiral view; Wall texture SEM images of **(O)** umbilical view, **(P)** spiral view. No evidence of spine holes. Scale bars: 100 µm (whole specimens) and 10 µm (close-up images).

**Figure 32.** *Subbotina eocaena* **(NHMUK PM PF XXXXX, A-J)**, ODP 647A-36R-1, 19-22 cm, upper Eocene, Zone E15, south of Greenland in the deep-water masses of the southern Labrador Sea: Z-stacker images of **(A)** umbilical view, **(B)** edge view, **(C)** spiral view; SEM images of **(D)** umbilical view, **(E)** edge view not obtained, **(F)** spiral view; Wall texture SEM images of **(G)** umbilical view, **(H)** edge view, **(I)** spiral view, **(J)** spiral view. No evidence of spine hole. Scale bars: 100 µm (whole specimens) and 10 µm (close-up images). *Subbotina eocaena* **(NHMUK PM PF XXXXX, K-R)**, ODP Sample 865C-3H-5, 110-112 cm, upper Eocene Zone E15, Allison Guyot, Mid-Pacific Mountains in the Western Pacific Ocean: Z-stacker images of **(K)** umbilical view, **(L)** edge view, **(M)** spiral view; SEM images of **(N)** umbilical view, **(O)** edge view, **(P)** spiral view; Wall texture SEM image of **(Q)** umbilical view, **(R)** spiral view. Evidence of spine holes. Scale bars: 100 µm (whole specimens) and 10 µm (close-up images).

**Figure 33.** *Subbotina gortanii* **(NHMUK PM PF XXXXX, A-H)**, ODP Sample 1052B-12H-5, 3-6 cm, middle Eocene Zone E13, Blake Nose in the Western North Atlantic Ocean: Z-stacker images of **(A)** umbilical view, **(B)** edge view, **(C)** spiral view; SEM images of **(D)** umbilical view, **(E)** edge view, **(F)** spiral view; Wall texture SEM images of **(G)** umbilical view, **(H)** spiral view. No evidence of spine hole. Scale bars: 100 µm (whole specimens) and

10 µm (close-up images). *Subbotina gortanii* **(NHMUK PM PF XXXXX, I-Q)**, ODP Sample 1263B-9H-5W, 139-141 cm, middle Eocene Zone E11, below the crest of a North-South-trending segment of Walvis Ridge off the coast of Africa in the Eastern Atlantic Ocean: Z-stacker images of **(I)** umbilical view, **(J)** edge view, **(K)** spiral view; SEM images of **(L)** umbilical view, **(M)** edge view not obtained, **(N)** spiral view; Wall texture SEM images of **(O)** umbilical view, **(P)** umbilical view, **(Q)** spiral view. Evidence of spine holes. Scale bars: 100 µm (whole specimens) and 10 µm (close-up images).

**Figure 34.** *Subbotina projecta* **(NHMUK PM PF XXXXX, A-H)**, ODP Sample 763B-2X-5W, 120-122 cm, upper Eocene Zone E15, central Exmouth Plateau off the coast of north Western Australia: Z-stacker images of **(A)** umbilical view, **(B)** edge view, **(C)** spiral view; SEM images of **(D)** umbilical view, **(E)** edge view not obtained, **(F)** spiral view; Wall texture SEM images of **(G)** umbilical view, **(H)** spiral view. Evidence of spine holes. Scale bars: 100 µm (whole specimens) and 10 µm (close-up images). *Subbotina projecta* **(NHMUK PM PF XXXXX, I-P)**, ODP Sample 763B-3X-5W, 145-147 cm, upper Eocene Zone E15, central Exmouth Plateau off the coast of north Western Australia: Z-stacker images of **(I)** umbilical view, **(J)** edge view, **(K)** spiral view; SEM images of **(L)** umbilical view, **(M)** edge view not obtained, **(N)** spiral view; Wall texture SEM images of **(O)** edge view, **(P)** spiral view. Evidence of spine holes. Scale bars: 100 µm (whole specimens) and 10 µm (close-up images).

| Leg/ Field trip | Site/ Hole | Core/ Type/ Section | Interval (cm) | Depth (mbsf) | C&K Age (Ma) | Reference |
|---|---|---|---|---|---|---|
| **105** | 647A | 35R-2 | 24-27 | 329.04 | 34.35 | Firth *et al.* (2013) |
| **105** | 647A | 36R-1 | 19-22 | 339.45 | 34.4 | Firth *et al.* (2013) |
| **122** | 763B | 2X-5W | 120-122 | 198.46 | 34 | Wade, unpublished |
| **122** | 763B | 3X-5W | 145-147 | 208.25 | 34.1 | Wade, unpublished |
| **122** | 763B | 4X-3W | 46-48 | 217.46 | 35 | Wade, unpublished |
| **122** | 763B | 5X-2W | 55-57 | 222.3 | 37.5 | Wade, unpublished |
| **122** | 763B | 6X-5W | 42-44 | 234.74 | 42.3 | Wade, unpublished |
| **122** | 763B | 6X-6W | 53-55 | 236.49 | 42.8 | Wade, unpublished |
| **143** | 865C | 3H-5 | 110-112 | 18.9 | 34.8 | Coxall (2000) |
| **143** | 865C | 3H-6 | 46-48 | 20.4 | 35.2 | Coxall (2000) |
| **143** | 865C | 4H-2 | 110-112 | 22.50-32 | 37.6 | Coxall (2000) |
| **143** | 865C | 4H-6 | 63-65 | 29.90 | 39.7 | Coxall (2000) |
| **143** | 865C | 5H-6 | 70-72 | 40-41.5 | 41.4 | Coxall (2000) |
| **143** | 865C | 7H-3 | 110-112 | 54.80 | 44.1 | Coxall (2000) |
| **143** | 865C | 8H-3 | 70-72 | 63.40 | 44.3 | Coxall (2000) |
| **171B** | 1052B | 10H-6 | 13-16 | 79.75 | 37.55 | Wade (2004) |
| **171B** | 1052B | 12H-5 | 3-6 | 97.05 | 38.11 | Wade (2004) |
| **208** | 1263B | 7H-5W | 138-140 | 103.00 | 38.1 | Wade, unpublished |
| **208** | 1263B | 8H-5W | 139-141 | 112.50 | 39.2 | Wade, unpublished |
| **208** | 1263B | 9H-5W | 139-141 | 122.00 | 41.5 | Wade, unpublished |
| **Shubuta Formation** | BW10 | M1-2 | | | 33.8 | Wade, unpublished |

**Table 4.** Age references for studied sites. 'C&K' stands for Cande & Kent.

| Figure | Genus/Species | Planktonic Foraminiferal Zone according to W. *et al.* (2011) | Site/ Hole | Core/ Type/ Section | Preser- vation | Evidence of spine holes | Pustules |
|---|---|---|---|---|---|---|---|
| 6 | *D. galavisi* | E13 | 1052B | 12H-5 | Fair | Yes | No |
| | *D. galavisi* | E13 | 865C | 4H-6 | Fair | Yes | No |
| 7 | *D. galavisi* | E16 | 763B | 2X-5W | Fair | Yes | No |
| | *D. galavisi* | E15 | 763B | 4X-3W | Fair | Yes | No |
| 8 | *D. galavisi* | E15 | 763B | 4X-3W | Fair | Yes | No |
| | *D. galavisi* | E14 | 763B | 5X-2W | Good | No | No |
| 9 | *D. galavisi* | E13 | 1263B | 7H-5W | Poor | Yes | Yes |
| | *D. galavisi* | E11 | 763B | 6X-5W | Poor | No | No |
| 10 | *D. pseudovenezuelana* | E14 | 1052B | 10H-6 | Fair | Yes | Yes |
| | *D. pseudovenezuelana* | E14 | 1052B | 10H-6 | Fair | No | Yes |
| 11 | *D. pseudovenezuelana* | E13 | 1263B | 8H-5W | Fair | Yes | Yes |
| | *D. pseudovenezuelana* | E15 | 865C | 3H-5 | Fair | Yes | Yes |
| 12 | *D. pseudovenezuelana* | E15 | 865C | 3H-6 | Fair | Yes | Yes |
| | *D. pseudovenezuelana* | E15 | 865C | 3H-6 | Fair | No | Yes |
| 13 | *D. pseudovenezuelana* | E9 | 865C | 7H-3 | Good | Yes | Yes |
| | *D. pseudovenezuelana* | E14 | 763B | 5X-2W | Good | Yes | Yes |
| 14 | *Subbotina yeguaensis* | E11 | 763B | 6X-5W | Fair | Yes | No |
| | *Subbotina yeguaensis* | E11 | 763B | 6X-5W | Fair | Yes | No |
| 15 | *Subbotina* cf. *S. yeguaensis* | E13 | 1263B | 8H-5W | Poor | No | Yes |
| | *Subbotina* cf. *S. yeguaensis* | E15 | 865C | 3H-6 | Fair | Yes | Yes |
| 16 | *Subbotina* cf. *S. yeguaensis* | E13 | 865C | 4H-6 | Fair | Yes | Yes |
| | *Subbotina* cf. *S. eocaena* | E10 | 763B | 6X-6W | Fair | Yes | No |
| 17 | *Subbotina* sp. 1 | E9 | 865C | 7H-3 | Fair | Yes | Yes |
| | *Subbotina* sp. 1 | E9 | 865C | 7H-3 | Fair | Yes | Yes |
| 18 | *?Subbotina or ?Dento* | E9 | 865C | 7H-3 | Fair | Yes | Yes |
| 19 | *'D.' eotripartita* | E16 | BW10 | M1-2 | Fair | No | No |
| | *'D.' eotripartita* | E15 | 865C | 3H-5 | Poor | No | No |
| 20 | *'D.' eotripartita* | E14 | 865C | 4H-2 | Fair | No | No |
| | *'D.' eotripartita* | E14 | 865C | 4H-2 | Fair | No | No |
| 21 | *'D.' eotripartita* | E13 | 865C | 4H-6 | Fair | No | No |
| | *'D.' eotripartita* | E9 | 865C | 7H-3 | Fair | No | No |
| 22 | *'D.' eotripartita* | E9 | 865C | 7H-3 | Fair | No | No |
| | *Acarinina mcgowrani* | E9 | 865C | 8H-3 | Fair | No | Yes |
| 23 | *Acarinina* cf. *A. triplex* | E9 | 865C | 8H-3 | Fair | No | Yes |
| | *Acarinina* cf. *A. primitiva* | E10 | 763B | 6X-6W | Poor | No | Yes |

**Table 5.** Taxonomic name, pustulose and spinose characters of selected specimens of *Dentoglobigerina* and morphological intermediates for each sites of the Eocene interval. 'W. *et al.* (2011)' stands for Wade *et al.* (2011) and '*Dento*' for *Dentoglobigerina*.

| Figure | Genus/Species | Planktonic Foraminiferal Zone according to W. *et al.* (2011) | Site/ Hole | Core/ Type/ Section | Preser-vation | Evidence of spine holes | Pustules |
|---|---|---|---|---|---|---|---|
| **29** | *D. venezuelana* | E16 | 763B | 3X-5W | Poor | No | No |
| | *S. corpulenta* | E13 | 1263B | 7H-5W | Fair | Yes | No |
| **30** | *S. crociapertura* | E11 | 1263B | 9H-5W | Fair | No | Yes |
| | *S. crociapertura* | E11 | 865C | 5H-6 | Poor | Yes | No |
| **31** | *S. eocaena* | E15 | 647A | 35R-2 | Fair | Yes | No |
| | *S. eocaena* | E15 | 647A | 35R-2 | Good | No | No |
| **32** | *S. eocaena* | E15 | 647A | 36R-1 | Good | No | Yes |
| | *S. eocaena* | E15 | 865C | 3H-5 | Poor | Yes | No |
| **33** | *S. gortanii* | E13 | 1052B | 12H-5 | Fair | No | No |
| | *S. gortanii* | E11 | 1263B | 9H-5W | Fair | Yes | Yes |
| **34** | *S. projecta* | E16 | 763B | 2X-5W | Fair | Yes | No |
| | *S. projecta* | E16 | 763B | 3X-5W | Fair | Yes | No |

**Table 6.** Taxonomic name, pustulose and spinose characters of recognized *Subbotina* and *Dentoglobigerina* specimens for each sites of the Eocene interval. 'W. *et al.* (2011)' stands for Wade *et al.* (2011).

| Site/Hole | Core/Type/Section | Interval (cm) | Picking size |
|---|---|---|---|
| **647A** | 35R-2 | 24-27 | >250 µm |
| **647A** | 36R-2 | 19-22 | >250 µm |
| **763B** | 2X-5W | 120-122 | >250 µm |
| **763B** | 3X-5W | 145-147 | >355 µm |
| **763B** | 4X-3W | 46-48 | >250 µm |
| **763B** | 5X-2W | 55-57 | >355 µm |
| **763B** | 6X-5W | 42-44 | >250 µm |
| **763B** | 6X-6W | 53-55 | >355 µm |
| **865C** | 3H-5 | 110-112 | >250 µm |
| **865C** | 3H-6 | 46-48 | >355 µm |
| **865C** | 4H-2 | 110-112 | >250 µm |
| **865C** | 4H-6 | 63-65 | >250 µm |
| **865C** | 5H-6 | 70-72 | >355 µm |
| **865C** | 7H-3 | 110-112 | >355 µm |
| **865C** | 8H-3 | 70-72 | >355 µm |
| **1052B** | 10H-6 | 13-16 | >355 µm |
| **1052B** | 12H-5 | 3-6 | >355 µm |
| **1263B** | 7H-5W | 138-140 | >250 µm |
| **1263B** | 8H-5W | 139-141 | >250 µm |
| **1263B** | 9H-5W | 139-141 | >250 µm |
| **BW10** | M1-2 | | >355 µm |

**Table 7.** Picking size of selected specimens obtained for each samples of the Eocene and Miocene intervals

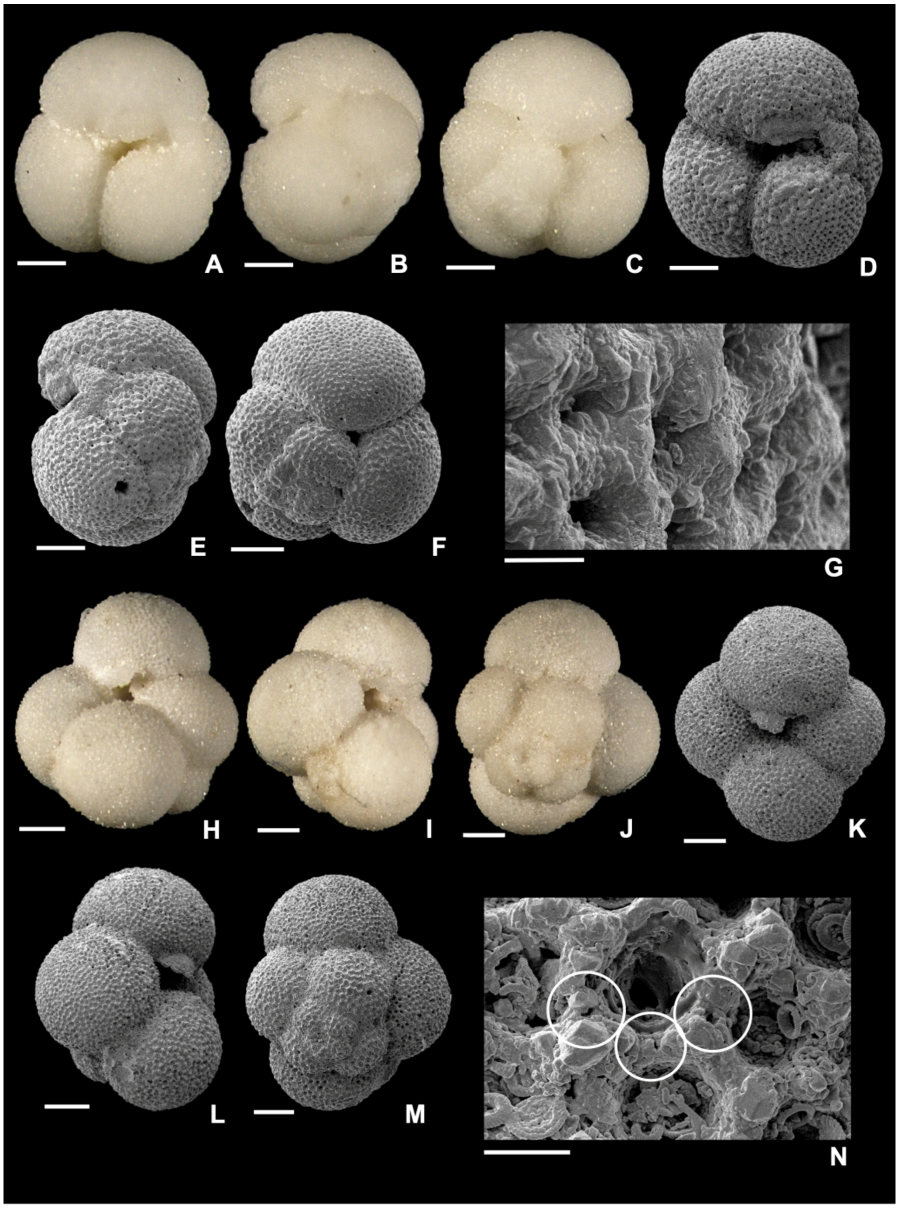


172x232mm (300 x 300 DPI)

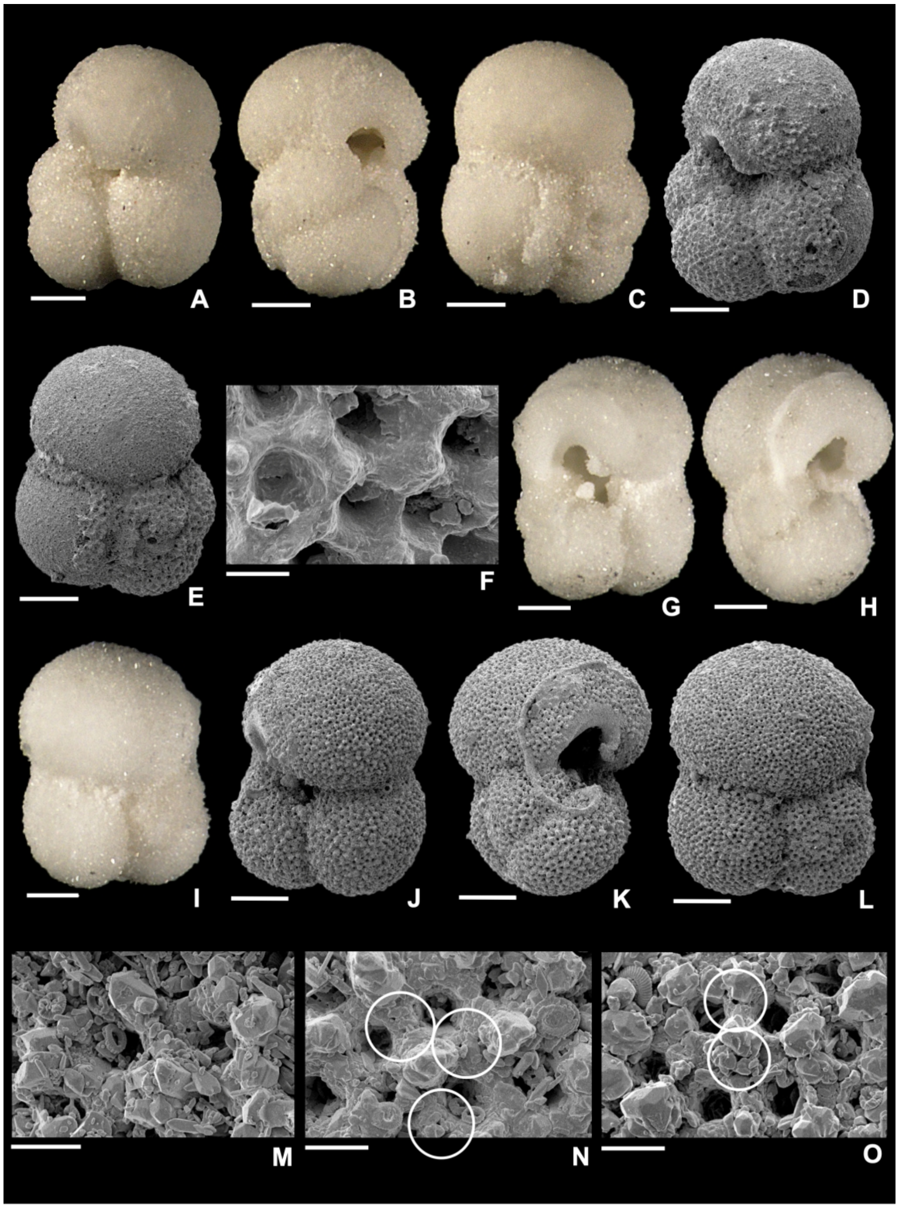


172x232mm (300 x 300 DPI)

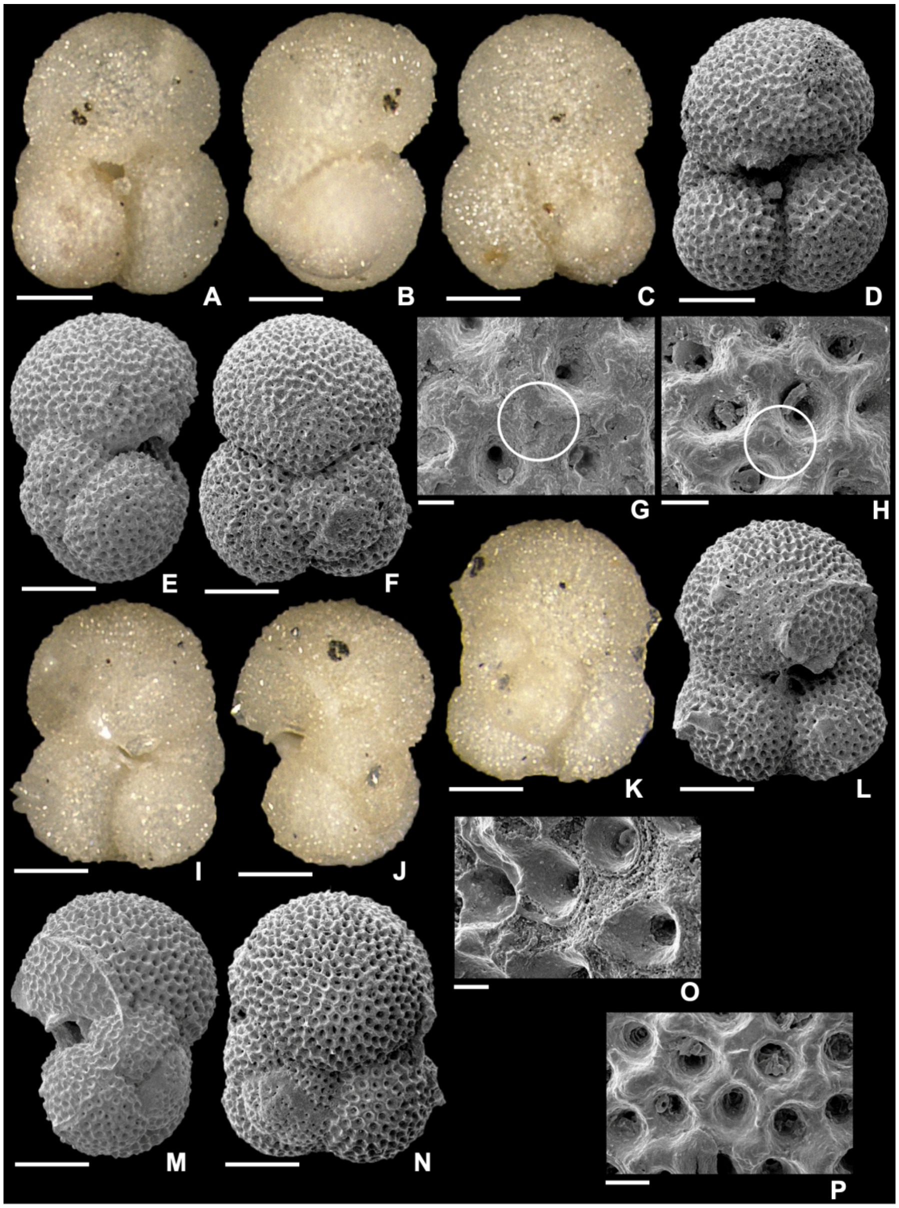


172x232mm (300 x 300 DPI)

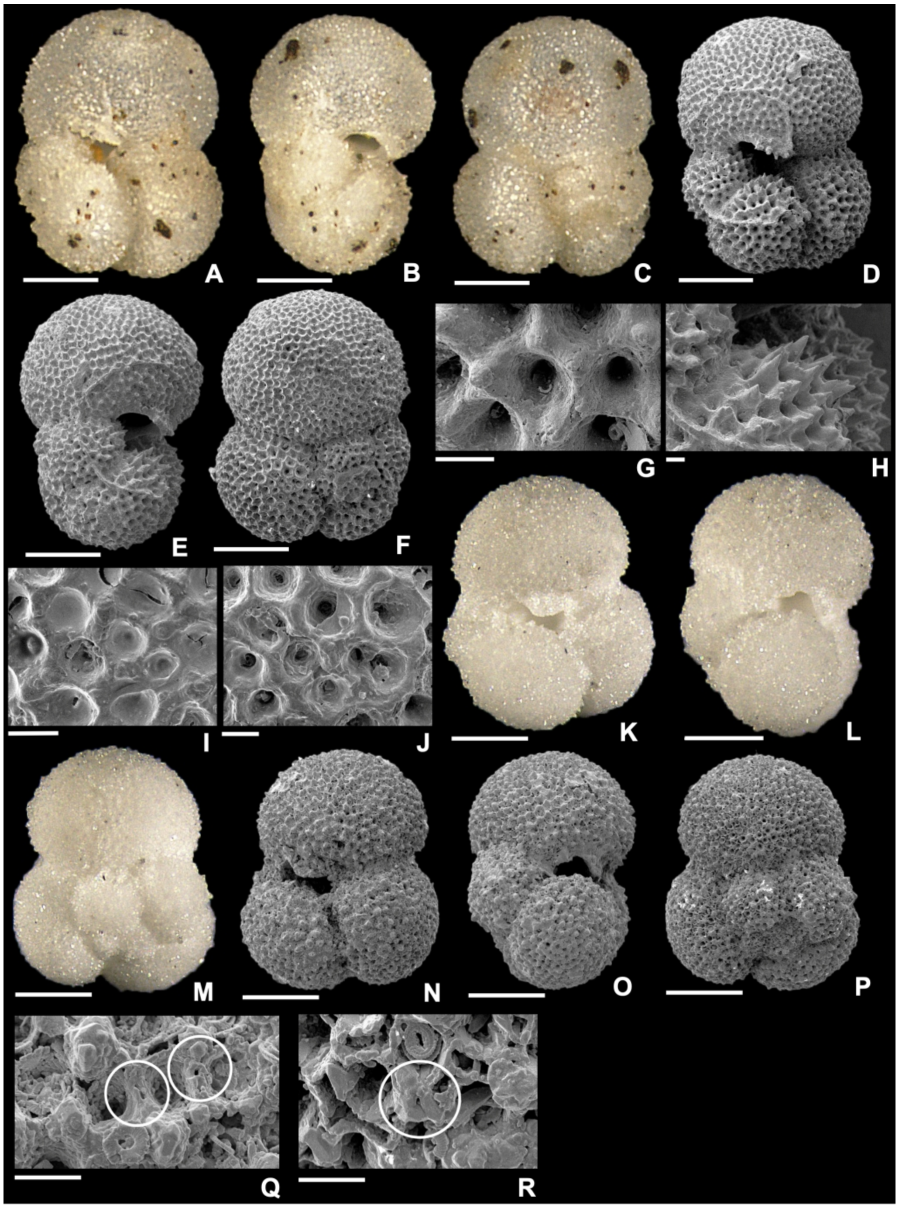


172x232mm (300 x 300 DPI)

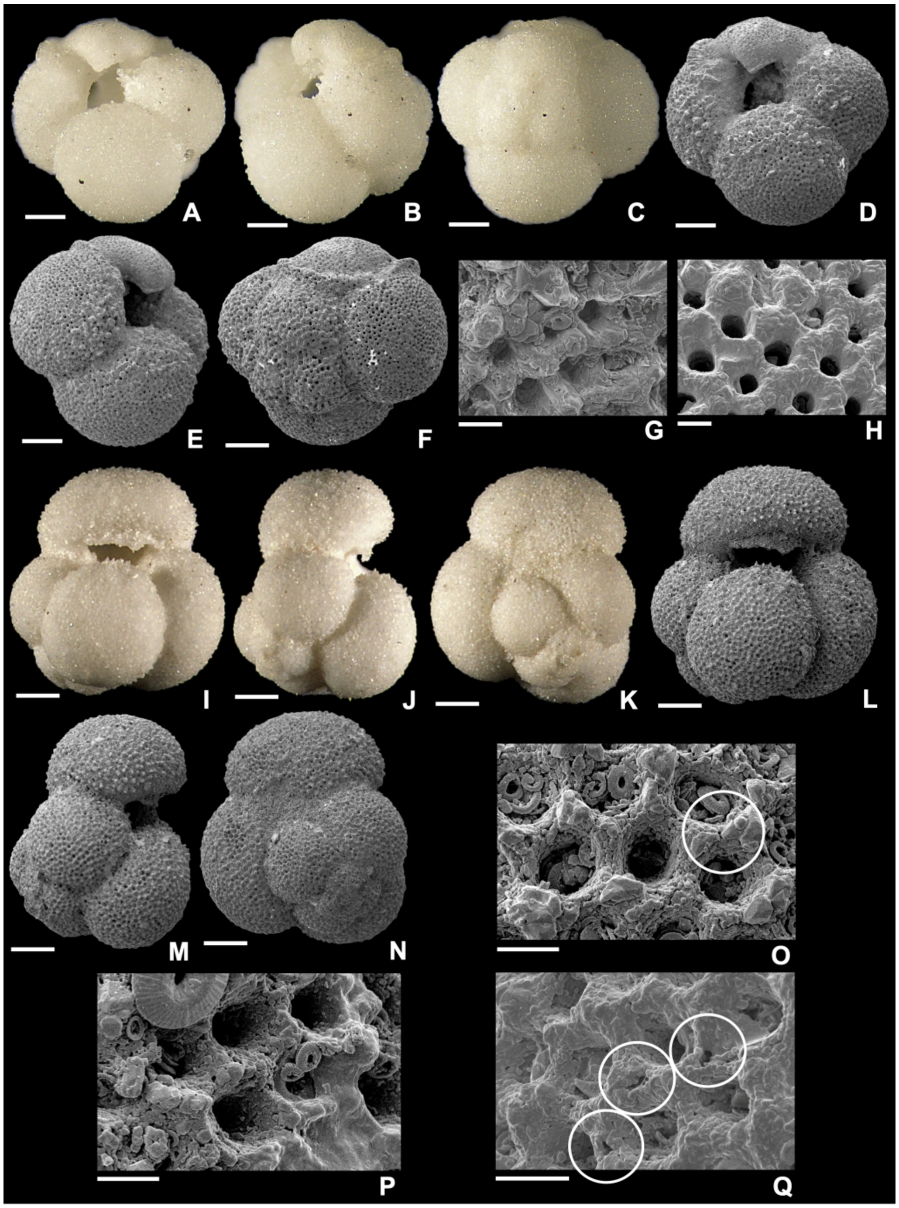


172x232mm (300 x 300 DPI)

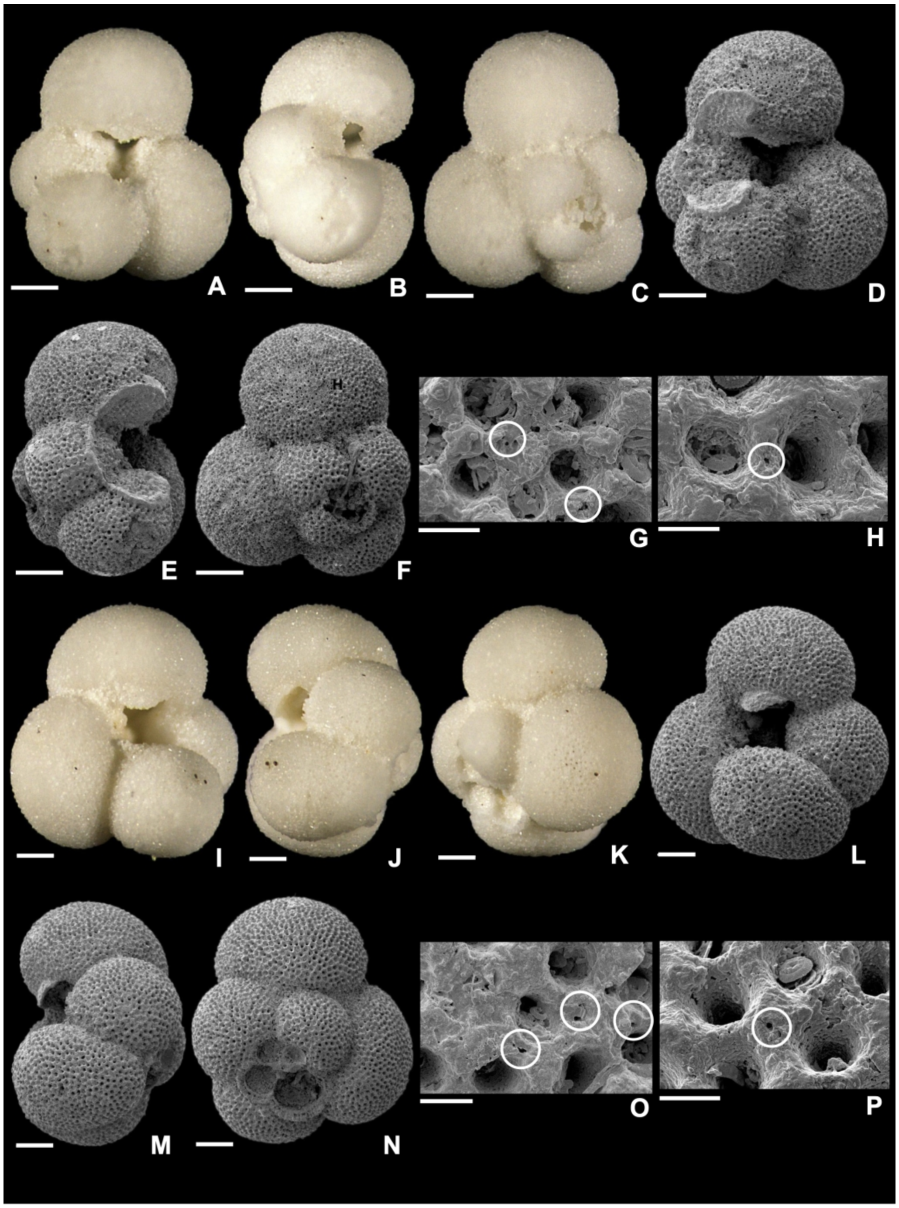


172x232mm (300 x 300 DPI)